NAVAL POSTGRADUATE SCHOOL
Monterey, California

THESIS

V6B65

DEEP NULL ANTENNAS
AND THEIR APPLICATIONS TO TACTICAL
VHF RADIO COMMUNICATIONS

by

Kenneth A. Vincent

March 1989

Co-Advisor	Richard W. Adler
Co-Advisor	James K. Breakall

Approved for public release; distribution is unlimited.

T24241

SCHOOL
CALIFORNIA 95943-5002

nclassified

urity classification of this page

REPORT DOCUMENTATION PAGE

Report Security Classification Unclassified		1b Restrictive Markings	
Security Classification Authority		3 Distribution Availability of Report Approved for public release; distribution is unlimited.	
Declassification Downgrading Schedule			
Performing Organization Report Number(s)		5 Monitoring Organization Report Number(s)	
Name of Performing Organization Naval Postgraduate School	6b Office Symbol *(if applicable)* 32	7a Name of Monitoring Organization Naval Postgraduate School	
Address *(city, state, and ZIP code)* Monterey, CA 93943-5000		7b Address *(city, state, and ZIP code)* Monterey, CA 93943-5000	
Name of Funding Sponsoring Organization	8b Office Symbol *(if applicable)*	9 Procurement Instrument Identification Number	
Address *(city, state, and ZIP code)*		10 Source of Funding Numbers	
		Program Element No	Project No / Task No / Work Unit Accession No

Title *(include security classification)* DEEP NULL ANTENNAS AND THEIR APPLICATIONS TO TACTICAL VHF RADIO COMMUNICATIONS

Personal Author(s) Kenneth A. Vincent

13a Type of Report	13b Time Covered	14 Date of Report *(year, month, day)*	15 Page Count
Master's Thesis	From To	March 1989	99

Supplementary Notation The views expressed in this thesis are those of the author and do not reflect the official policy or position of the Department of Defense or the U.S. Government.

17 Cosati Codes			18 Subject Terms *(continue on reverse if necessary and identify by block number)*
Field	Group	Subgroup	thesis, antenna, cardioidal radiation pattern.

Abstract *(continue on reverse if necessary and identify by block number)*

This study examines antennas with a characteristic cardioid radiation pattern, their applications to VHF radio communications and their design, construction and performance. Structures are investigated using both the Mini Numerical Electromagnetics Code (MININEC) and the Numerical Electromagnetics Code (NEC). A test structure is built, test data obtained, and a comparison of test results versus predicted results is made.

20 Distribution Availability of Abstract	21 Abstract Security Classification	
☒ unclassified unlimited ☐ same as report ☐ DTIC users	Unclassified	
22a Name of Responsible Individual Richard W. Adler	22b Telephone *(include Area code)* (408) 646-2352	22c Office Symbol 62Ab

D FORM 1473,84 MAR 83 APR edition may be used until exhausted
All other editions are obsolete

security classification of this page

Unclassified

Approved for public release; distribution is unlimited.

Deep Null Antennas and their Applications to Tactical VHF Radio Communications

by

Kenneth A. Vincent
Major, United States Marine Corps
B.S., Oregon State University, 1972

Submitted in partial fulfillment of the
requirements for the degree of

MASTER OF SCIENCE IN ELECTRICAL ENGINEERING

from the

NAVAL POSTGRADUATE SCHOOL
March 1989

ABSTRACT

This study examines antennas with a characteristic cardioid radiation pattern, their applications to VHF radio communications and their design, construction and performance. Structures are investigated using both the Mini Numerical Electromagnetics Code (MINNEC) and the Numerical Electromagnetics Code (NEC). A test structure is built, test data obtained, and a comparison of test results versus predicted results is made.

V6
C.1

TABLE OF CONTENTS

LIST OF TABLES

LIST OF FIGURES

ACKNOWLEDGEMENTS

Completion of this thesis would not have been possible without the guidance and encouragement rendered by Professors Richard W. Adler and James K. Breakall, and the patience of my wife Kay. Additionally, the author wishes to acknowledge the assistance provided by EW1 John Alexakos USN, EWC Max Cornell USN, ETCS Mark Delagasse USN, Mrs. Janeen Grohsmeyer, and Mr. Joe Vitale during testing of the prototype antenna, to Cpt McCoy, Communication-Electronics Staff Officer of the 3d Brigade, 9th Regiment, 7th Infantry Division (Light) for loan of equipment used in testing, and to Mr. Steve Blankschein who helped with fabrication of the prototype antenna.

I. INTRODUCTION

A. PURPOSE OF STUDY

In tactical military communications systems it is often advantageous for a radio to transmit and receive well in most directions but poorly or not at all in a few directions, or in one sector. Mutual interference from co-sited transmitters operating on adjacent frequencies and jamming by enemy electronic warfare activities are typical examples. Figures 1 and 2 illustrate these situations. While modern signal processing techniques and equipment can do much to reduce or eliminate such interference, two or three decibels of improvement is often prohibitively expensive, impractical, or in the worst case, impossible to produce. The use of antenna characteristics to get additional immunity to jamming and interference is thus attractive from the standpoints of both cost and practicality.

B. METHODOLOGY

This study examines a class of antennas having a characteristic cardioidal radiation pattern. Such antennas offer the prospect of putting sources of interference in the null portion of the radiation pattern, thereby reducing or eliminating the unwanted signals. Since it is usually desirable not to radiate transmitted signals in the direction of the enemy, reciprocity of receiving and transmitting characteristics is an advantage in this case.

The most common configuration in a tactical communications network is that of several stations, all within normal transmission range and located in relative directions covering up to about 270 degrees of horizontal coverage. This configuration is usually dictated by the operational situation, and is seldom based on communications considerations.

Use of directional antennas is often a means of coping with marginal or inadequate signal strength, but frequently using such antennas creates new problems, since they do not radiate well in all directions, and are in some cases nearly unidirectional. While such antennas are usually available to communicators, their often complex or unpredictable patterns of gain and loss (lobes and nulls) frequently makes them impractical to use on any but point-to-point circuits. Development of practical antennas with a single well-defined null covering a 45 to 90 degree sector and having as much gain as possible in all other directions is attractive, since it offers the possibility of getting a significant improvement in immunity to jamming and coverage range in most directions, at relatively

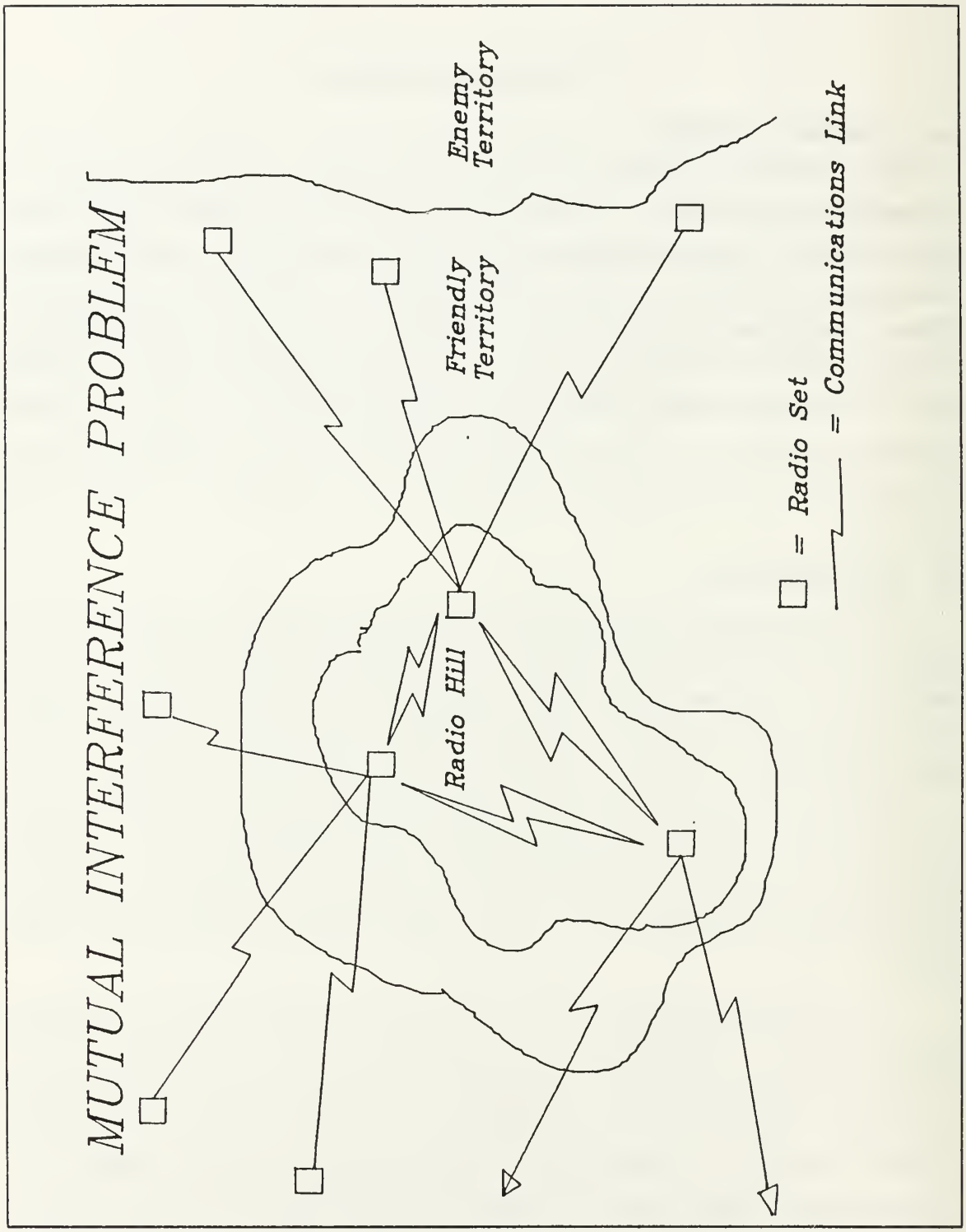

Figure 1. Typical Mutual Interference Situation

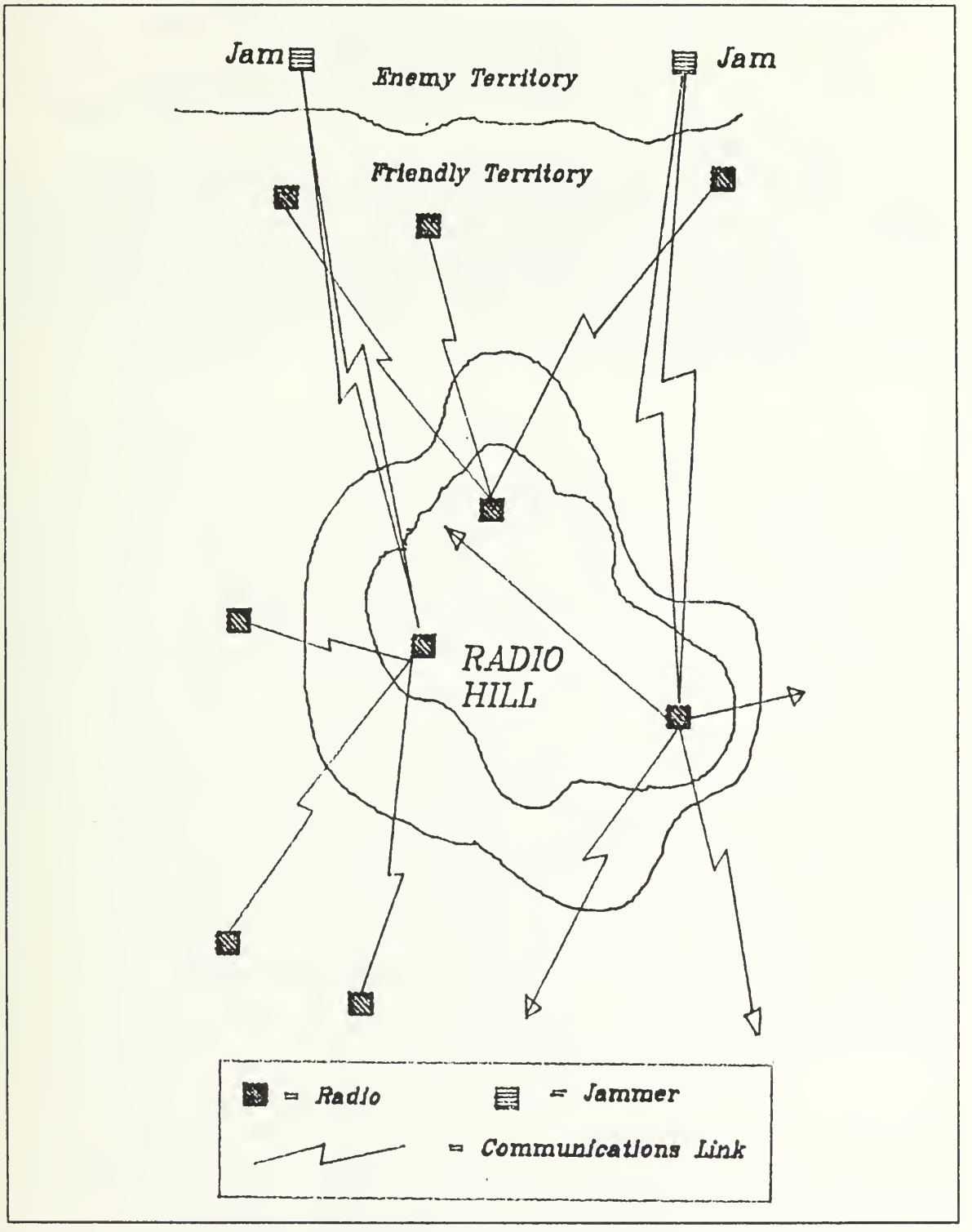

Figure 2. Typical Electronic Warfare Threat Situation

low cost. This thesis examines the possibilities for such antennas, develops a design for a prototype antenna having a characteristic cardioidal radiation pattern, models the prototype design over several combinations of ground and structure height, and evaluates actual performance of the implemented prototype versus predicted performance obtained through modeling.

The performance criteria of interest in this study are the radiation pattern, input impedance, and usable frequency range for a single structure. The shape and depth of the null in the radiation pattern are of special interest, since that single characteristic is unique to the category of antennas under study. Specific measures for these characteristics are developed when needed.

II. SURVEY OF PREVIOUS WORK

A. EARLY FINDINGS

Antennas with characteristic deep nulls have been known since the early days of radio, and are well documented in most texts on basic antenna theory. Review of some classic and current texts [Refs. 1, 2] reveals that the desired cardioidal deep null radiation pattern may be obtained by correct phasing of currents in the elements of an array of elements. Further research of the literature produced several practical structures having the desired radiation pattern, along with useful insight on productive lines of research [Refs. 3, 4].

B. FAMILIARIZATION WITH THE PROBLEM

Initial simplified studies of two vertical monopoles over perfect ground were conducted using the Mini Numerical Electromagnetics Code (MINNEC) antenna modeling program [Ref. 5] running on a personal computer. This preliminary work immediately revealed the need to know the characteristic impedance of each monopole and the mutual impedance between monopoles in order to provide the input arguments required by the MINNEC program. Appendix A addresses this problem and presents two methods which can be used to find the necessary information. A few runs of the MINNEC program provided initial insight into the scope and nature of the design task at hand. Figures 3, 4, and 5, each produced using a MINNEC simulation of a structure similar to one used in Christman's study [Ref. 4] indicate that while a well defined cardioidal far field radiation pattern can be obtained using an array of proper dimensions with properly phased currents of equal magnitude flowing in the elements, the desired pattern is essentially a narrowband phenomenon and deteriorates quite rapidly as the frequency varies from that for which the structure was designed. In addition to deterioration of the desired radiation pattern, the input impedance of the structure varies over a wide range as the frequency varies from the design frequency of the array.

In order to characterize the results of this study in quatntiative terms, the null depth in decibels relative to the front-lobe, the angle over which various null depths were exhibited, and the input impedance variations that occurred in each of several simulations are summarized in tables which follow. While null depth relative to an isotropic radiator is of interest from an analytical standpoint, the null depth relative to the gain from the

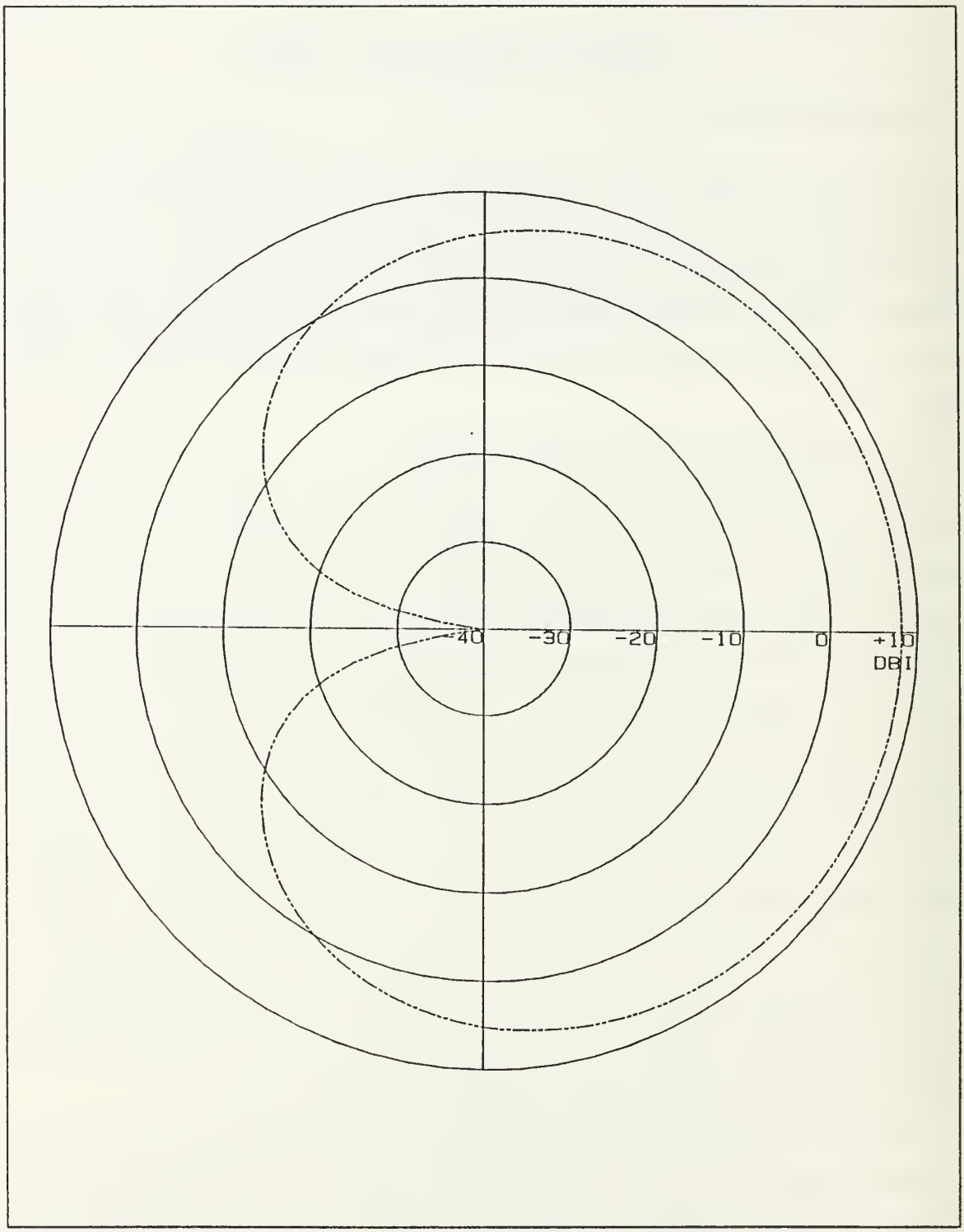

Figure 3. Far Field Pattern of Phased 60 MHz Monopoles at Resonance

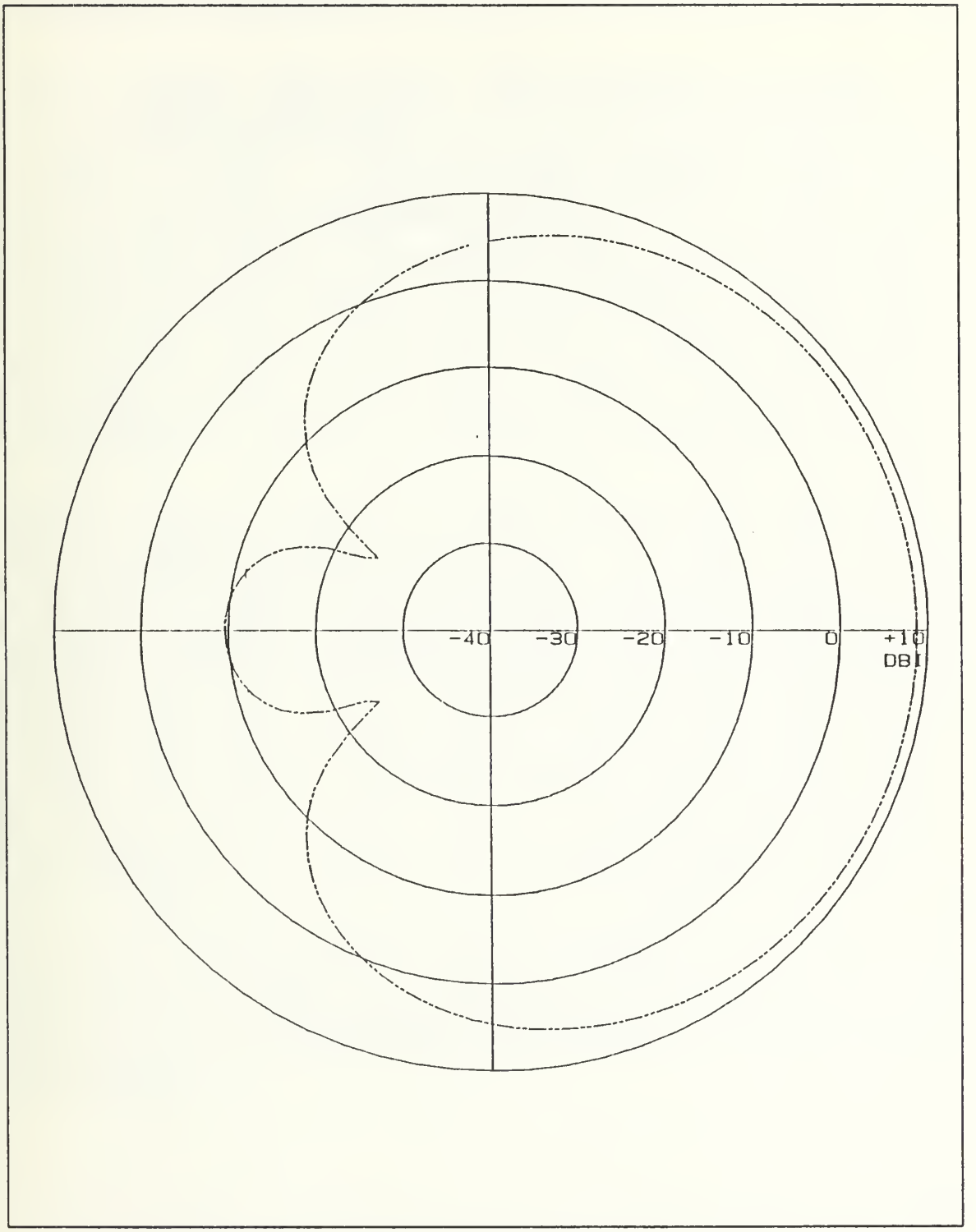

Figure 4. Far Field Pattern of Phased 60 MHz Monopoles Excited at 59 MHz

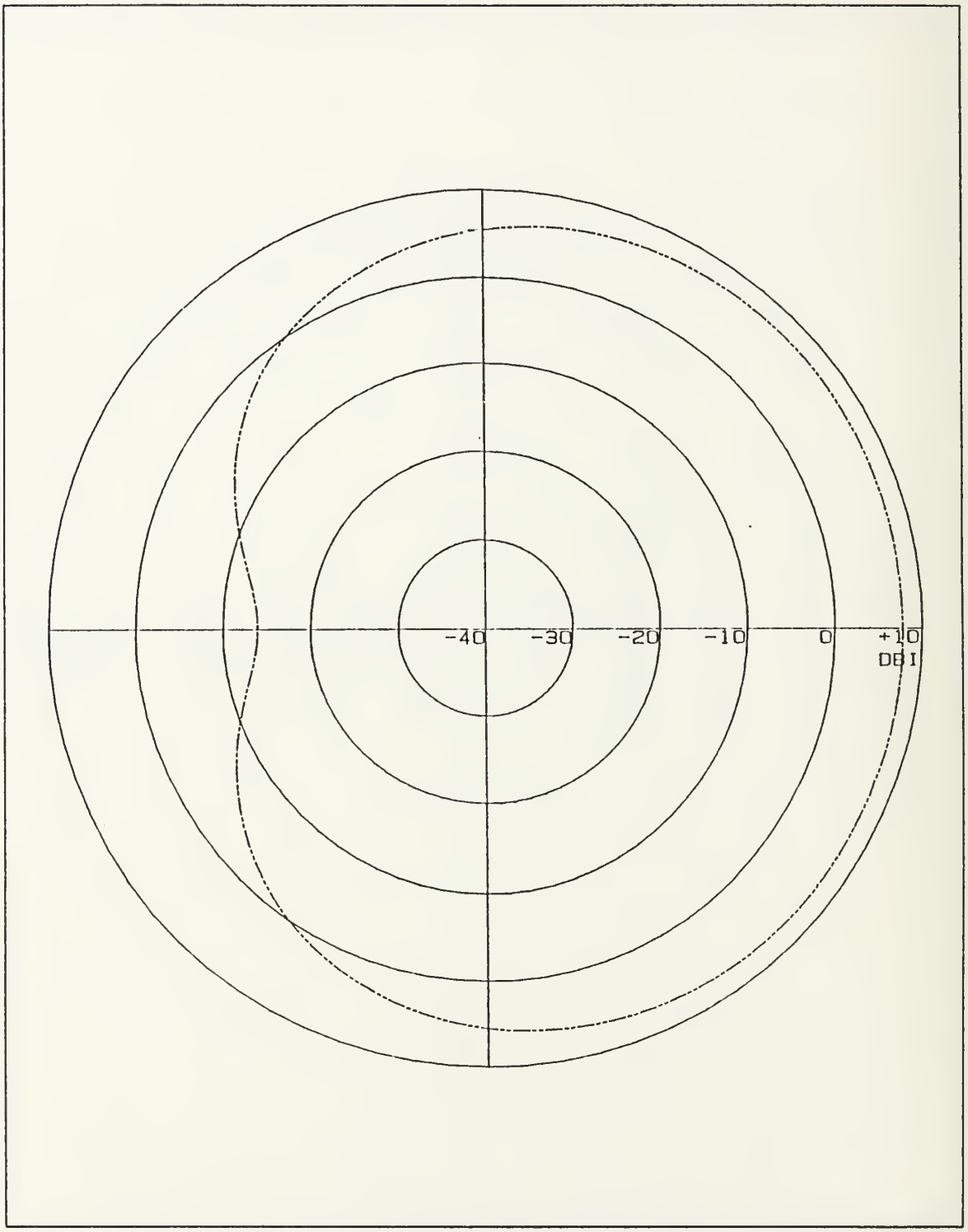

Figure 5. Far Field Pattern of Phased 60 MHz Monopoles Excited at 61 MHz

front lobe of the antenna is a more practical and useful measure of deep null effect and is therefore included in the tables.

Table 1. PHASED MONOPOLES CHARACTERISTICS, ELEMENT RADIUS = .001 METER

Freq (MHz)	0 dBi Angle (degrees)	-10 dBi Angle (degrees)	-20 dBi Angle (degrees)	20 dB F B (degrees)	Null Depth (dB)
58	156	62	32*	38*	-26.2
59	138	90	14*	60*	-24.8
60	120	64	36	56	-49.6
61	112	42		26	-14.0
62	102				-9.4
* = Two nulls					

Table 2. PHASED MONOPOLES CHARACTERISTICS, ELEMENT RADIUS = .01 METER

Freq (MHz)	0 dBi Angle (degrees)	-10 dBi Angle (degrees)	-20 dBi Angle (degrees)	20 dB F B (degrees)	Null Depth (dB)
58	160	18*	56*	98	-27.0
59	152	24*	60	136	-27.0
60	140	64	36	58	-47.4
61	132	48		42	-19.2
62	126	34		22	-13.5
* = Two nulls					

Examination of the foregoing tables shows that element radius has an effect on the shape of the radiation pattern, and also affects the bandwidth over which appreciable nulls are exhibited. The input impedance variations predicted by these simulations are summarized below:

Table 3. PHASED MONOPOLES IMPEDANCE VARIATIONS

Freq (MHz)	Monopole 1 Input Z (radius = .001 M)	Monopole 2 Input Z (radius = .001 M)	Monopole 1 Input Z (radius = .01M)	Monopole 2 Input Z (radius = .01 M)
58	14.8	44.0	17.2	56.6
59	18.8	60.0	20.2	66.6
60	23.0	70.6	23.2	62.5
61	27.4	78.1	26.2	80.5
62	32.2	85.1	29.5	86.1

From this summary of monopole impedance characteristics it can be seen that the impedance of both monopoles increases as the frequency of excitation increases and drops as the excitation frequency decreases below the structure design frequency. Figures 3, 4, and 5 illustrate the deep null performance of the two monopoles. Note that these three plots show the narrowband behavior of the structure when the magnitude and phase of the excitation voltages are not changed to compensate for changing element and mutual impedances as the excitation frequency varies. The effects of optimizing these excitations is explored in later chapters.

C. INITIAL PERSPECTIVES

This preliminary investigation indicated that there are many ways to implement an array of elements that have the desired characteristics, but also revealed that all the methods found have the common disadvantage that their cardioidal patterns are not exhibited over a wide band of frequencies and that input impedances vary over a wide range. Investigation of dipole arrays and folded dipole arrays did not produce a structure of substantially better characteristics. These structures were therefore discarded in order to limit the investigation to a manageable scope.

D. LIMITATIONS OF MININEC

While a MININEC simulation of monopoles over perfect ground is useful in a preliminary investigation, simulation of a phased monopole array over real ground using a realistic support structure and a practical feed system is beyond the capabilities of the

MININEC program. This dictates that the remainder of the simulation work be carried out using the Numerical Electromagnetics Code (NEC).

III. INVESTIGATION

A. FORMULATING THE PROBLEM USING NEC

Having narrowed the investigation to a specific monopole array using the NEC simulation system, a whole new set of requirements arises. First, since this study is oriented toward study of practical antenna systems, the simulations must be carried out over less than perfect grounds. Review of the Antenna Engineering Handbook, Vol. I [Ref. 6] provided the needed dielectric and conductivity values for good, average and poor grounds.

Since the structure must be elevated above the (imperfect) ground in order to provide satisfactory line-of-sight coverage, a support structure must be used. Since practical antennas must often be erected at varying heights above ground, it is necessary to simulate the structures investigated at varying heights above the terrain. The NEC program can easily handle this requirement if the coordinates describing the test structure are translated along the "Z" axis (chosen as the vertical axis).

B. FEED SYSTEM CONSIDERATIONS

Real antennas must have some feed system, and, in the case of the family of arrays chosen for study using NEC, the feed system is a key consideration. This is due to the critical effects of current magnitude and phase in the elements upon the radiation pattern produced. This current phasing can be accomplished in a variety of ways, as indicated by Christman and Melody [Refs. 7, 8]. Unfortunately, a simple and practical means of getting the desired phase and magnitude relationships was not found, and as mentioned in the ARRL Antenna Book [Ref. 3: pp. 8-14], a number of designers are still looking for a simple and practical means of accomplishing a constant phase equal current feed over a wide bandwidth. As a means of further exploration of this problem, the antenna feed method of Christman [Ref. 7] was chosen since it provides a computer program which in most cases provides at least one solution which is physically realizable, and since it provides a rigorous (but difficult) derivation of the theory behind the published program. This program, written by Roy Lewallen, is listed in Appendix B since it was central to the work done.

Finally, each time the test structure is changed, or the frequency used to excite the structure changes, the characteristic impedance of the monopoles and their mutual impedance changes. A mechanized way of manipulating the complex impedance matrix

describing the antenna's characteristics is almost mandatory since it is necessary to invert the characteristic admittance matrix to get the antenna's impedance matrix. Once the impedance matrix is found, the element impedances and mutual impedances are known, and the entry arguments of Lewallen's feed harness length calculation program [Ref. 7] can be supplied. A simple routine to do the required matrix manipulations was written using the MATHCAD © [Ref. 9] program running on a personal computer. This routine is included at the end of Appendix A.

At this point, all the necessary tools and information elements were at hand to proceed with a NEC-based simulation of phased monopoles over imperfect ground, employing a practical feed system.

C. EFFECTS OF SUPPORT MAST ON RADIATION PATTERN

A NEC dataset describing the model to be studied was constructed and initial test runs were made. During this sequence of tests it became clear that something was wrong, in that the radiation patterns obtained from the test structure elevated above ground by means of a metallic mast were not the same as those obtained earlier at the same height without the metallic support structure. Since the support structure was the only difference between the two cases, a one meter long insulating section was inserted between the metallic mast and the antenna. This immediately cured the problem, and the model then performed as expected. Figures 6 through 11 illustrate the problem, its remedy, and the resultant radiation pattern.

D. EFFECTS OF VARYING STRUCTURE HEIGHT

In order to explore the effects of raising and lowering the test antenna, the NEC dataset was modified by adding the vertical height to be used to all the wire Z-coordinates. Test heights of 2.5, 5 and 10 meters were chosen as those most likely to be used in practice. The effects of running the program at these heights can be seen in Figures 12 through 14. The structure and operating frequency (60 MHz) are unchanged and only the antenna height is varied. The deterioration of the deep null is evident when the structure is close to the ground.

E. EFFECTS OF VARYING GROUND CHARACTERISTICS

The effects of varying the ground over which the test antenna is used can be simulated by varying the relative dielectric constant and the conductivity (epsilon and sigma values) in the GN card of the NEC dataset describing the antenna and its environment. In order to simulate the full range of conditions that might be encountered in practice,

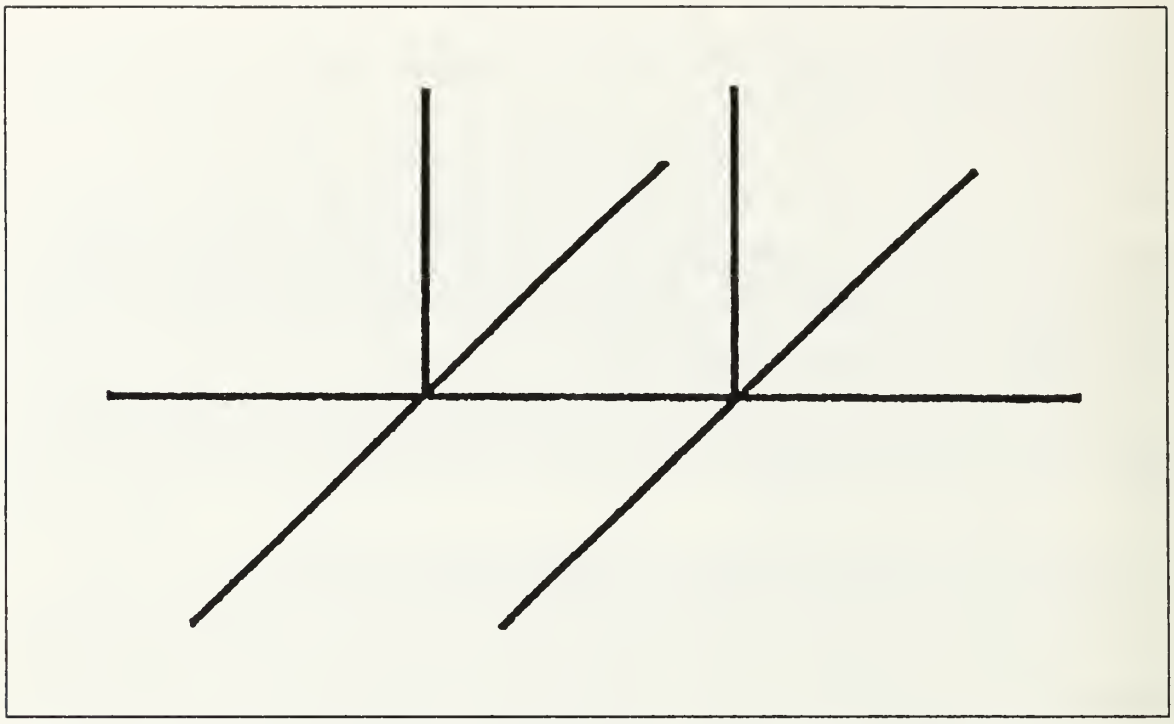

Figure 6. Initial Test Structure Geometry

three cases were chosen: rice paddy (epsilon = 34, sigma = 0.15), average ground (epsilon = 10, sigma = 0.003) and poor ground such as desert or rocky areas (epsilon = 2.5, sigma = 0.00022). The effects of changing ground characteristics can easily be misinterpreted if the angle from the zenith is not considered. To illustrate this hazard, Figures 15 through 17 show the patterns obtained over average ground at a zenith angle of 80 degrees. The same antenna at the same frequency, but viewed at an angle from the zenith of 89 degrees produced the radiation patterns shown in Figures 18 through 20. The effect of imperfect ground is clearly evident at very low angles.

From these plots it is evident that the poorer the ground is, the less the available signal strength at very low radiation angles (i.e., theta angles close to 90 degrees). This phenomenon holds in general for all antennas over imperfect ground. Its effects on the test antenna's radiation pattern are as expected.

F. EFFECTS OF VARYING GROUND PLANE STRUCTURE GEOMETRY

Since the input impedance of the test antenna is of interest, the effects of varying the angle of the ground plane radials with respect to the radiating elements was explored. The NEC datasets used to conduct this study are included in Appendix D, and the plots

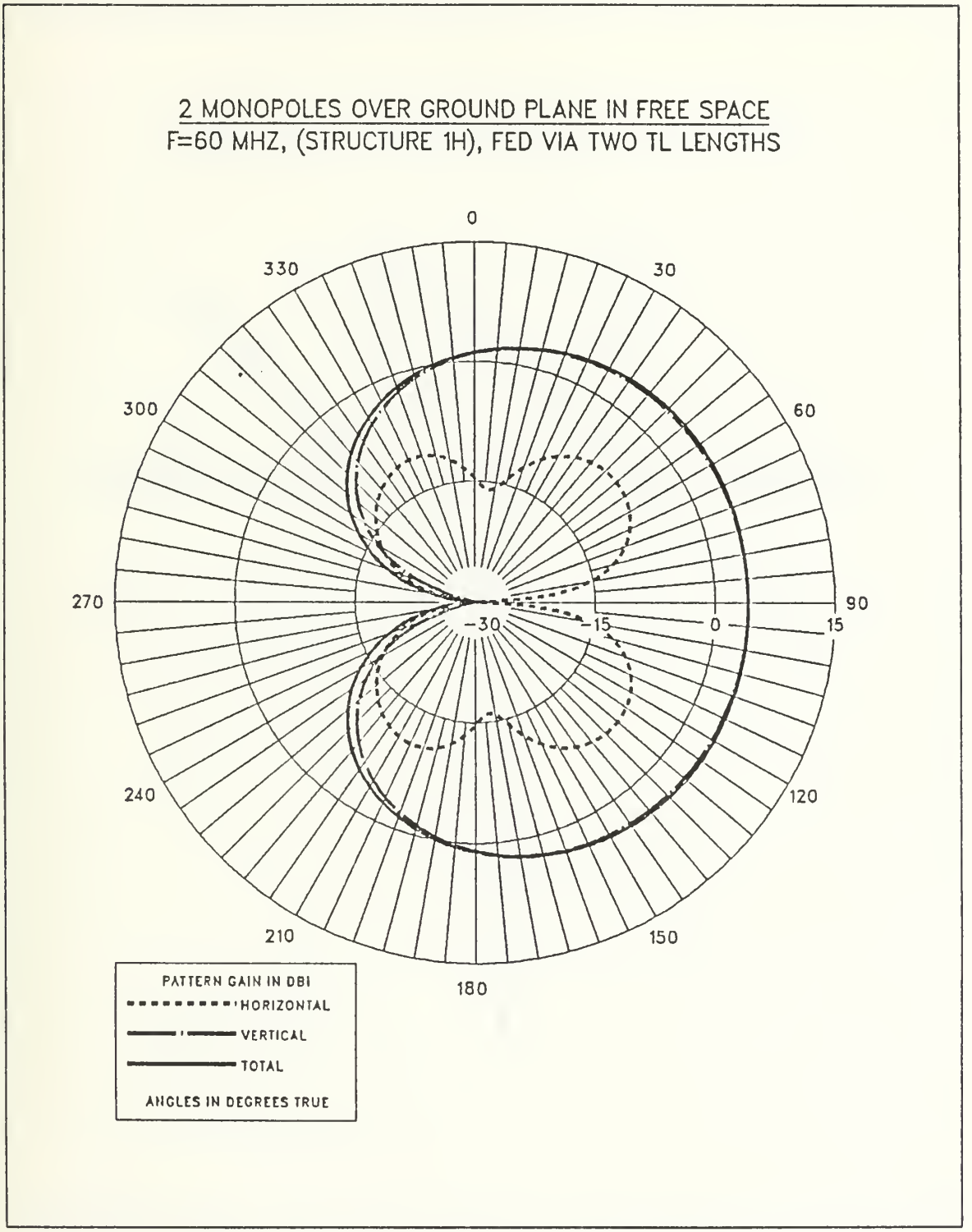

Figure 7. Initial Test Structure Radiation Pattern at Design Frequency

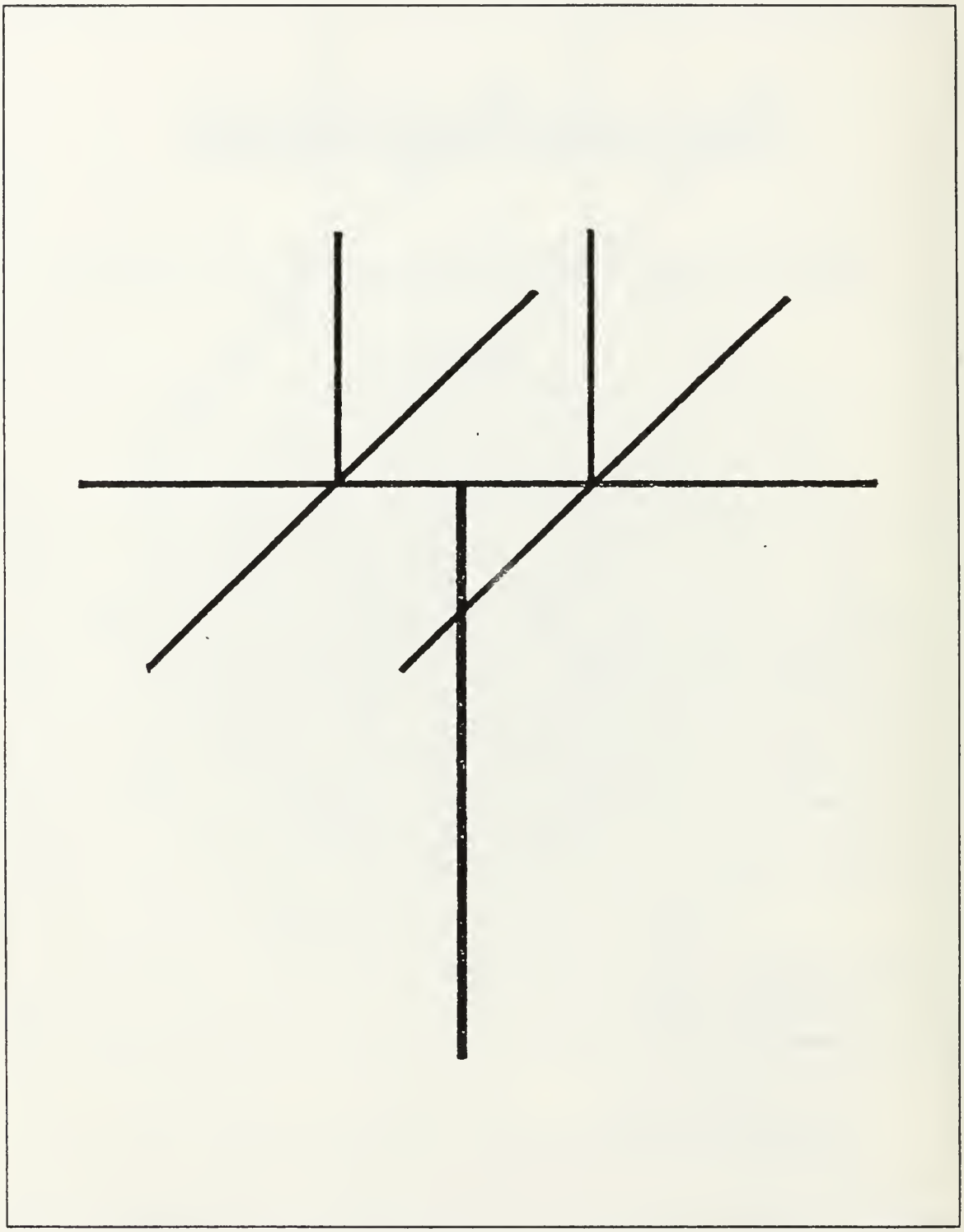

Figure 8. Test Structure Elevated by Metallic Mast

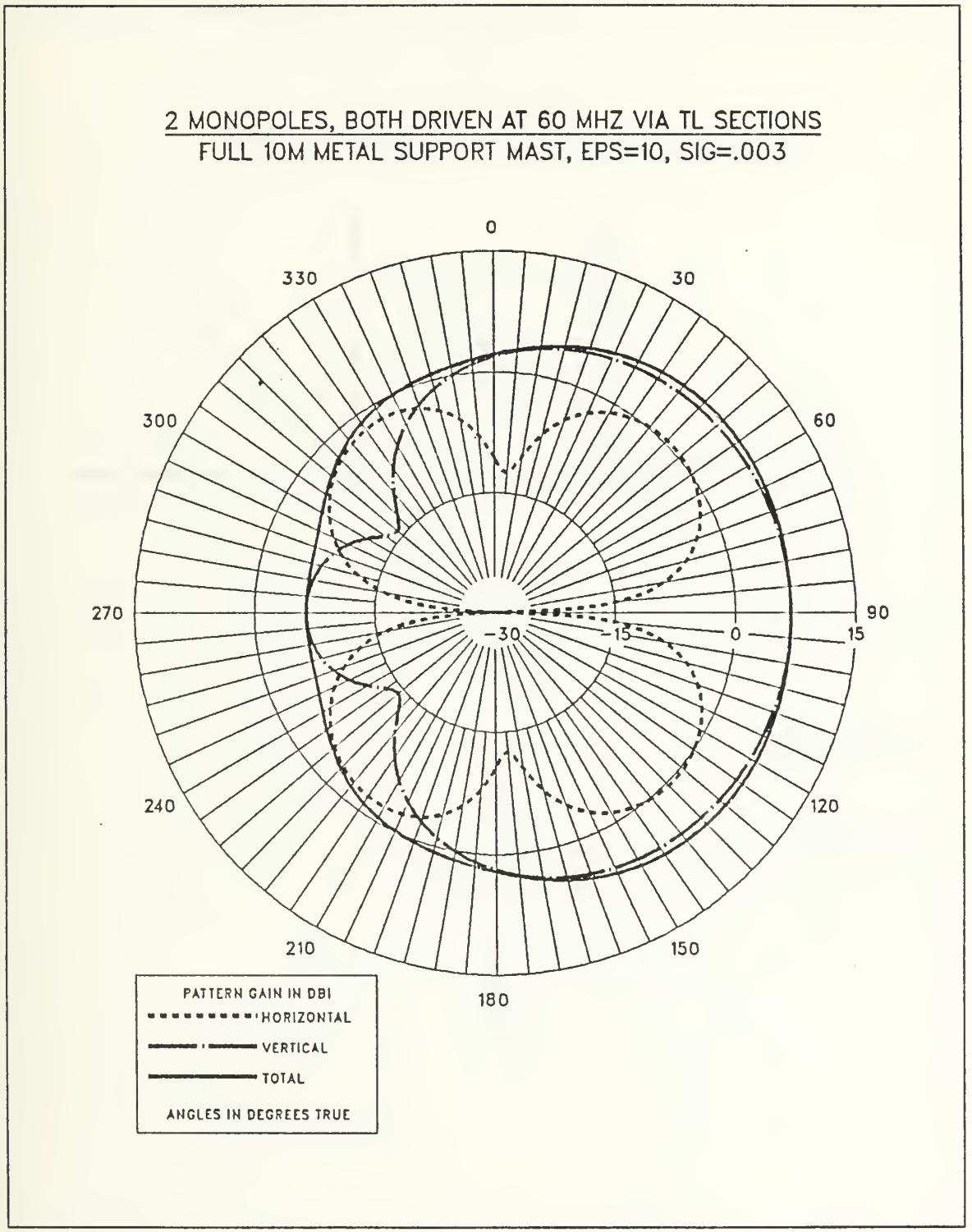

Figure 9. Radiation Pattern Distortion Caused by Metallic Mast

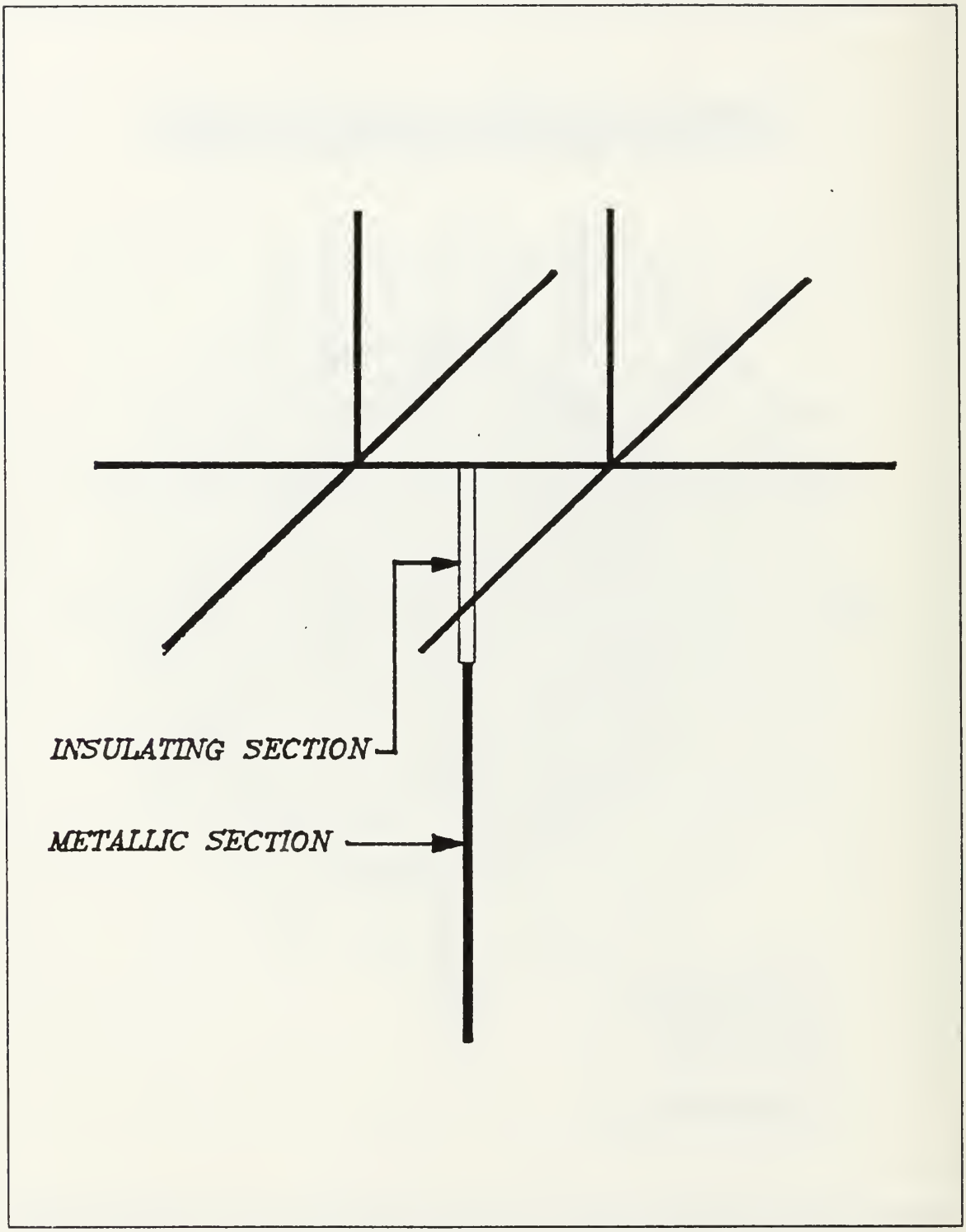

Figure 10. Insulating Section Inserted in Metallic Support Mast

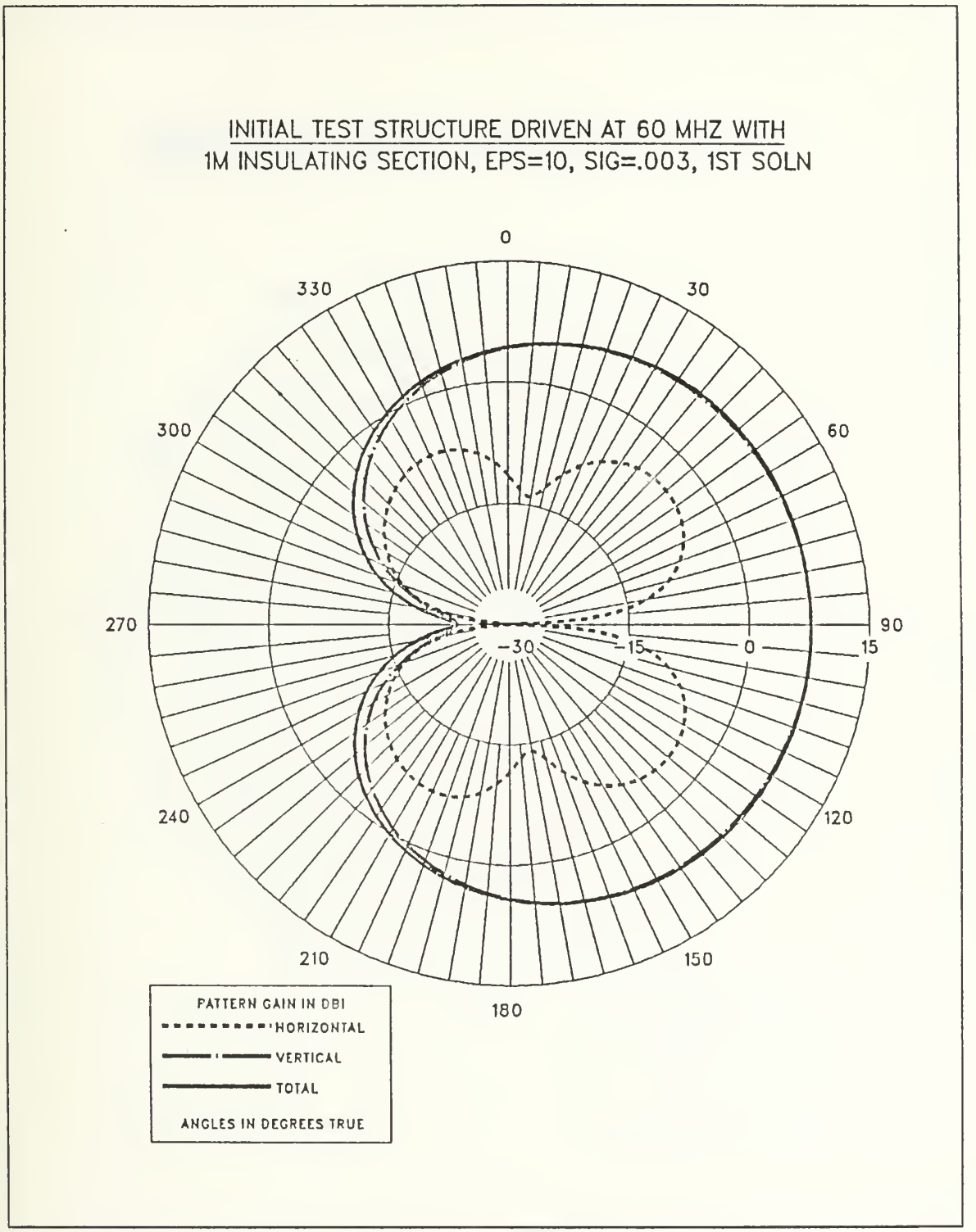

Figure 11. Radiation Pattern with Insulating Section Inserted

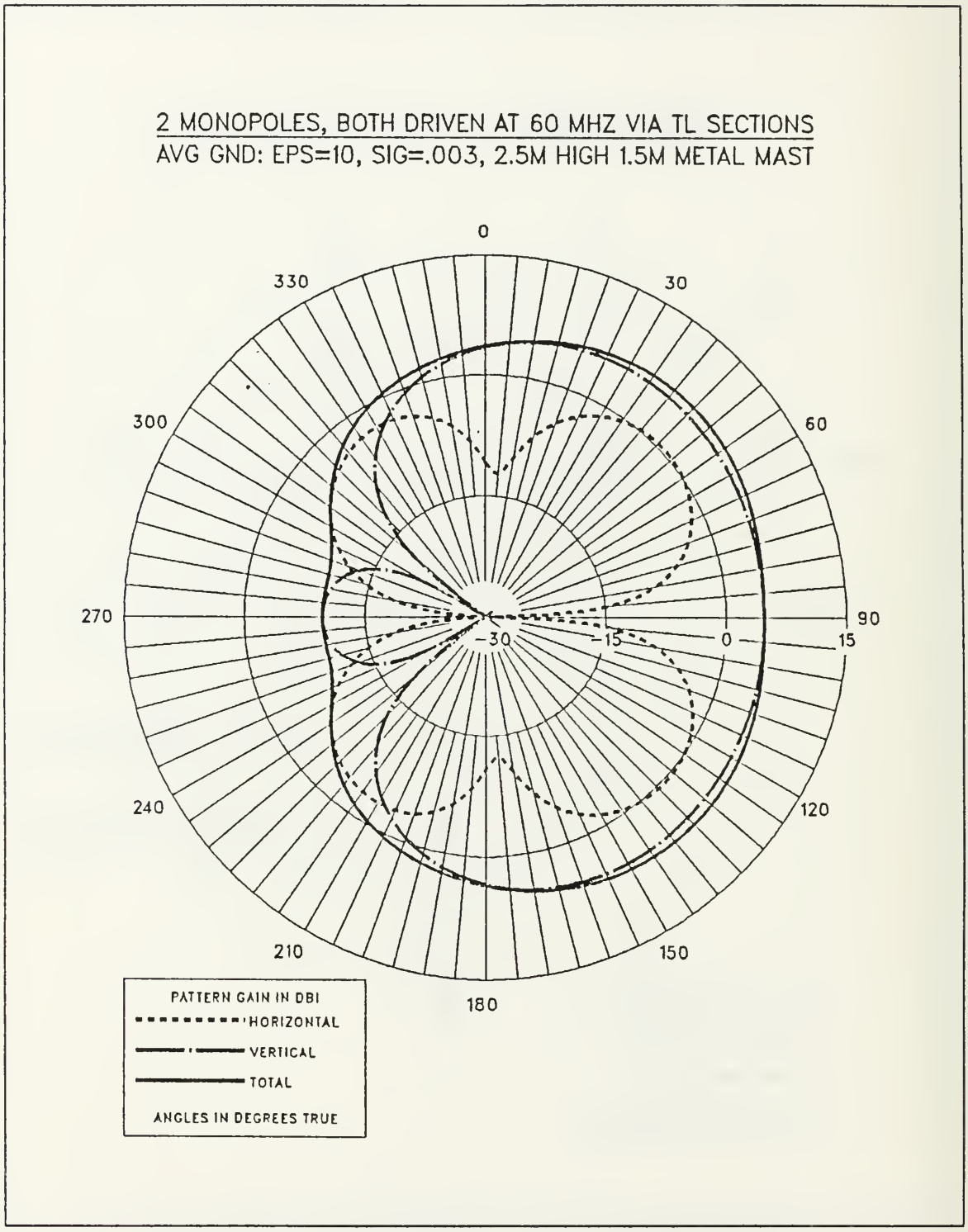

Figure 12. Radiation Pattern with Test Antenna 2.5 Meters Above Ground

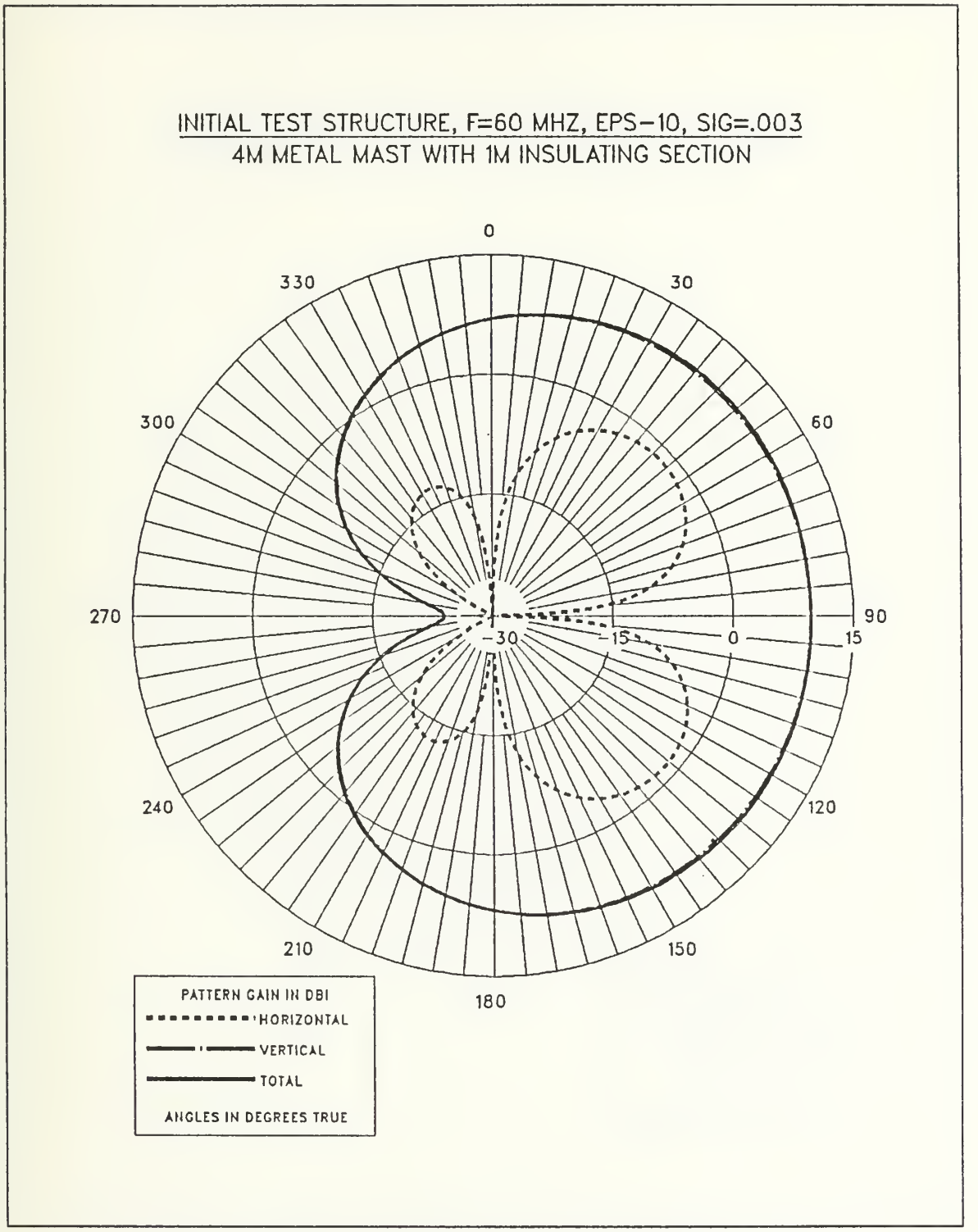

Figure 13. Radiation Pattern with Test Antenna 5 Meters Above Ground

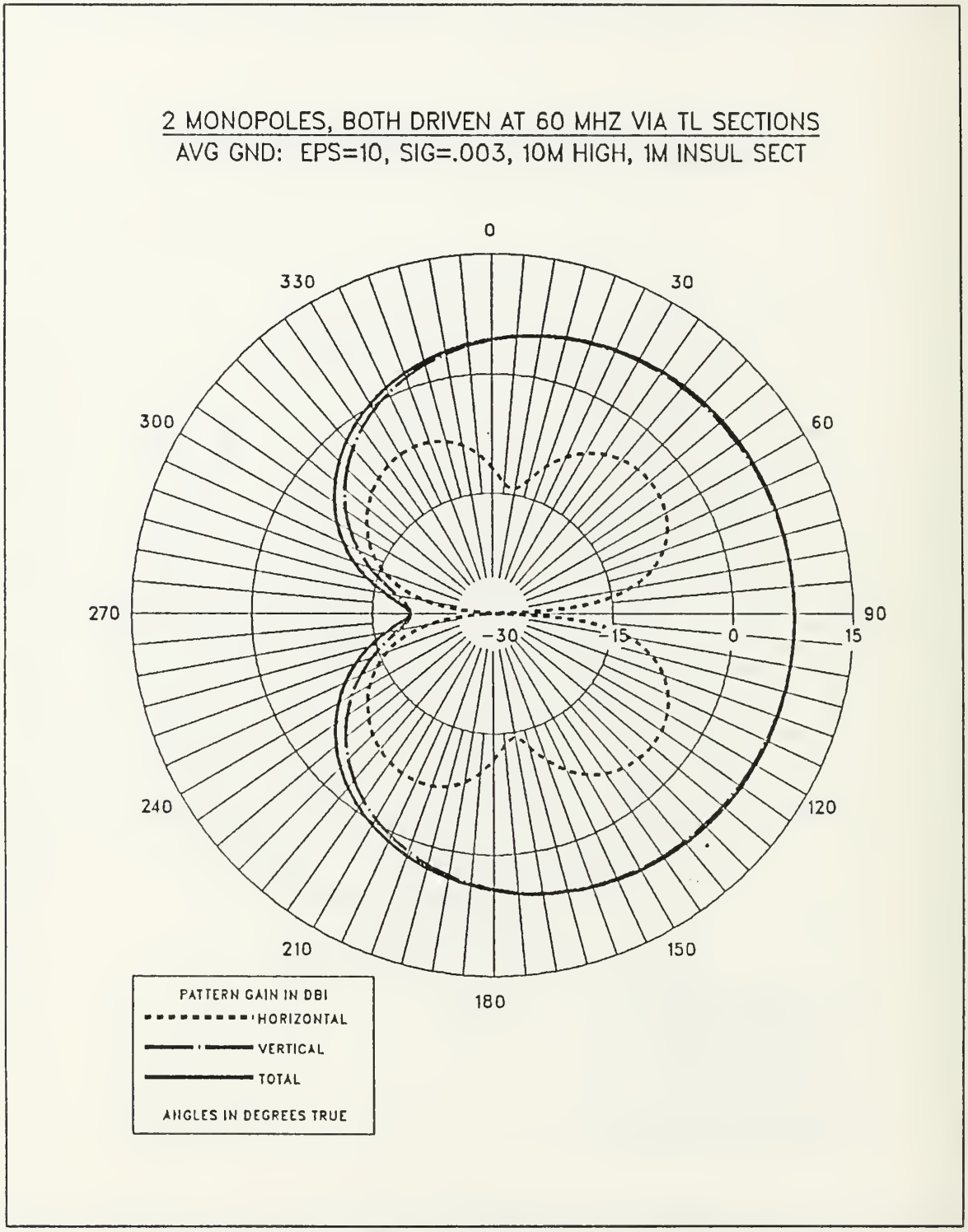

Figure 14. Radiation Pattern with Test Antenna 10 Meters Above Ground

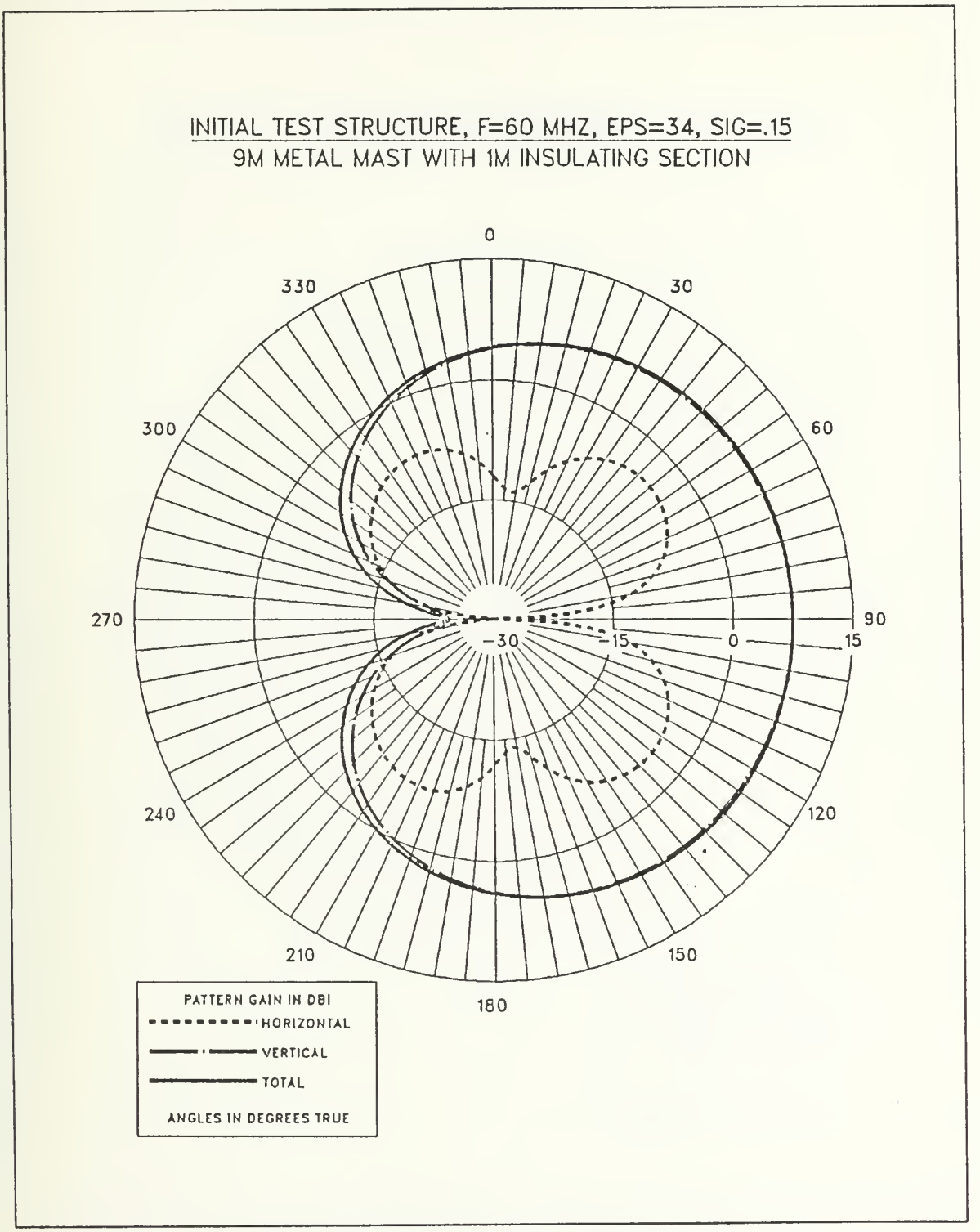

Figure 15. Pattern of Test Antenna Over Rice Paddy (Theta = 80 Degrees)

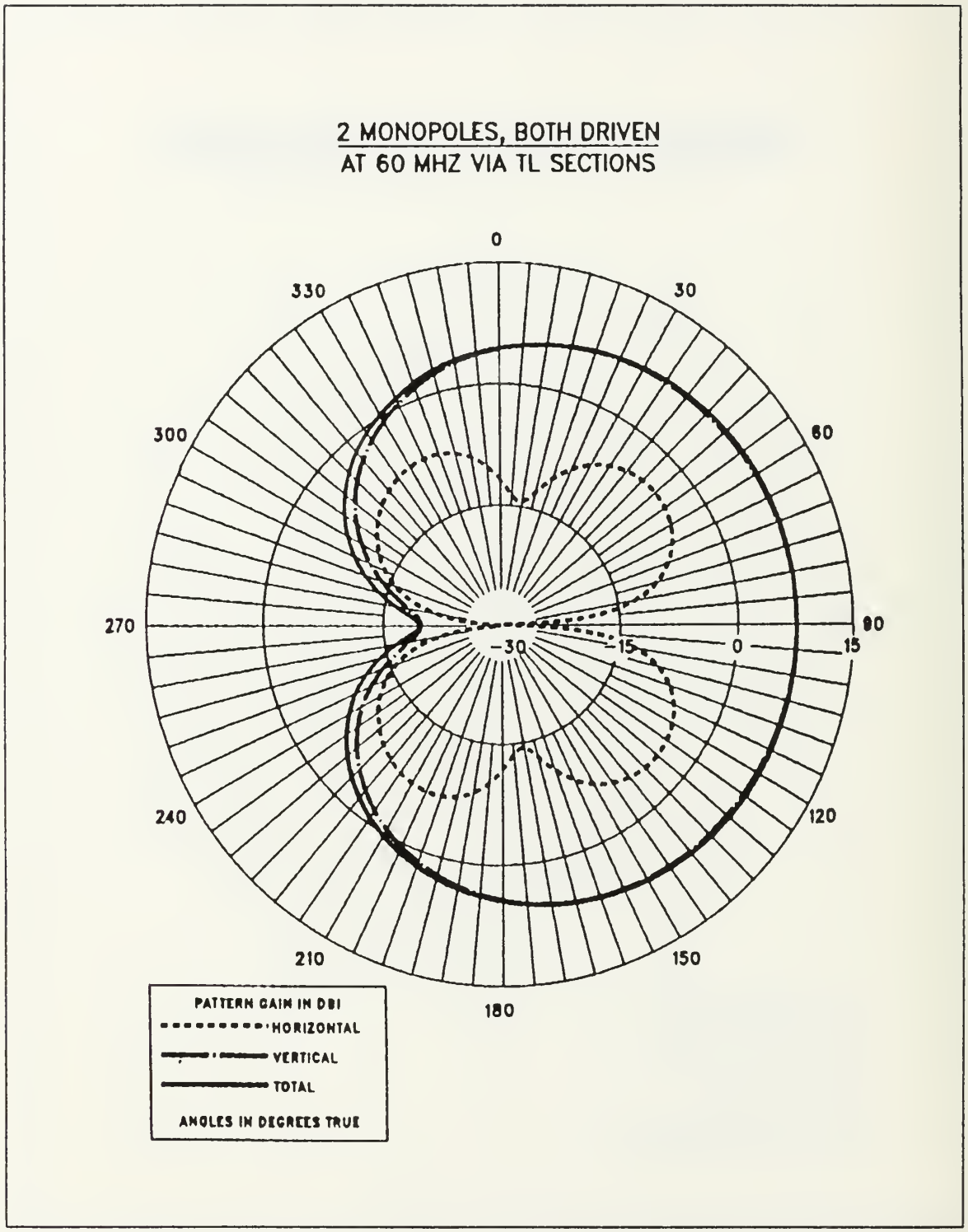

Figure 16. Pattern Over Average Ground (Theta = 80 Degrees)

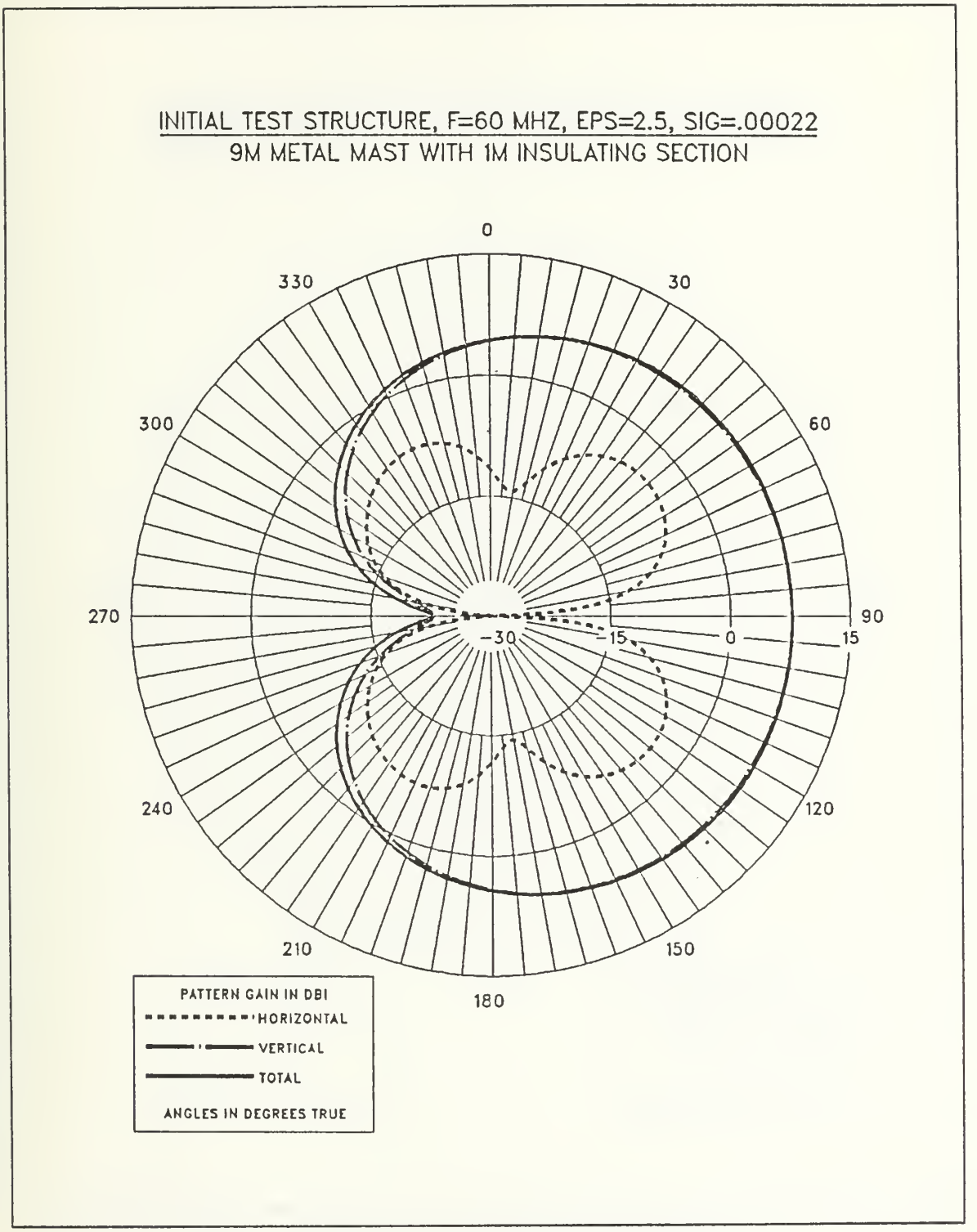

Figure 17. Pattern Over Poor Ground (Theta = 80 Degrees)

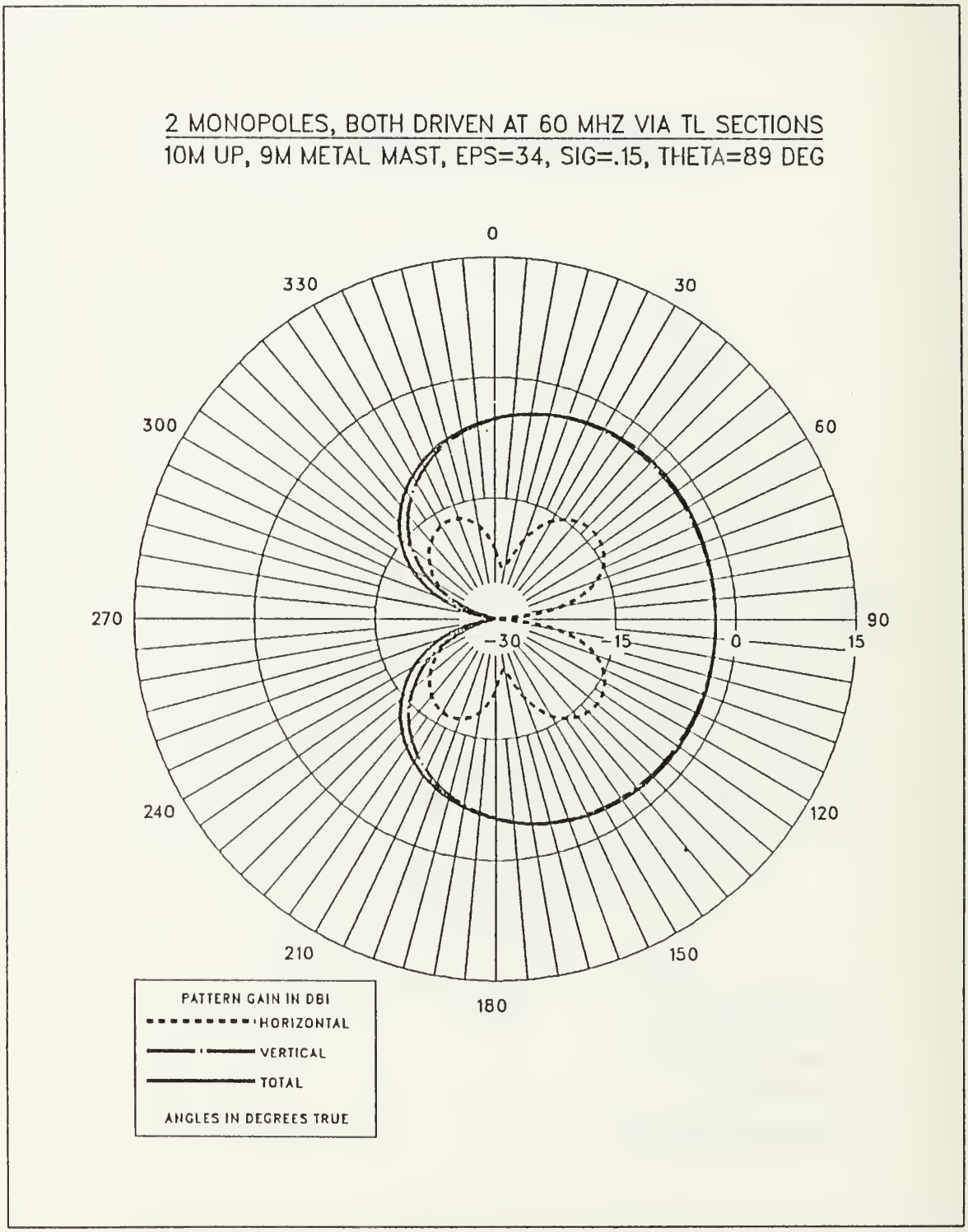

Figure 18. Pattern Over Rice Paddy (Theta = 89 Degrees)

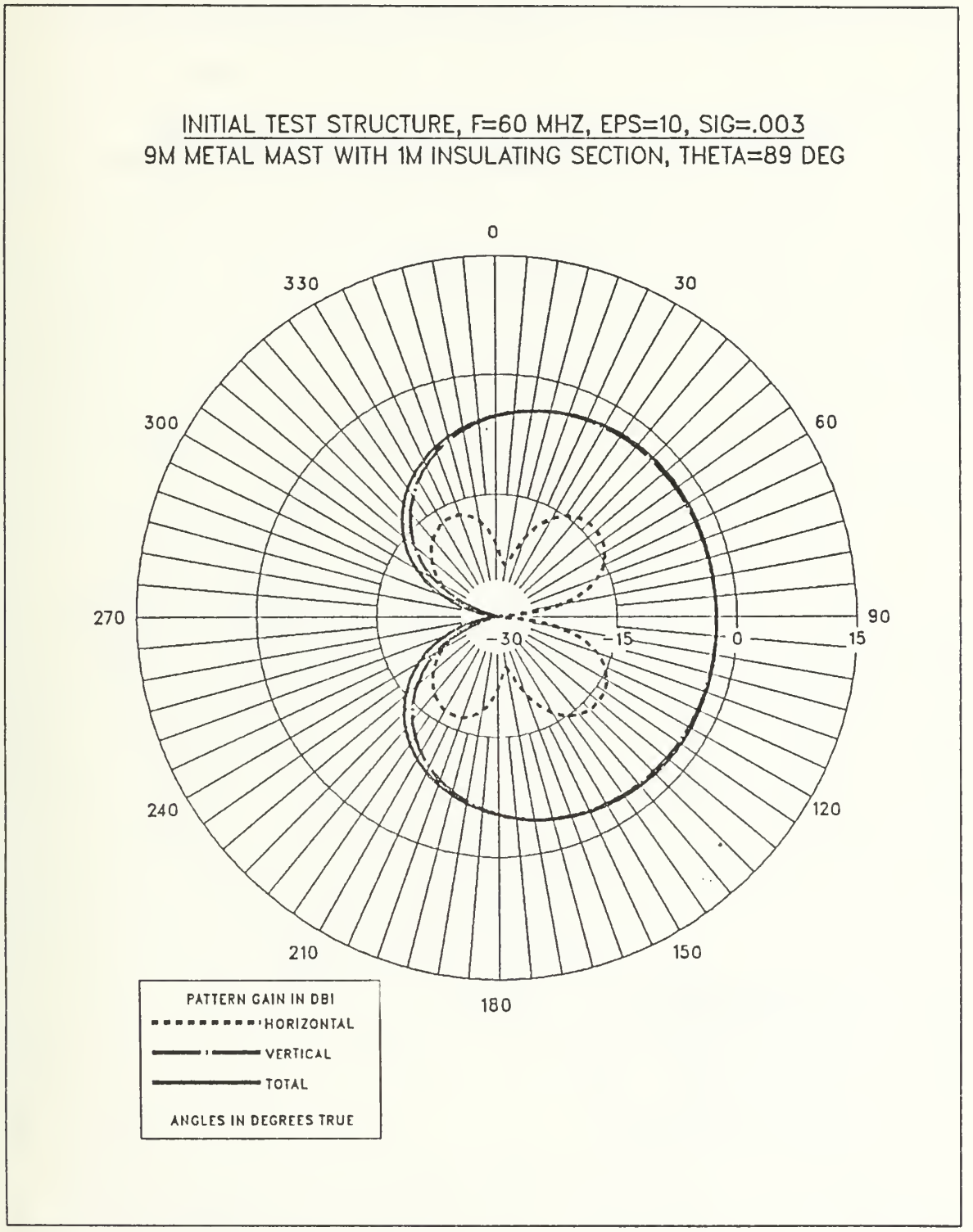

Figure 19. Pattern Over Average Ground (Theta = 89 Degrees)

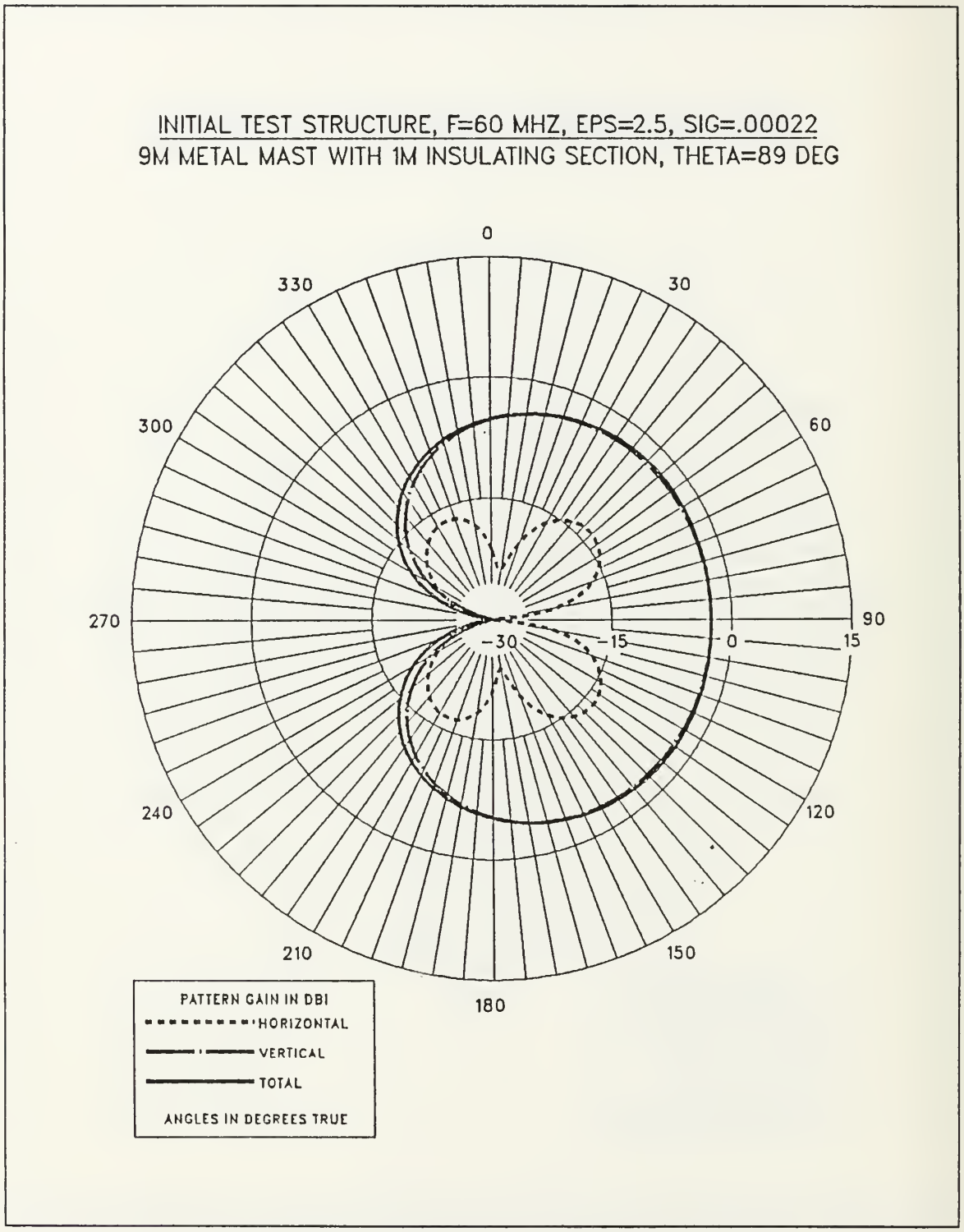

Figure 20. Pattern Over Poor Ground (Theta = 89 Degrees)

used are included in Appendix C. With each variation of the geometry, it was necessary to recompute the impedance matrix for the structure, in order to adjust the transmission line feed harness lengths. The conclusion drawn from this study was that while feedpoint impedances can indeed be varied by changing the angle of the ground plane radials with respect to the driven elements, deep null characteristics disappear as the ground plane elements are varied from a perpendicular orientation to the driven elements.

In order to investigate the effect of removing ground plane elements on the structure radiation pattern, elements were removed, characteristic impedances found, and excitations recalculated and applied to the modified structure. It was found through modeling that the ground radials on the ends of the structure could be removed while maintaining good deep null performance, yet simplifying the test structure. Figure 23 shows this configuration. Subsequent modeling revealed that this structure has deeper nulls in most cases than did the initial test structure. Subsequent work was therefore done using this structure vice that of the initial test structure.

G. EFFECTS OF SURFACE WAVES

In order to investigate the effects of surface waves on the radiation patterns produced by the test structure, the NEC dataset was modified to include surface wave effects. This required using the Sommerfeld ground option of NEC. Before running a simulation using this option, it is necessary to create a ground characteristics lookup table for use by NEC during calculation. The table is created by SOMNEC which uses a data card containing the frequency, dielectric constant, and conductivity values characteristic of the ground over which the simulation is to be done. The NEC input dataset and SOMNEC data card used are included in Appendix D.

The results of the surface wave-included study were surprising in that the nulls predicted were deeper than those obtained over similar ground without surface wave effects included. This result offers the hope that very deep nulls may be encountered during field testing of a prototype antenna.

The effects of varying the test structure height above ground were quite noticeable, as can be seen from comparing Figures 21 and 22. While from a visual standpoint the difference is obvious, from the standpoint of a practical system, the case of Figure 22 represents a null of over 20 dB, which is still useful in practice.

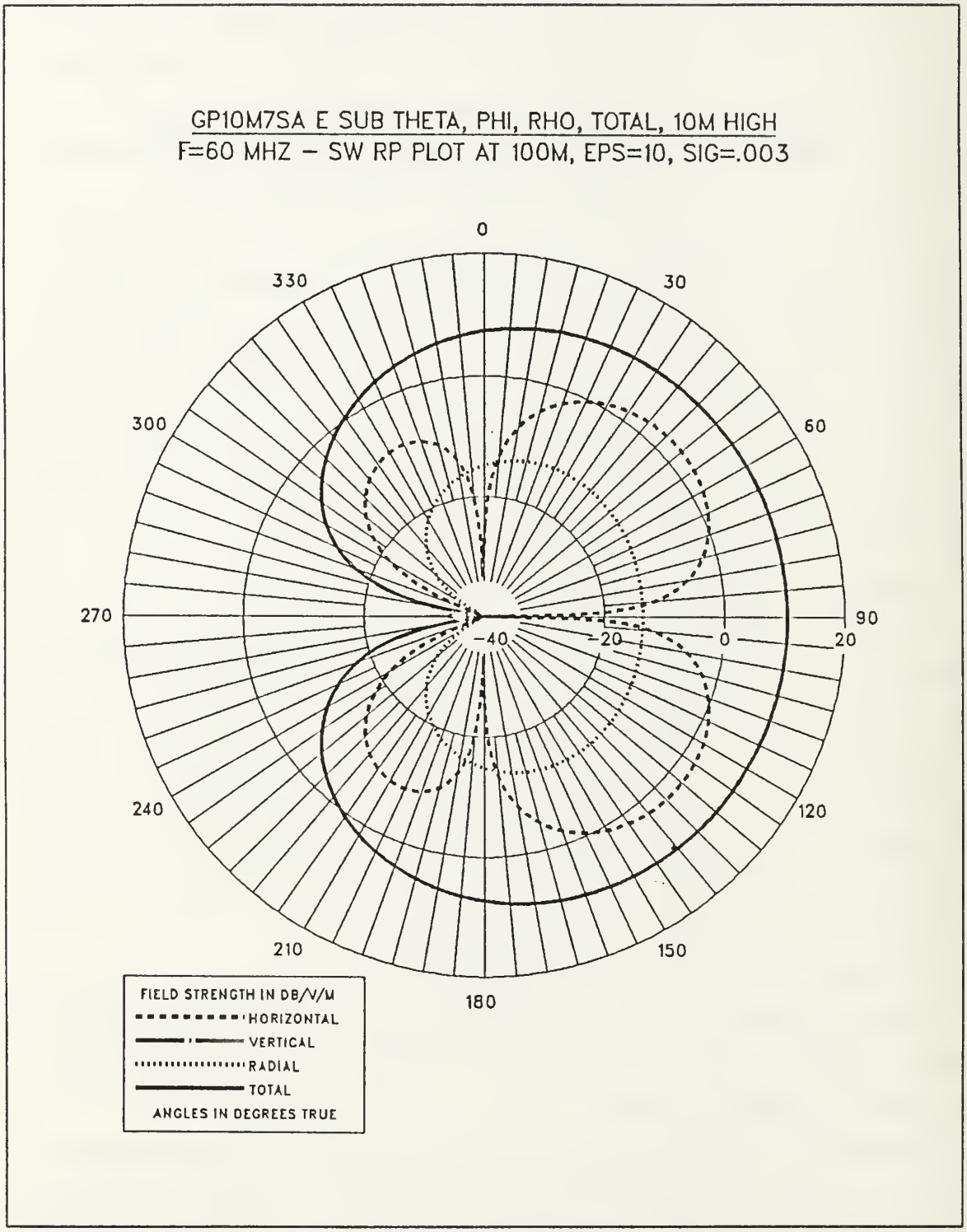

Figure 21. Surface Wave Included, F = 60 MHz, H = 10 M, Average Ground

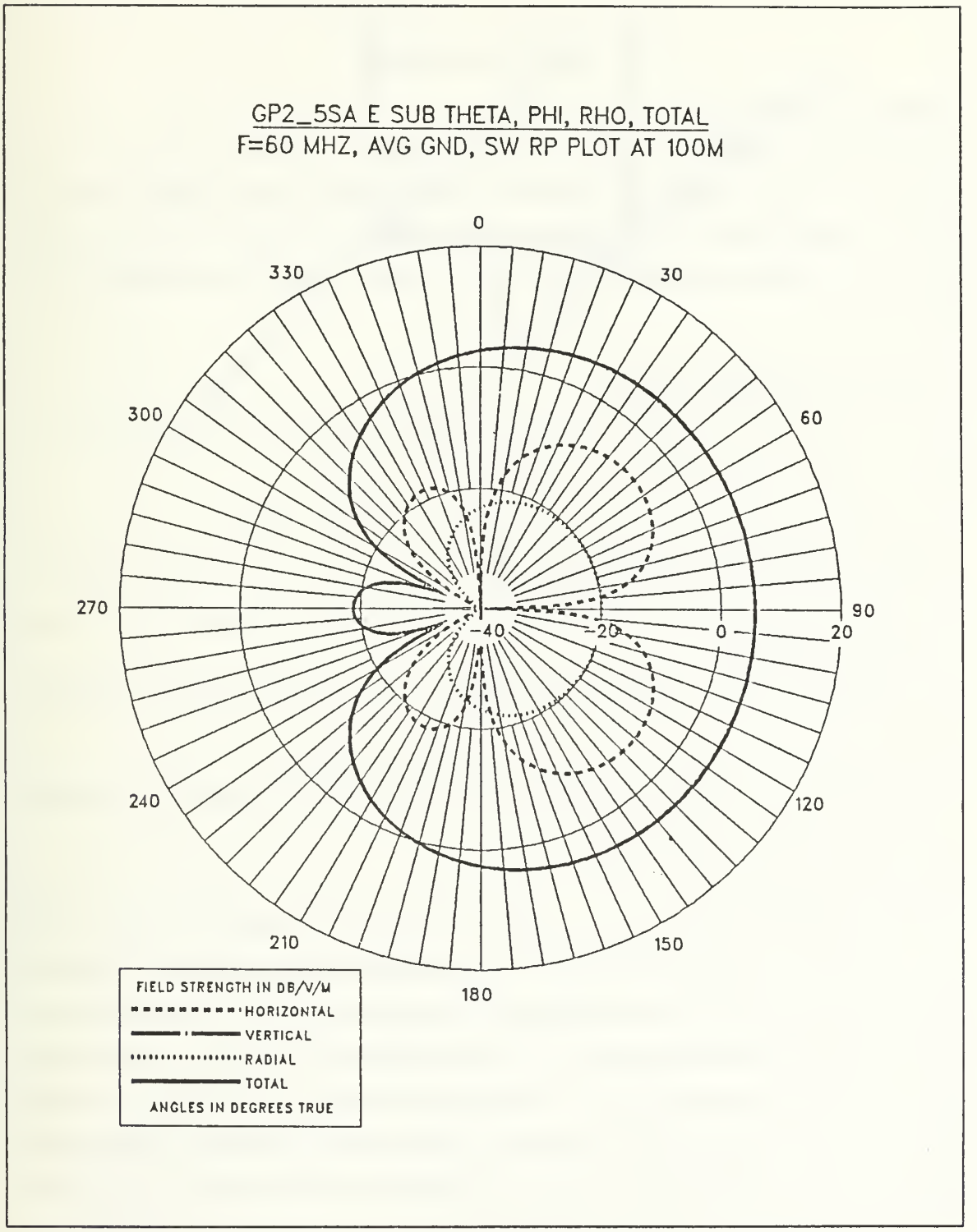

Figure 22. Surface Wave Included, F = 60 MHz, H = 2.5 M, Average Ground

IV. ANTENNA DESIGN

A. BASIS FOR DESIGN

The work presented to this point is based on computer simulation of various structures under varying conditions and explores certain structures that are likely candidates for further development. The structure geometry shown in Figure 23 was chosen for construction and further evaluation because of its relative simplicity and predicted null characteristics.

B. DESIGN CONSIDERATIONS

In order to keep the mechanical work of constructing the prototype antenna to a minimum, the following assumptions and decisions were made:

- A frequency of 60 MHz is used as the design operating frequency
- Half inch copper pipe is used for antenna elements due to its low cost, availability, and availability of fittings at nominal cost
- Belden 8219 type coaxial cable is used for the matching harnesses due to its low cost and availability
- An aluminum mast kit with two inch diameter and including a three foot dielectric section is used to elevate the prototype antenna as necessary
- Insulating plates are used to support the radiating elements
- UHF type coaxial connectors are used in building the prototype due to ease of assembly, availability and low cost

C. PROTOTYPE DESIGN

Having defined the essential characteristics of the prototype deep null antenna, the structure detailed by Figures 23 through 27 was constructed, keeping elements as close to a quarter wavelength at the 60 MHz design frequency as possible. A feed harness for 60 MHz was also constructed. Since the "Tee" connector at the junction of the two transmission line sections and the wire from the connectors at the antenna bases added about 3.5 cm to the length, that amount was subtracted from the length of each cable. The velocity factor of Belden 8219 cable is 0.78, and was also included in calculating physical feedline lengths for the 60 MHz feed harness.

In order to facilitate transporting the prototype antenna, hose clamps were used to hold elements in place, rather than solder. A wooden mounting bracket was made to

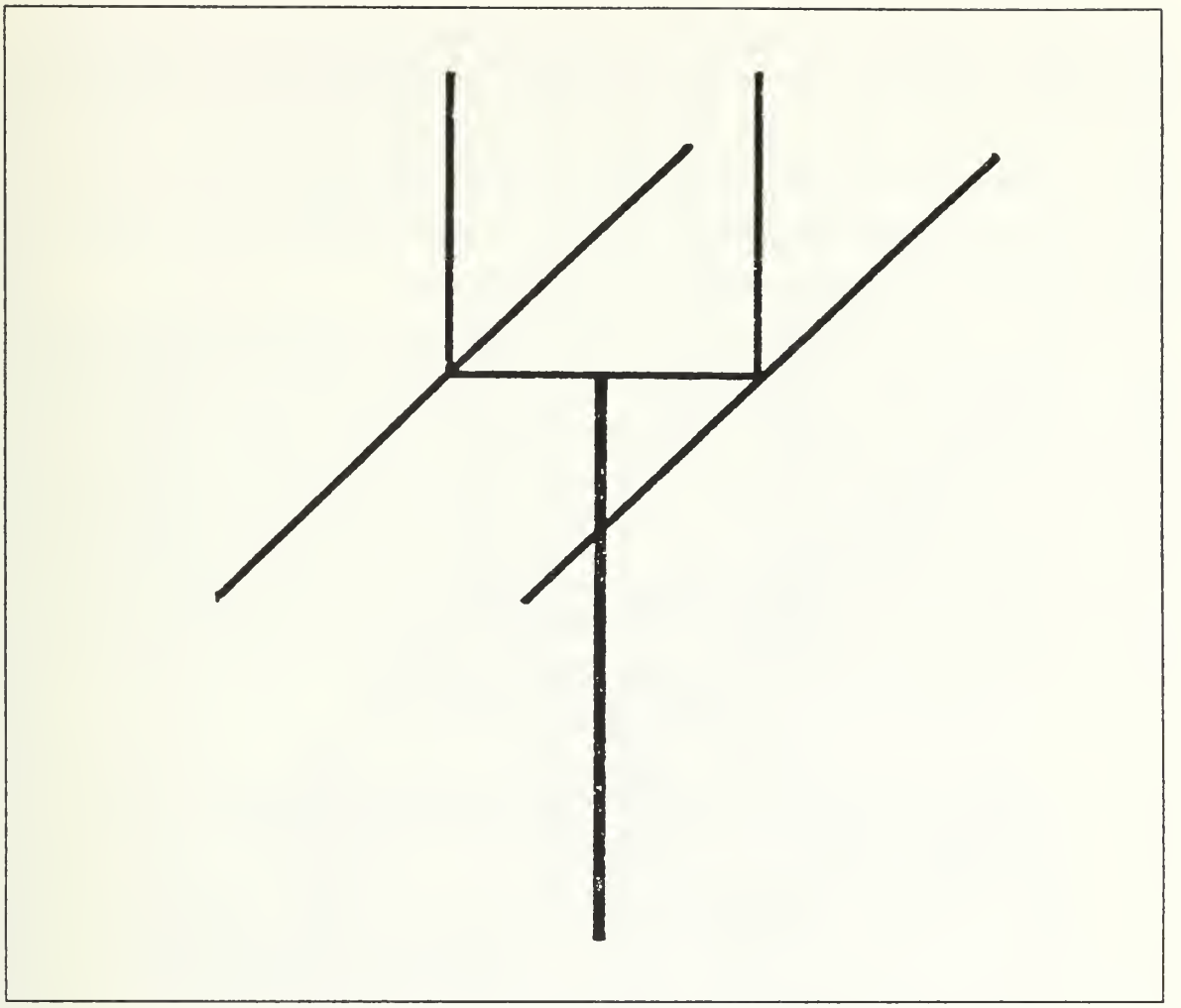

Figure 23. Structure Geometry of Prototype Deep Null Antenna

allow connection to the support structure, and an azimuth indicator was made for attachment to the support mast during field testing.

D. FEED HARNESS VARIATIONS

In order to get more usable bandwidth from the prototype antenna a way of maintaining the proper current relationships in the two driven elements at frequencies other than the structure design frequency was needed. It was noted that, as the frequency of excitation varies from the structure design frequency, the spacing between the driven elements departs from the ideal 90 electrical degrees. This effect can be compensated by varying the phase angle between excitation currents when calculating feed harness lengths using Christman's feed method. Minor adjustments to the current magnitude

ratio resulted in feed harness lengths that produced clean cardioidal deep null patterns when modeled using NEC. It was noted during this iterative process that the first solution from the feed harness length calculation program [Ref. 7] produced feed harness lengths that provided clean patterns, while the second solution from the program did not produce the desired deep null patterns. Due to the need to keep this work within a manageable scope, the cause of this effect was not pursued.

In order to test the validity of results obtained from NEC modeling, three feed harnesses were constructed for field testing. The 60 MHz harness length was obtained by direct application of Christman's feed method [Ref. 7], taking into account a 0.78 transmission line velocity factor and a 3.5 cm correction for the length of connectors and wires in the prototype antenna structure. The 55 and 66 MHz harness lengths were obtained by applying the compensation method described above, again using a 0.78 velocity factor and a 3.5 cm correction for connector and wire lengths. The results of these calculations and adjustments are summarized in Table 4 below.

Table 4. FEED HARNESS PHYSICAL LENGTHS

Harness Design Frequency (MHz)	L1 Length (Meters)	L2 Length (Meters)
55	0.715	2.578
60	1.577	1.859
66	1.459	2.795

E. ANTENNA TESTING

The objective of this phase of the study was to see if the results predicted through computer modeling agree with measurements. To check the predicted results, it was necessary to measure the far field radiation pattern and the input impedance of the prototype structure over a range of frequencies. In order to evaluate potential usefulness of this class of antennas for reduction of either mutual interference due to nearby transmitters on adjacent frequencies or reduction of jamming from a transmitter some distance away, two cases were tested, one where the prototype antenna's far field pattern was measured 100 meters away, and a second case where the antenna's pattern was measured 1000 meters away. Test data is then compared with predictions and conclusions drawn.

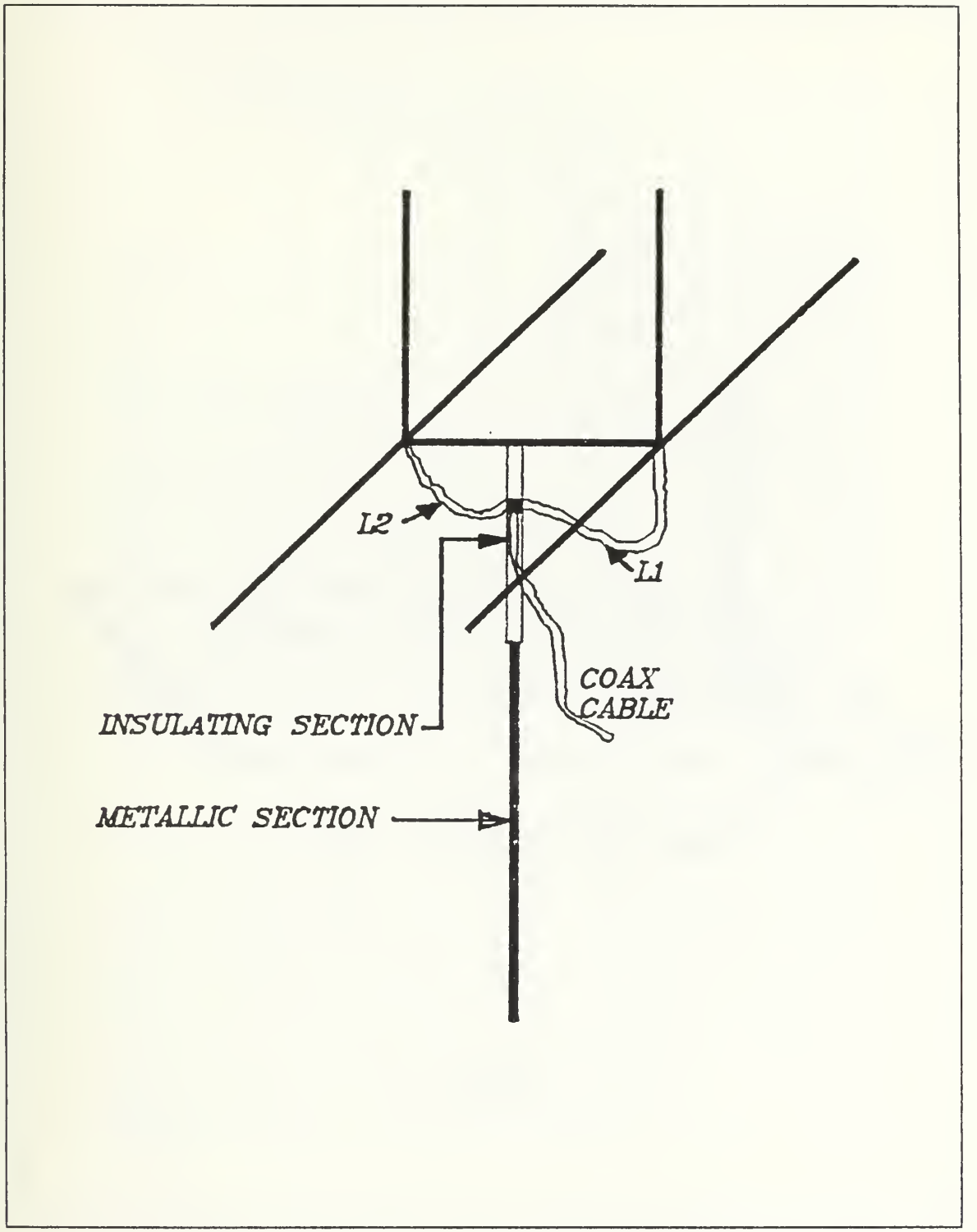

Figure 24. Prototype Antenna Details, Construction

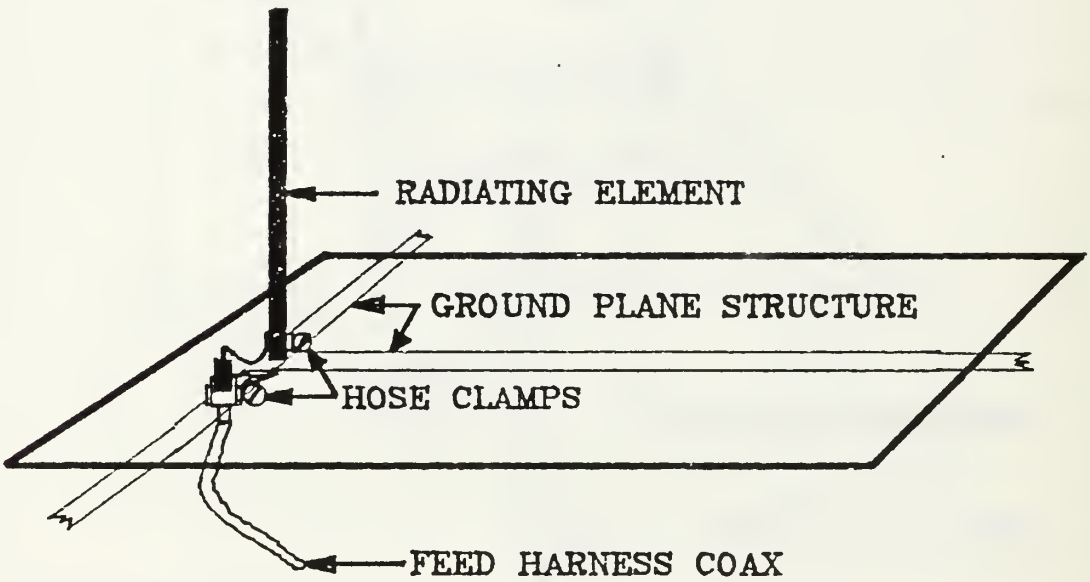

Figure 25. Feedpoint Details

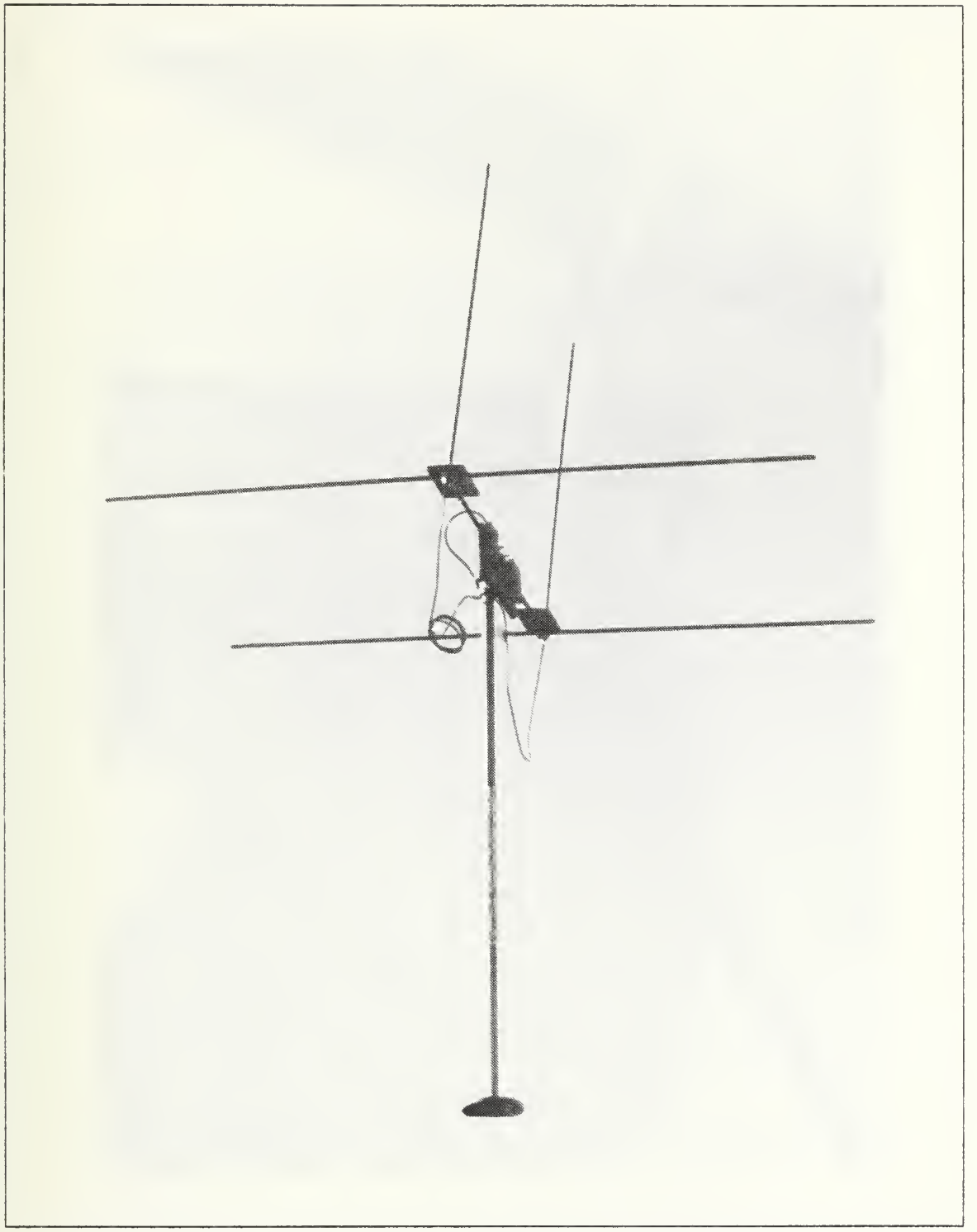

Figure 26. Photograph, Completed Prototype Deep Null Antenna

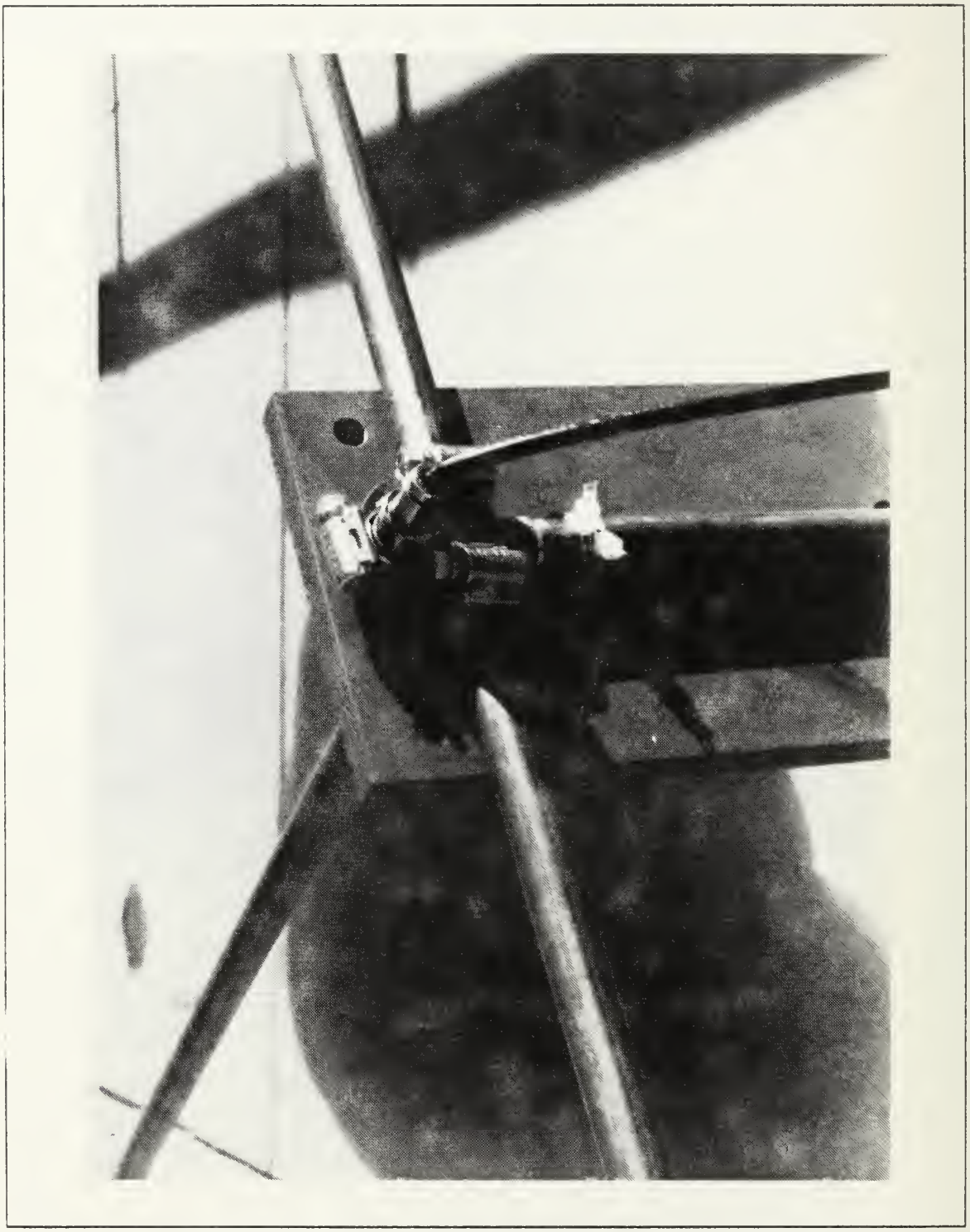

Figure 27. Photograph, Prototype Antenna Feedpoint Details

F. TEST SETUP

The setup to be used in the two tests is shown graphically in Figures 28 and 29. Volunteer assistants rotated the prototype antenna and collected data as necessary. A hilltop site was chosen to avoid reflections off nearby objects, and a line of sight path to the 1000 meter reception site was identified. The ground at the test site was moist sandy soil.

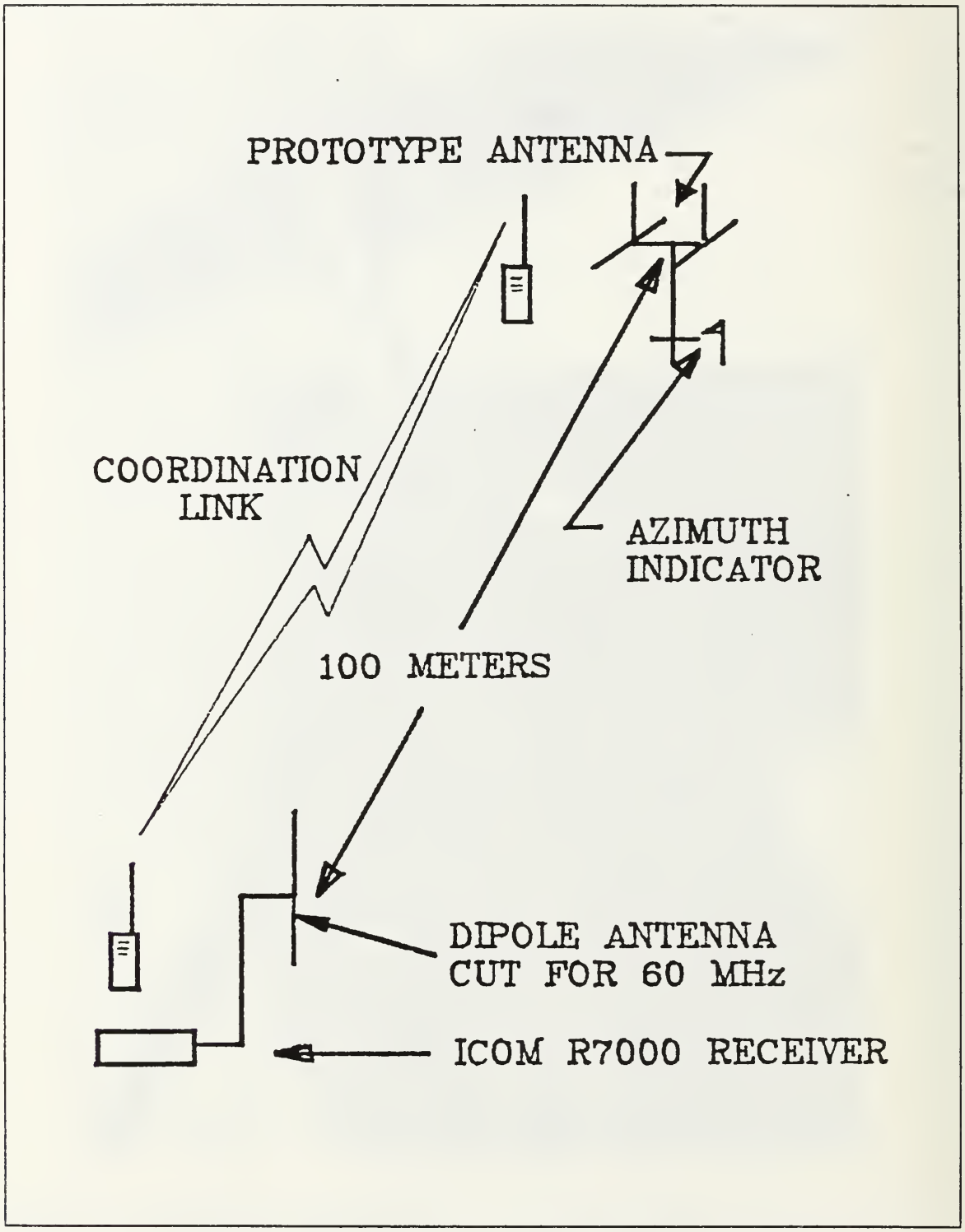

Figure 28. Test Setup for Measuring Radiation Pattern at 100 Meters

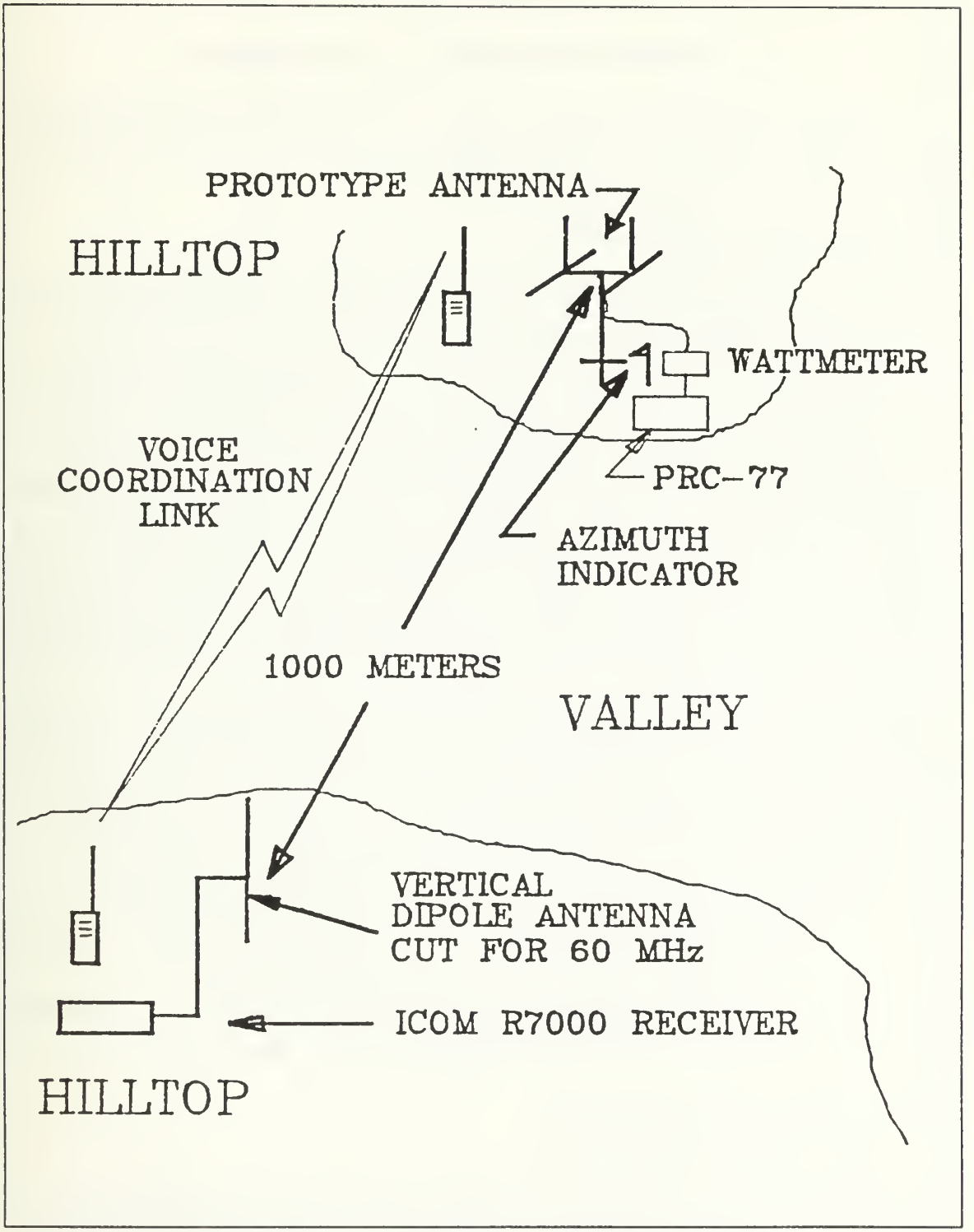

Figure 29. Test Setup for Measuring Radiation Pattern at 1000 Meters

V. PROTOTYPE ANTENNA EVALUATION

Testing of the prototype deep null antenna was conducted both in the laboratory and in the field as outlined in the previous chapter. Field tests were done to include the effects of real ground in the evaluation.

A. LABORATORY TESTS

Prior to conducting field tests of the prototype antenna, it was considered as prudent to conduct some preliminary tests under controlled conditions to see if the structure and feed scheme worked as predicted. This test was accomplished by raising the prototype antenna on a mast (with an insulating section), exciting a vertical monopole about 80 meters away with a signal generator, and using a receiver and rotator-turntable arrangement to produce a logarithmic polar plot of the received signal strength versus azimuth. Figures 30, 31 and 32 show the results of this test. It was discovered during the course of this test that the prototype antenna's actual resonant frequency was 59.25 MHz vice the 60.00 MHz design frequency. This 1.25% departure from the design frequency was viewed as minor, and the structure was not modified to correct this due to test schedule considerations.

From Figures 30-32 it is evident that the deep null performance of the structure is relatively narrowband, and that it deteriorates rather quickly as the frequency of excitation departs from the actual resonant frequency of the structure. During this sequence of tests it was noted that tuning in a television sound carrier at 59.75 MHz and then running a signal strength plot produced patterns that were neither cardioidal nor deep null. Since this signal was circularly polarized, the performance of the prototype deep null antenna on signals other than vertical linear polarization is suspect. Tactical VHF radio systems nearly always use vertical linear polarization, however, so the prototype antenna's response to other types of polarization was not of immediate concern.

B. FIELD TESTING PROCEDURE

1. Field Test at 100 Meter Range

The next stage of the testing procedure was to set up the prototype antenna in the field, excite it with an AN/PRC-77 tactical VHF FM radio set, and measure the signal strength at a range of 100 meters. The test antenna was then rotated and another measurement taken. This process was repeated at regular increments of azimuth until

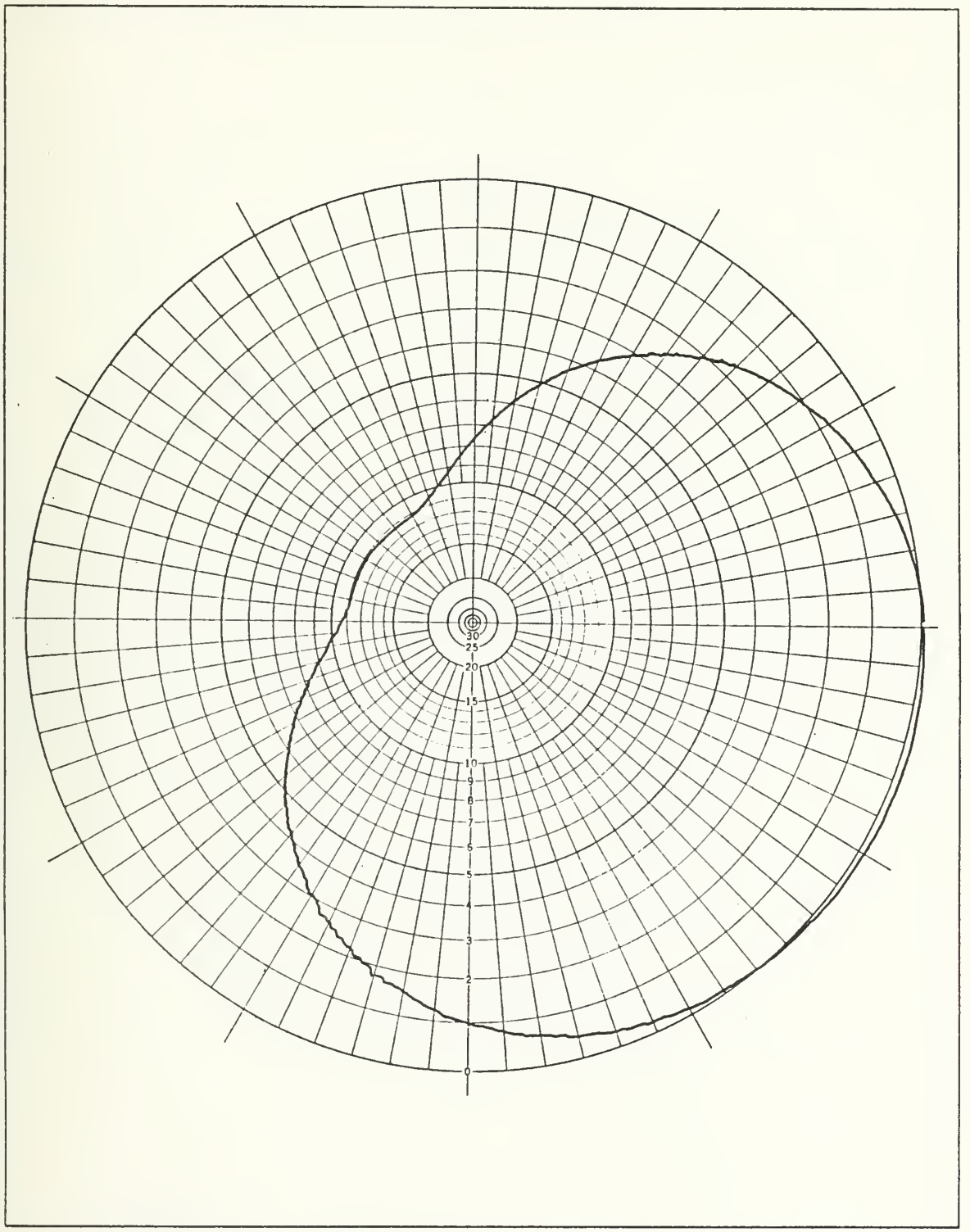

Figure 30. Laboratory Plot, F = 60.00 MHz, 60 MHz Feed Harness

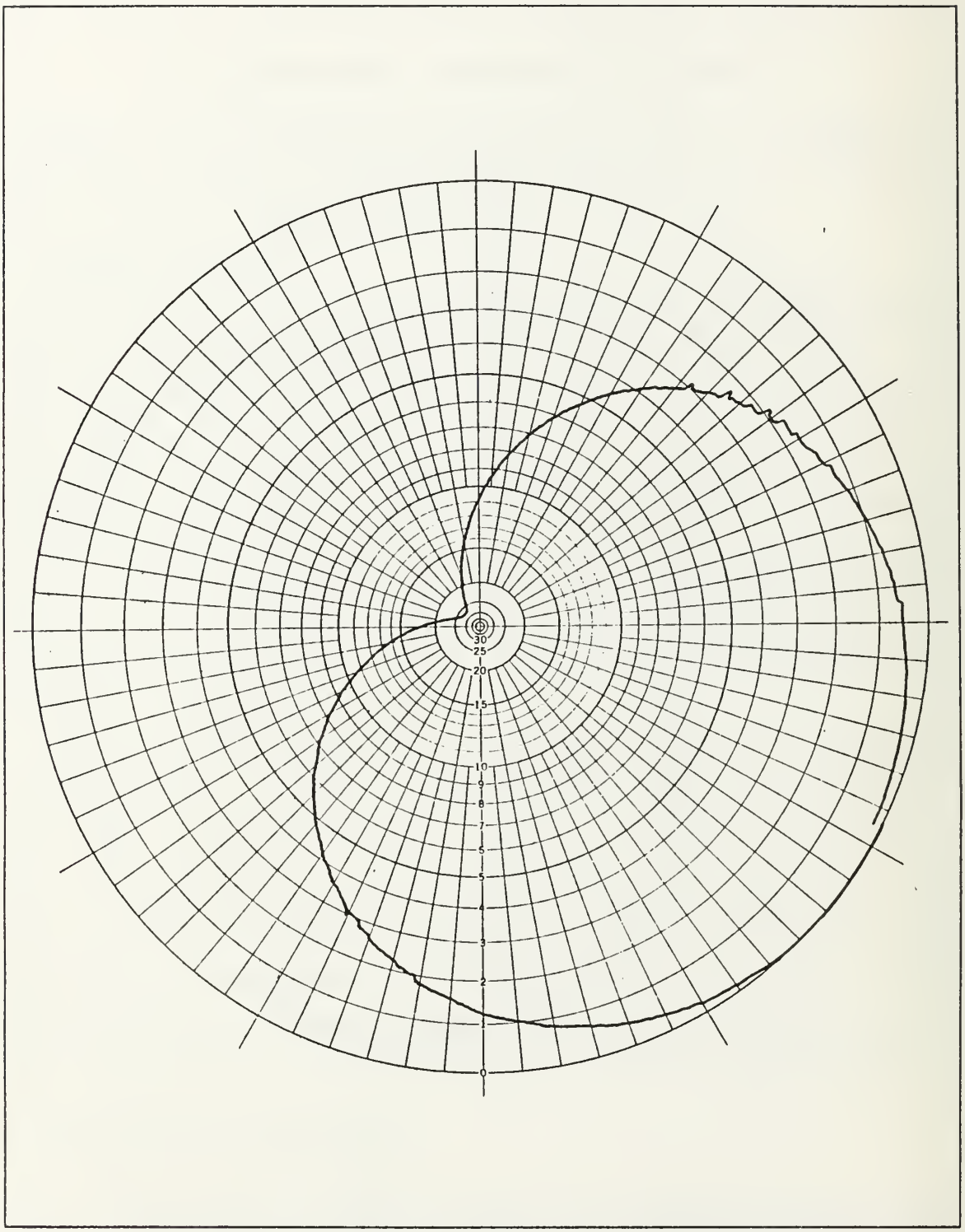

Figure 31. Laboratory Plot, F = 59.50 MHz, 60 MHz Feed Harness

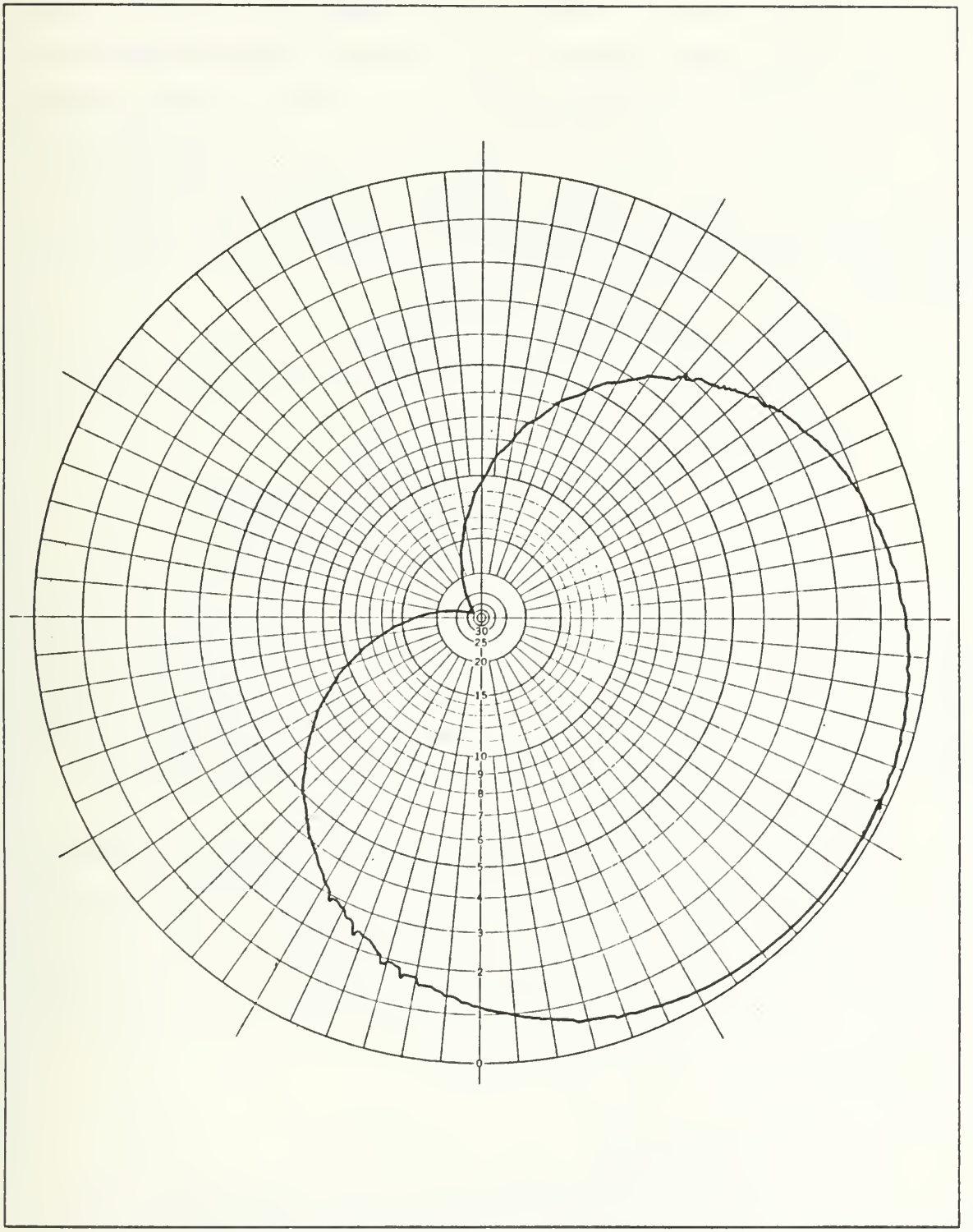

Figure 32. Laboratory Plot, F = 59.25 MHz, 60 MHz Feed Harness

sufficient data to construct a polar plot of the antenna radiation pattern was obtained. Signal strength readings were taken from the S-meter of an ICOM-R7000 receiver, and recorded on data collection forms. Additional passes through nulls were made as necessary to get accurate strength readings at the null azimuths. Since the characteristics of the receiver S-meter were not known, the receiver was connected to a signal generator, and input signal strength versus S-meter reading data was taken. This allowed all signal strength readings to be translated into microvolts, and the microvolt readings of signal strength at many azimuths were obtained. In order to plot these readings on polar logarithmic graph paper the voltage ratios had to be converted to decibels using the relationship:

$$dB = 20 \log \frac{V_2}{V_1} \tag{1}$$

where: V_2 = Reading for azimuth being plotted
V_1 = Maximum reading for any azimuth

The initial test run was done using the 60 MHz feed harness in order to make an early comparison with laboratory results. In order to test the validity of the feed harness compensation method outlined earlier, the test structure was next excited using the 55 and 66 MHz harnesses. Signal strength measurements were made for various frequencies while again varying the azimuth to the receiving antenna in increments.

2. Tests at 1000 Meter Range

In order to test the prototype antenna's potential usefulness in eliminating signals from jammers located in enemy controlled areas, the receiving setup was relocated to a hilltop about 1000 meters away, and another series of tests made. Since radiation pattern data and bandwidth measurements were made in detail at 100 meters, frequencies were chosen at which good null performance was expected. Feed harnesses for 55, 60, and 66 MHz were used, and data taken.

C. TEST RESULTS

1. Results at 100 Meter Range

In each of the cases tested radiation patterns with substantial nulls were obtained as shown by Figures 33, 34 and 35. The results obtained during this sequence of tests are in general agreement with the predictions obtained using NEC, and they show

that the predicted deep null behavior can be obtained in practical structures. Furthermore, the test sequence demonstrated the behavior of the structure and feed harness at frequencies above and below the structure and feed harness design frequencies. While the figures shown above are indicative of the results obtained, additional test data is included in Appendix C.

2. Results of Tests at 1000 Meter Range

Figures 36-38 show the prototype antenna's deep null characteristics at 1000 meters, and are in good agreement with plots taken at the 100 meter range. Since the radiation patterns obtained agree with those obtained for the same configuration at 100 meters, testing at close range can be done with some confidence that similar results would be obtained at greater distances.

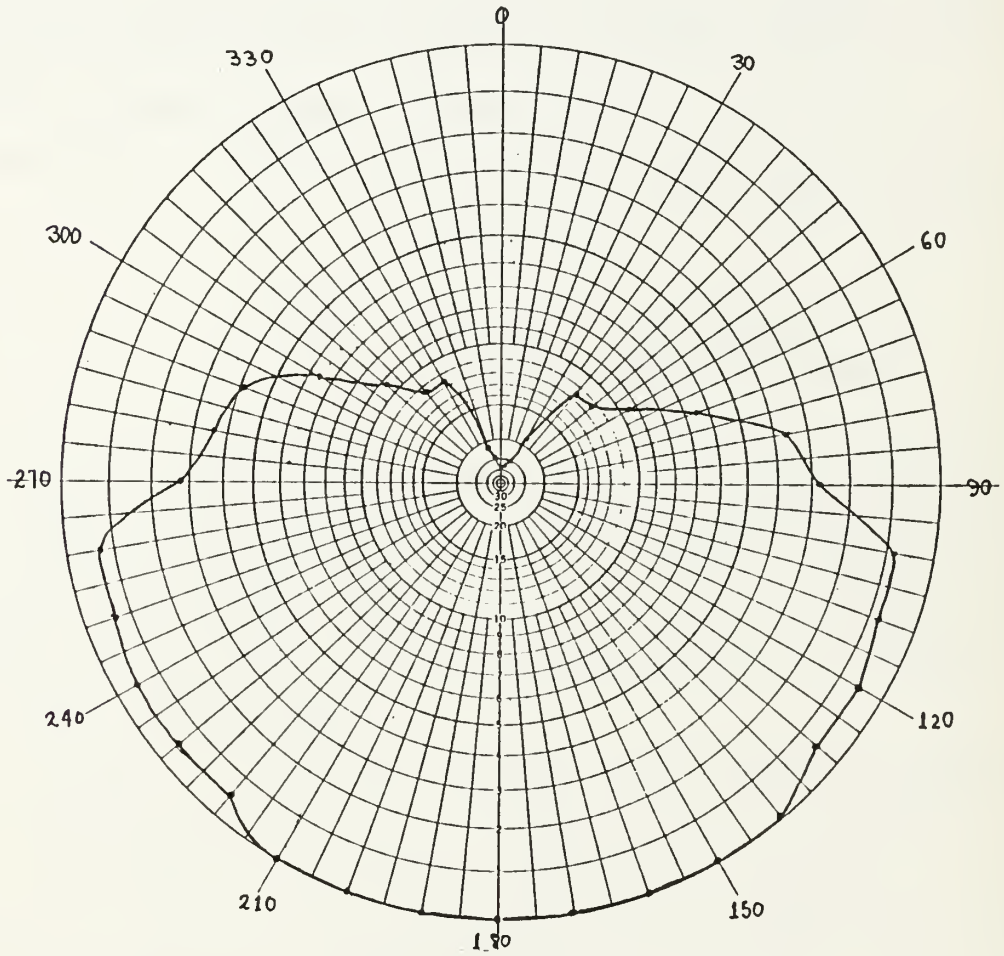

Figure 33. Radiation Pattern at 100 M, F = 59.25 MHz, 60 MHz Feed Harness

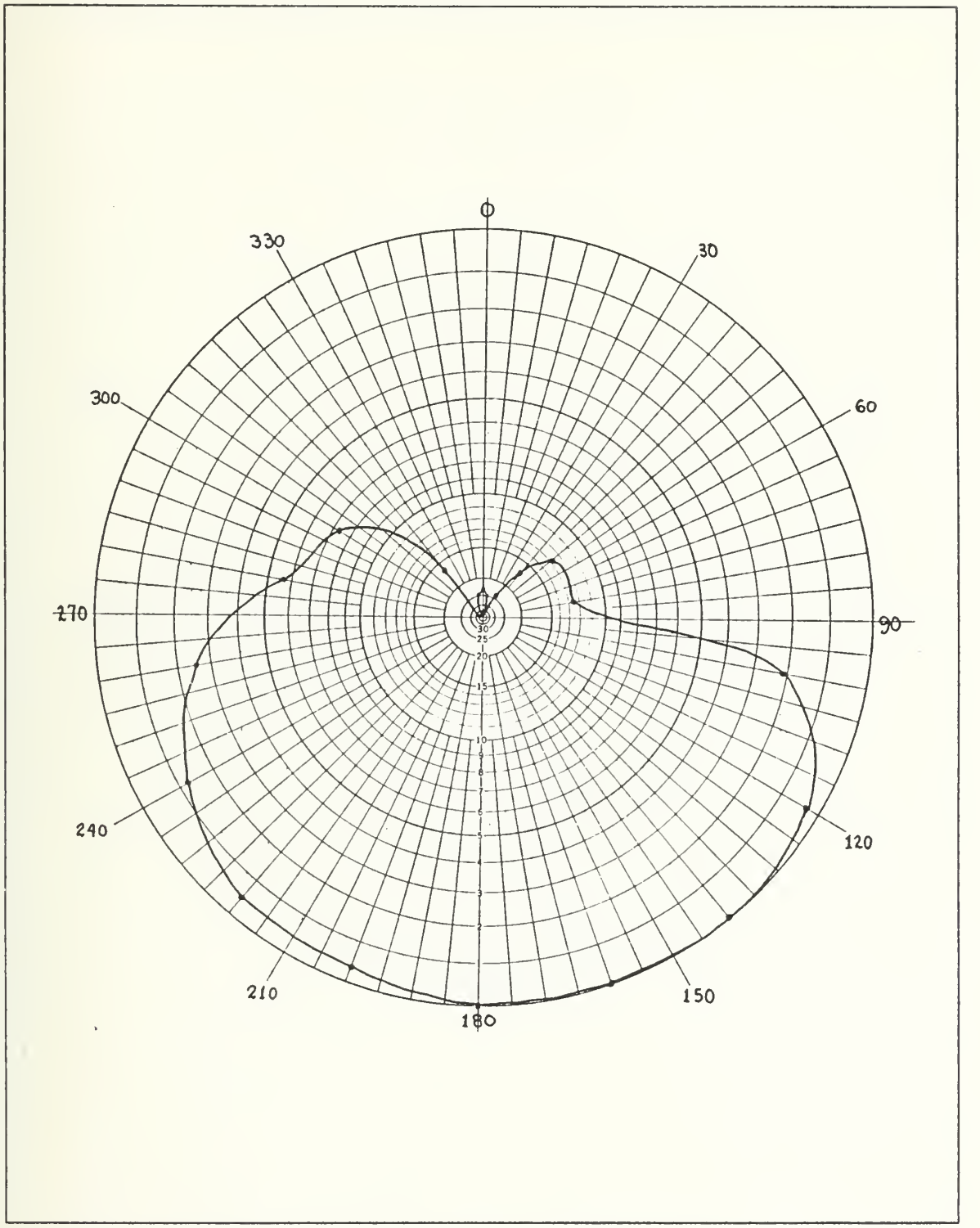

Figure 34. Radiation Pattern at 100 M, F = 53.00 MHz, 55 MHz Feed Harness

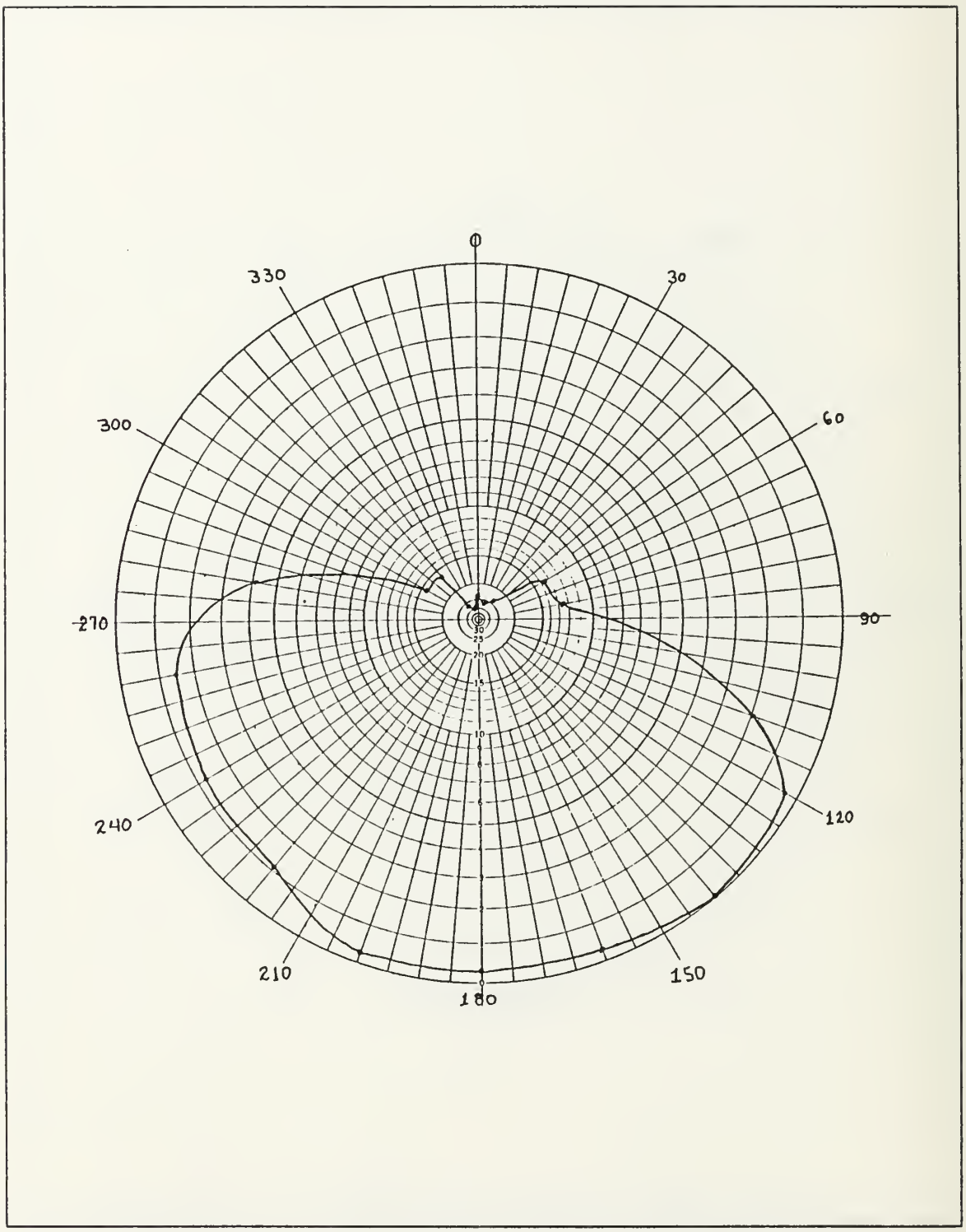

Figure 35. Radiation Pattern at 100 M, F = 65.75 MHz, 66 MHz Feed Harness

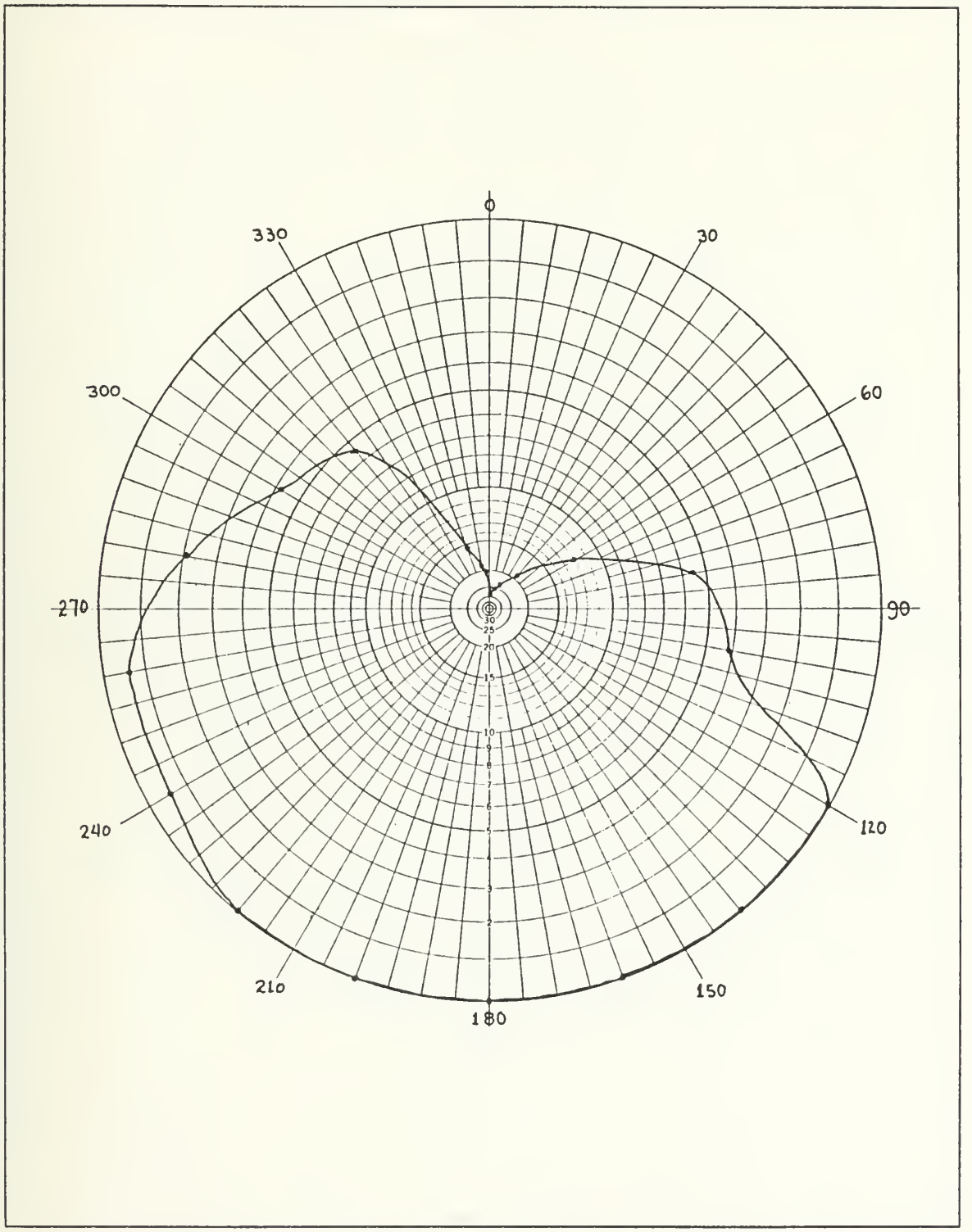

Figure 36. Radiation Pattern at 1 Km, F = 59.25 MHz, 60 MHz Feed Harness

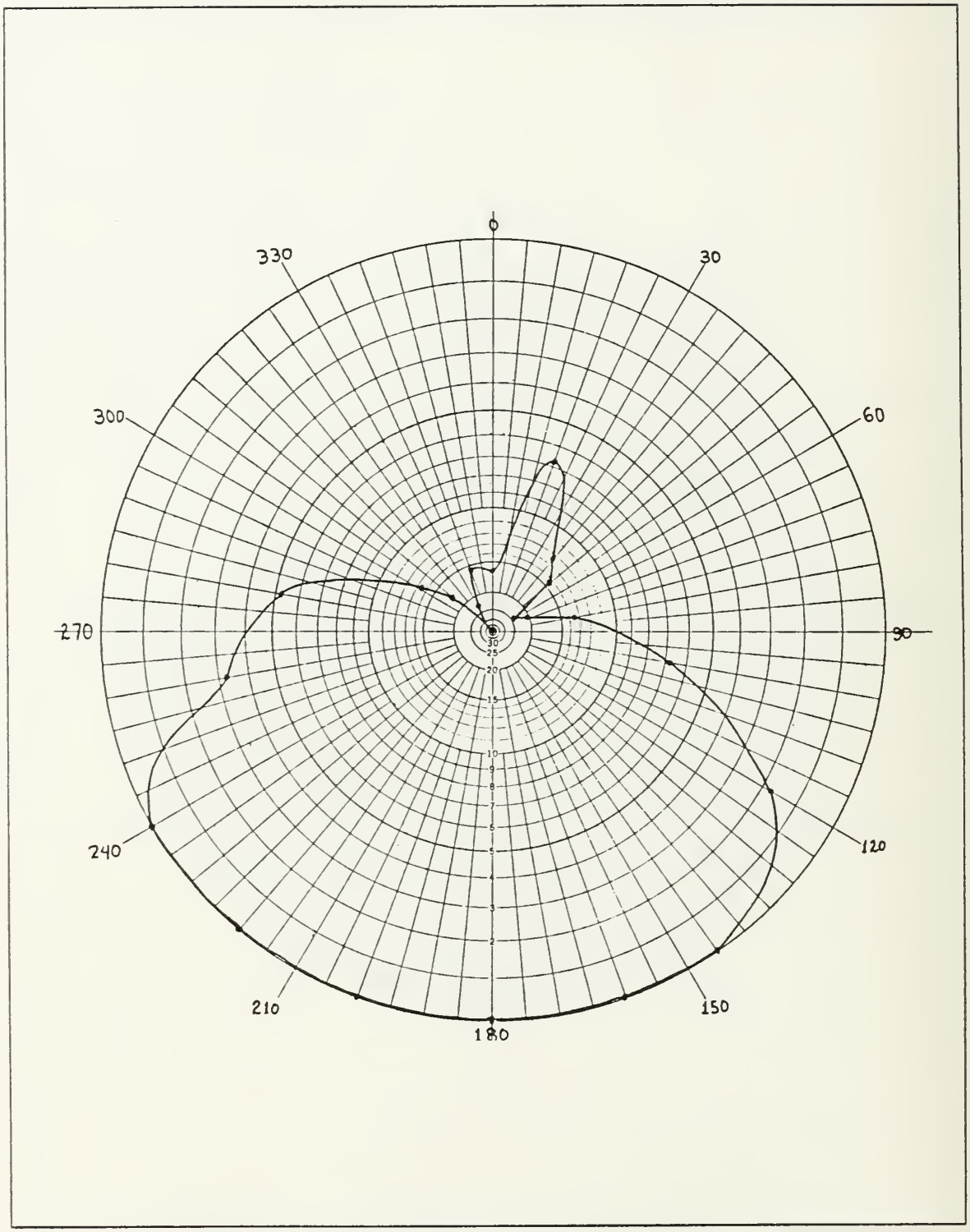

Figure 37. Radiation Pattern at 1 Km, F = 54.00 MHz, 55 MHz Feed Harness

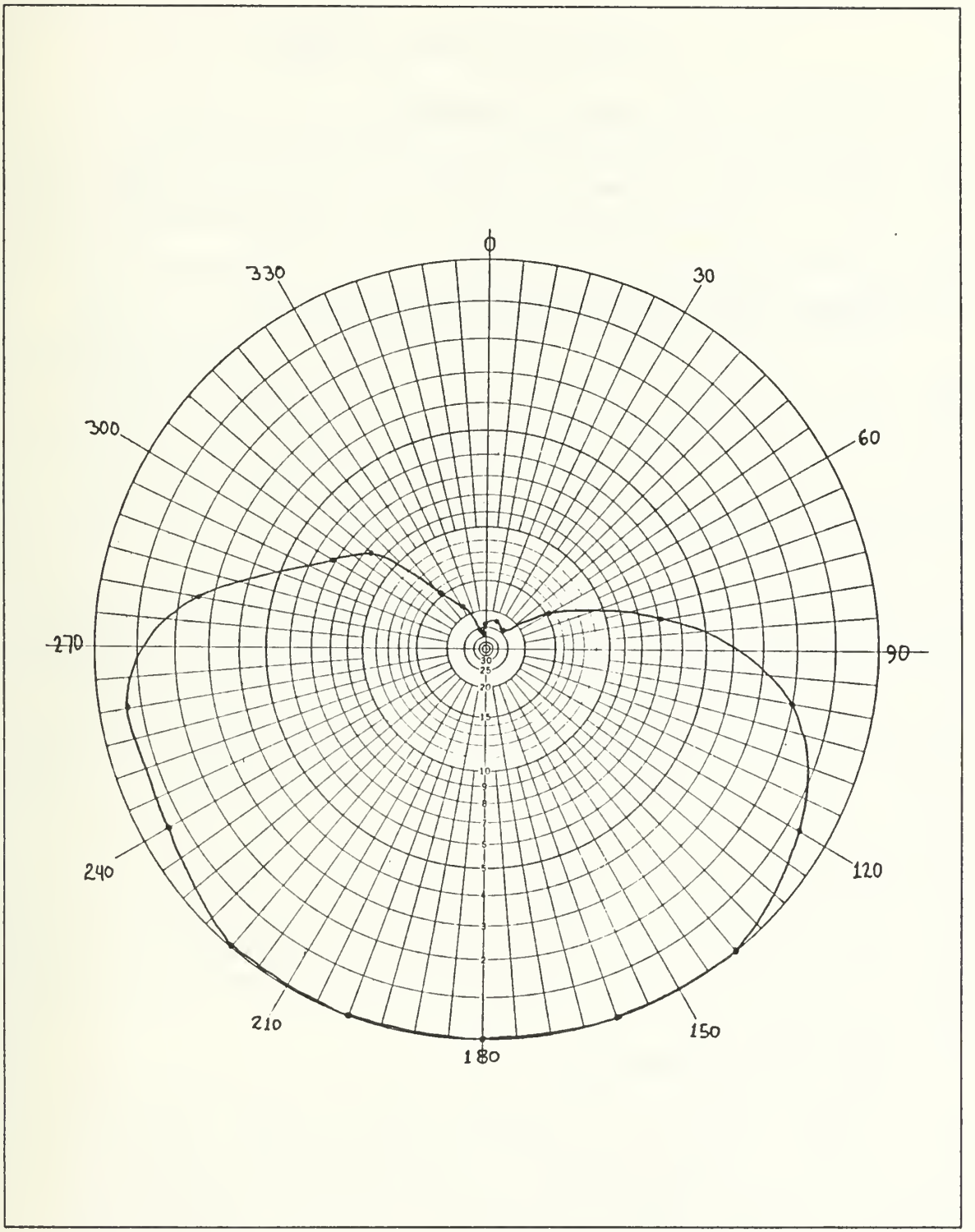

Figure 38. Radiation Pattern at 1 Km, F = 66.00 MHz, 66 MHz Feed Harness

VI. ANALYSIS AND CONCLUSIONS

A. COMPARISON OF RESULTS TO PREDICTIONS

Having predicted the performance of the prototype antenna under various configurations, excitations, and environments, and having field tested the antenna under some (but not all) of the conditions simulated during computer modeling, some useful conclusions can be drawn and some observations made.

1. Bandwidth and Standing Wave Ratio (SWR) Characteristics

The bandwidth characteristics of the prototype antenna are such that current military radios can operate into the antenna over a substantial range of frequencies. A usable bandwidth of over 20% of the design frequency was predicted, and field testing confirmed that prediction. At the resonant frequency of the structure, the SWR was computed (based on forward and reflected power readings) as 1.75 : 1. This is an acceptable SWR for a practical antenna system, but could probably be improved by "pruning" the antenna structure for resonance at exactly 60 MHz. At the edges of the usable bandwidth, SWR's of 3.4 : 1 were calculated (again from forward and reflected power measurements). While these values are substantially higher than that obtained at the structure resonant frequency, they are still within the usable range, as demonstrated by the ability of the AN PRC-77 radio to work into the prototype antenna during testing. Use of low loss coaxial cable would be advisable in this situation, but even with standard RG-8 type cable, transmission line losses at the SWR's encountered are acceptable. Addition of a simple matching network between the transmitter and transmission line would be advisable in high power systems, or where the transmitter in use is not designed to couple into high SWR loads. Location of a matching device at the feed harness "Tee" is another possible means of reducing SWR losses and improving transmitter matching.

2. Radiation Pattern Comparisons

The radiation patterns obtained during field and laboratory testing agreed closely with those predicted by NEC modeling. The laboratory plots were much more precise than those derived from field data, but overall agreement was remarkably close, considering the limitations imposed by construction techniques, measurement equipment, and normal experimental error. The prototype deep-null antenna appears to have considerable potential for development into a militarized antenna for tactical use. Fur-

ther testing to better define its performance on signals other than vertical linear polarization is advisable, however.

B. RECOMMENDATIONS

While this study has resulted in confirmation of several predictions, it has also raised numerous questions that, due to their nature and the need to limit the scope of this study, were not pursued beyond noting their existence and immediate impact on the goals of the study as previously defined. These questions include:

- Can Christman's feed method be replaced with a network optimized for various frequencies throughout a desired operational bandwidth? If so, this would offer greater control over radiation pattern shape, and might also allow reduction of the standing wave ratio seen by the radio attached to the antenna.
- How far can the bandwidth of the prototype structure be stretched using Christman's feed method?
- Can the prototype structure be modeled at a higher frequency in order to ease the burden of further laboratory testing?
- Can the vertical plane radiation pattern of the prototype structure be modified to improve low angle radiation while preserving deep null performance?
- What are the performance characteristics of the prototype structure on signals of polarization other than vertical linear?
- What other structures exhibit deep null characteristics, and are they better or worse candidates for development than the structure investigated herein?

These questions are the basis for further work in this area, and provide an indicator of the scope of the subject.

APPENDIX A. CURRENT CALCULATION PROCEDURE

A. PURPOSE

Both MININEC and NEC require that the specified structure be excited by a voltage of magnitude and phase specified by the user. Since the antenna radiation characteristics of interest derive from equal magnitude currents of specific phase relationships flowing in the structure elements, a procedure for calculating these excitation voltages is needed.

This Appendix describes two procedures by which the required excitation voltages may be found. Since both magnitude and phase are involved, and since the structure impedance involves both real and imaginary components, it is advantageous to do all such calculations on a computer. Improved accuracy and less time expended are the benefits of this approach.

B. TWO PORT NETWORK APPROACH

In order to find the excitation voltage that will produce equal magnitude currents of the proper phase relationship, it is necessary to know the admittance of each element to be driven, and the mutual admittance between driven elements. This is accomplished by exciting one element with one volt at a phase angle of zero degrees while shorting the other element to the ground structure. This produces a current value for the driven element and a current value at the base of the element shorted to ground.

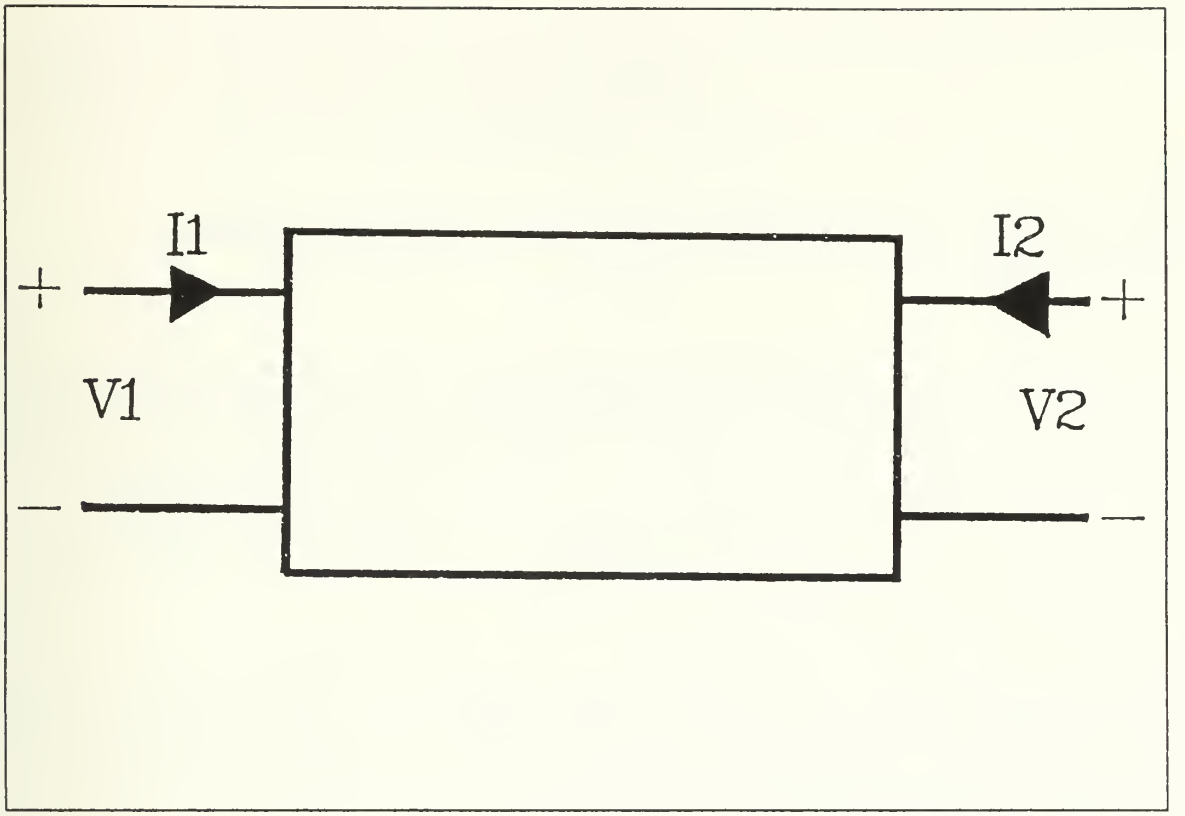

Figure 39. Two Port Network.

Starting with the equation set for a two port network,

$$I_1 = Y_{11}V_1 + Y_{12}V_2 \tag{2}$$

$$I_2 = Y_{21}V_1 + Y_{22}V_2 \tag{3}$$

It can be seen that when the other monopole of the structure (the one that is not excited) is connected to the ground plane elements, $V_2 = 0$. Thus:

$$Y_{11} = \left.\frac{I_1}{V_1}\right|_{V_2 = 0.} \tag{4}$$

Since the monopoles are identical, it follows that

$$Y_{22} = \frac{I_2}{V_2}\bigg|_{V_1 = 0.} \tag{5}$$

The mutual admittance can be found by following the same line of reasoning:

$$Y_{12} = \frac{I_1}{V_2}\bigg|_{V_1 = 0} \tag{6}$$

$$Y_{21} = \frac{I_2}{V_1}\bigg|_{V_2 = 0.} \tag{7}$$

Note that $Y_{21} = I_2$ when $V_1 = 0$ volt at a phase angle of zero. Since in this case the current magnitudes in the two monopoles are equal, it can be seen that the admittance matrix is symmetric, i.e., $Y_{11} = Y_{22}$ and $Y_{12} = Y_{21}$.

While it is convenient to develop the above argument in terms of admittances, element impedances and mutual impedances are needed when working with Christman's feed line matching arrangement [Ref. 7]. By inverting the admittance matrix the impedance matrix can be obtained:

$$\begin{bmatrix} Z_{11} & Z_{12} \\ Z_{21} & Z_{22} \end{bmatrix} = \begin{bmatrix} Y_{11} & Y_{12} \\ Y_{21} & Y_{22} \end{bmatrix}^{-1} \tag{8}$$

A MATHCAD © routine [Ref. 9] was written to accomplish this matrix inversion in order to avoid tedium and errors. The impedance values are then accessible for further use. The MATHCAD © routine used is listed at the end of this appendix. When the impedance values are found, the feed system described in [Ref. 7] can be calculated using the BASIC program presented therein. These transmission line lengths can then be modeled using NEC TL "cards."

C. A SHORTCUT METHOD

While the above method is more general, it is possible to avoid much of the work by placing a large resistance in the structure, then exciting it with a known voltage. The resulting element current is then essentially constant, so the impedance can be calculated

directly and then the loading resistance subtracted out. If the loading resistance is high enough, the remainder after the subtraction is then:

$$V_1 = I_1 Z_1 \tag{9}$$

$$V_2 = I_2 Z_2 \tag{10}$$

These voltages can then be used to excite the two monopoles of the structure under study. The correctness of this approach can be easily checked by looking at the currents in the segments of the two monopoles nearest the ground plane structure. The currents should be equal in magnitude and differ in phase by 90 degrees.

D. MATRIX INVERSION ROUTINE

- USE THIS ROUTINE TO FIND MUTUAL IMPEDANCE BETWEEN ANTENNA ELEMENTS THEN USE THE MUTUAL IMPEDANCE WITH LEWALLEN'S PROGRAM TO FIND TRANSMISSION LINE LENGTHS TO GET DESIRED CURRENT RELATIONSHIPS. (F=58 MHz HERE)

$i := \sqrt{-1}$ $\qquad \theta 11 := \frac{28.892}{360} \cdot 2 \cdot \pi$ angle of I1 current

$Y11 := .04443 \cdot e^{i \cdot \theta 11}$ complex form of I1 = Y11

$\theta 12 := \frac{-150.784}{360} \cdot 2 \cdot \pi$ angle of I2 current

$Y12 := .02206 \cdot e^{i \cdot \theta 12}$ complex form of I2 = Y12

$Y22 := Y11 \qquad Y21 := Y12$

from symmetry, Y11 = Y22 and Y12 = Y21,
thus the admittance matrix is

$$Y := \begin{bmatrix} Y11 & Y12 \\ Y21 & Y22 \end{bmatrix}$$

$Z := Y^{-1}$ by applying Ohm's law to the admittance matrix

$$Z = \begin{bmatrix} 26.206 - 14.335i & 13.052 - 7.044i \\ 13.052 - 7.044i & 26.206 - 14.335i \end{bmatrix}$$

the element impedance for use with Lewallen's program is thus Z11 or Z12, and the mutual impedance is Z12 or Z21

APPENDIX B. FEEDLINE LENGTH CALCULATION METHOD

A. PURPOSE

The experimental approach used in this study makes extensive use of Christman's feed [Ref. 7]. In order to provide better documentation of the methods used in this work, the program is listed here. The theoretical work that provides the basis for this program is presented in Christman's paper [Ref. 7] and is not repeated due to its length and complexity.

B. BASIC PROGRAM LISTING

```
100 REM
110 REM SIMPLIFIED FEED SYSTEM FOR TWO-ELEMENT ARRAYS
120 REM ROY W. LEWALLEN, W7EL
130 REM 7 JAN. 1985
140 REM
150 REM ANGULAR CALCULATIONS ARE DONE IN RADIANS;
160 REM INPUTS AND OUTPUTS ARE IN DEGREES.
170 REM
180 PRINT
190 PRINT
200 PRINT "R,X OF LEADING ELEMENT (OHMS)"
210 INPUT R1,X1
220 PRINT "R,X OF LAGGING ELEMENT (OHMS)"
230 INPUT R2,X2
240 PRINT "MUTUAL R,X (OHMS)"
250 INPUT R3,X3
260 PRINT "EL. 2:EL. 1 CURRENT MAGNITUDE, PHASE"
270 PRINT "--PHASE MUST BE ZERO OR NEGATIVE (DEGREES)"
280 INPUT M,P
290 IF P<=0 THEN 340
300 PRINT "PHASE MUST BE NON-POSITIVE, SINCE EL. 2 IS"
310 PRINT "DEFINED AS BEING THE LAGGING ELEMENT"
320 PRINT
330 GO TO 260
340 PRINT "FEEDLINE 1,2 IMPEDANCE (OHMS)"
350 INPUT F1,F2
360 LET P1=3.14159
370 LET J=0
380 LET C1=COS(P*P1/180)/M
390 LET S1=SIN(P*P1/180)/M
400 LET H=R2+C1*R3+S1*X3
410 LET A=(R3+C1*R1+S1*X1)/H
420 LET B=S1*F1/H
430 LET C=((X3+C1*X1-S1*R1)*H-(X2+C1*X3-S1*R3)*(R3+C1*R1+S1*X1))/F2/H
440 LET D=F1*(C1*H-S1*(X2+C1*X3-S1*R3))/F2/H
500 LET Q=2-(A*A+B*B+C*C+D*D)
510 LET E=(A*A+C*C-B*B-D*D)/Q
```

```
520 LET F=2*(A*B+C*D)/Q
530 LET R=E
540 LET I=F
550 GOSUB 810
560 LET G1=V
570 IF U<1 THEN 910
580 LET X=ATN(SQR(U*U-1))
590 LET T1=(X+G1)/2
600 IF T1=>0 THEN 620
610 LET T1=T1+2*P1
620 IF T1<P1 THEN 640
630 LET T1=T1-P1
640 LET I=C*COS(T1)+D*SIN(T1)
650 LET R=A*COS(T1)+B*SIN(T1)
660 GOSUB 810
670 IF V=> THEN 690
680 LET V=V+2*P1
690 IF J=1 THEN 790
700 PRINT
710 PRINT " ","Z0=";F1;" OHMS","Z0=";F2;" OHMS"
720 PRINT " ","TO LEAD. EL.","TO LAG. EL."
730 PRINT " ","ELECT L.(DEG.)","ELECT. L.(DEG.)"
740 PRINT
750 PRINT "FIRST SOLN.",T1*180/P1,V*180/P1
760 LET J=1
770 LET X=2*P1-X
780 GO TO 590
790 PRINT "SECOND SOLN.",T1*180/P1,V*180/P1
800 GO TO 970
810 REM RECTANGULAR-POLAR SUBROUTINE
820 LET U=SQR(R*R+I*I)
830 IF U=0 THEN 870
840 IF ABS(U+R)<1.0E-7 THEN 890
850 LET V=2*ATN(I/(U+R))
860 RETURN
870 LET V=0
880 RETURN
890 LET V=P1
900 RETURN
910 PRINT
920 PRINT "NO SOLUTION FOR THE SPECIFIED PARAMETERS."
930 PRINT "WOULD YOU LIKE TO TRY DIFFERENT"
940 PRINT "FEEDLINE Z0'S (Y/N)?"
950 INPUT A$
960 IF A$="Y" THEN 340
970 PRINT
980 PRINT
990 END
```

APPENDIX C. ADDITIONAL TEST DATA

A. GROUND PLANE STRUCTURE VARIATION PLOTS

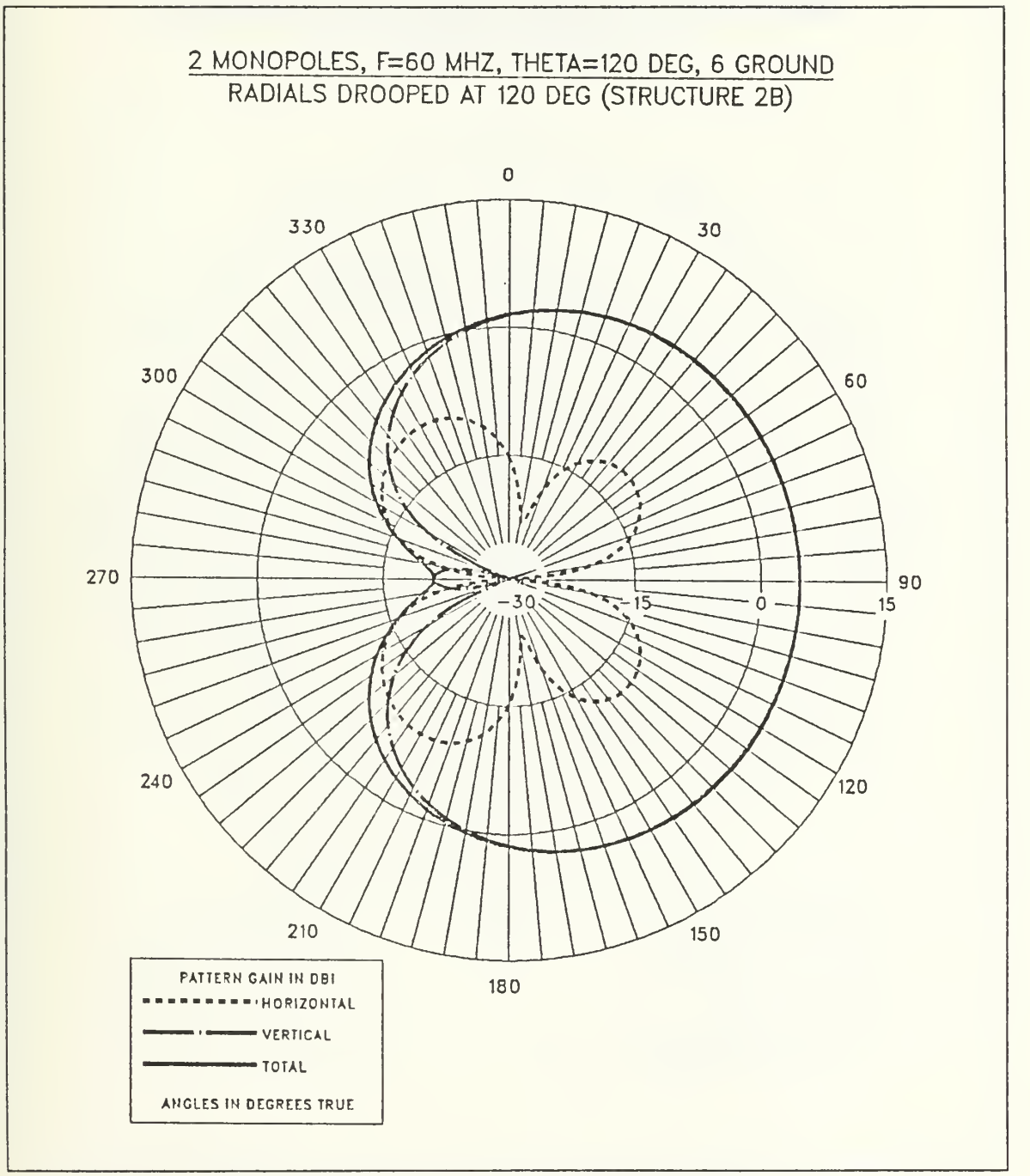

Figure 40. Radials Drooped at 120 Degrees from Monopoles

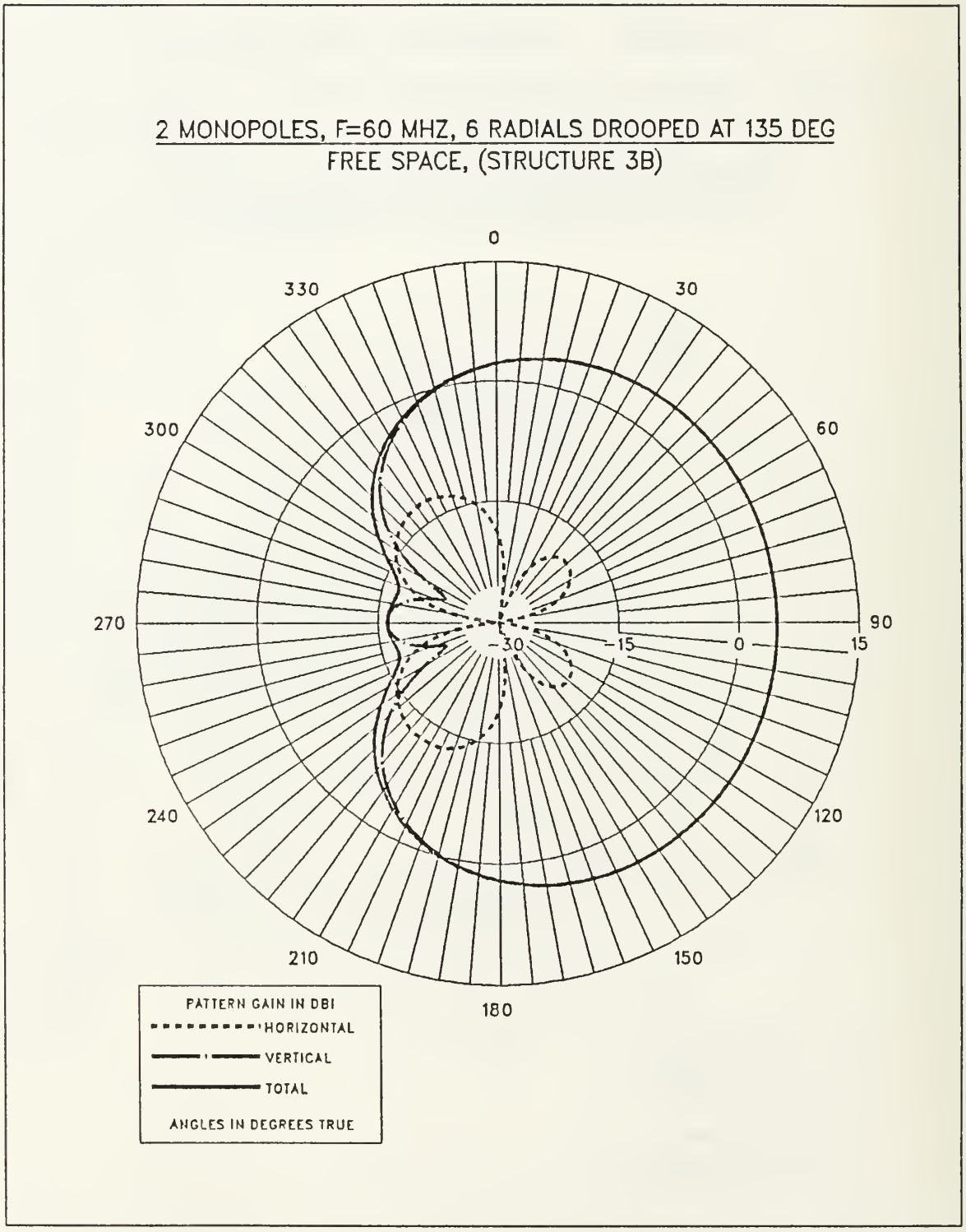

Figure 41. Radials Drooped at 135 Degrees from Monopoles

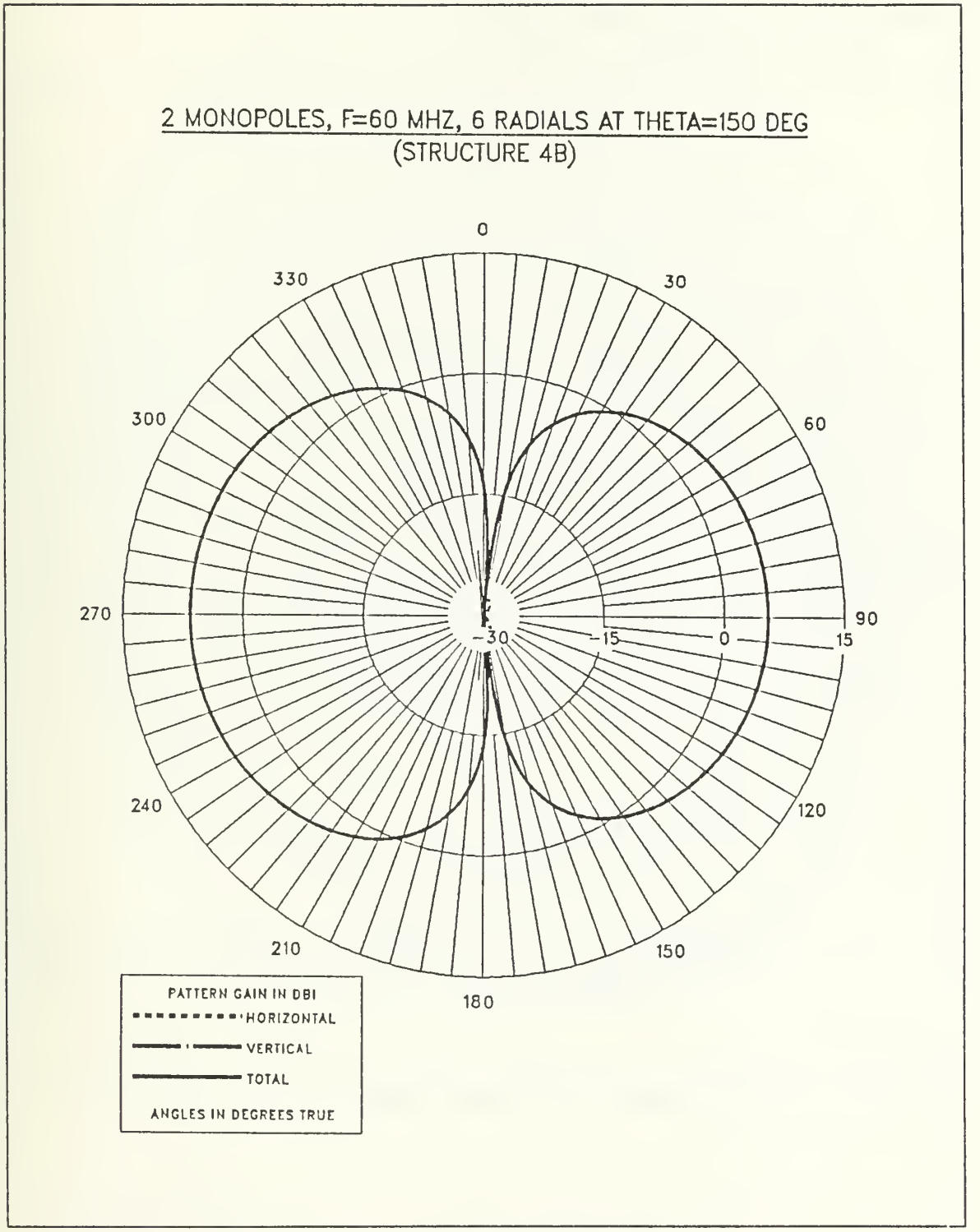

Figure 42. Radials Drooped at 150 Degrees from Monopoles

B. ADDITIONAL LABORATORY PLOTS

1. 55 MHz Feed Harness

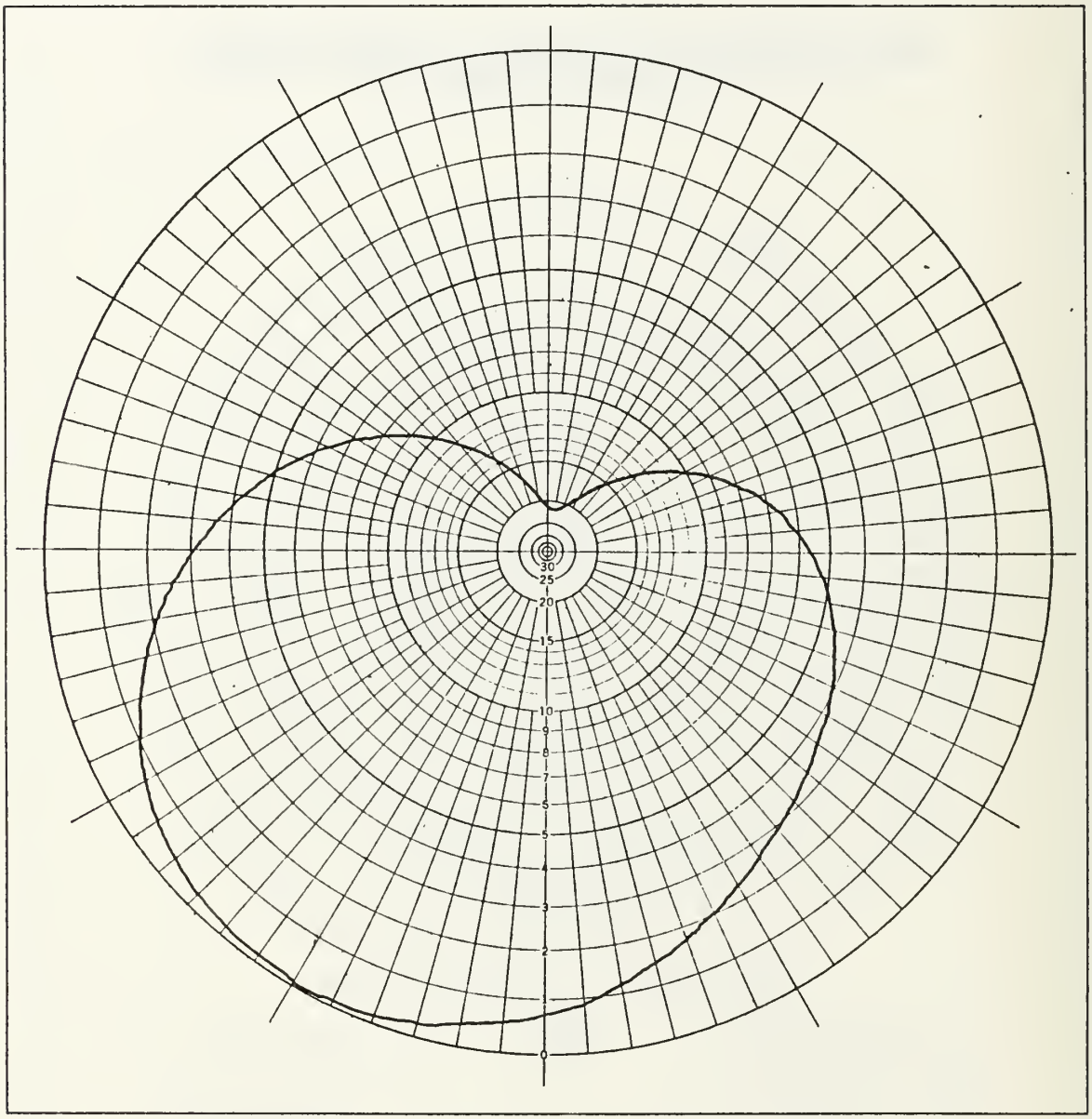

Figure 43. 55 MHz Harness, F = 53.75 MHz, Laboratory Plot

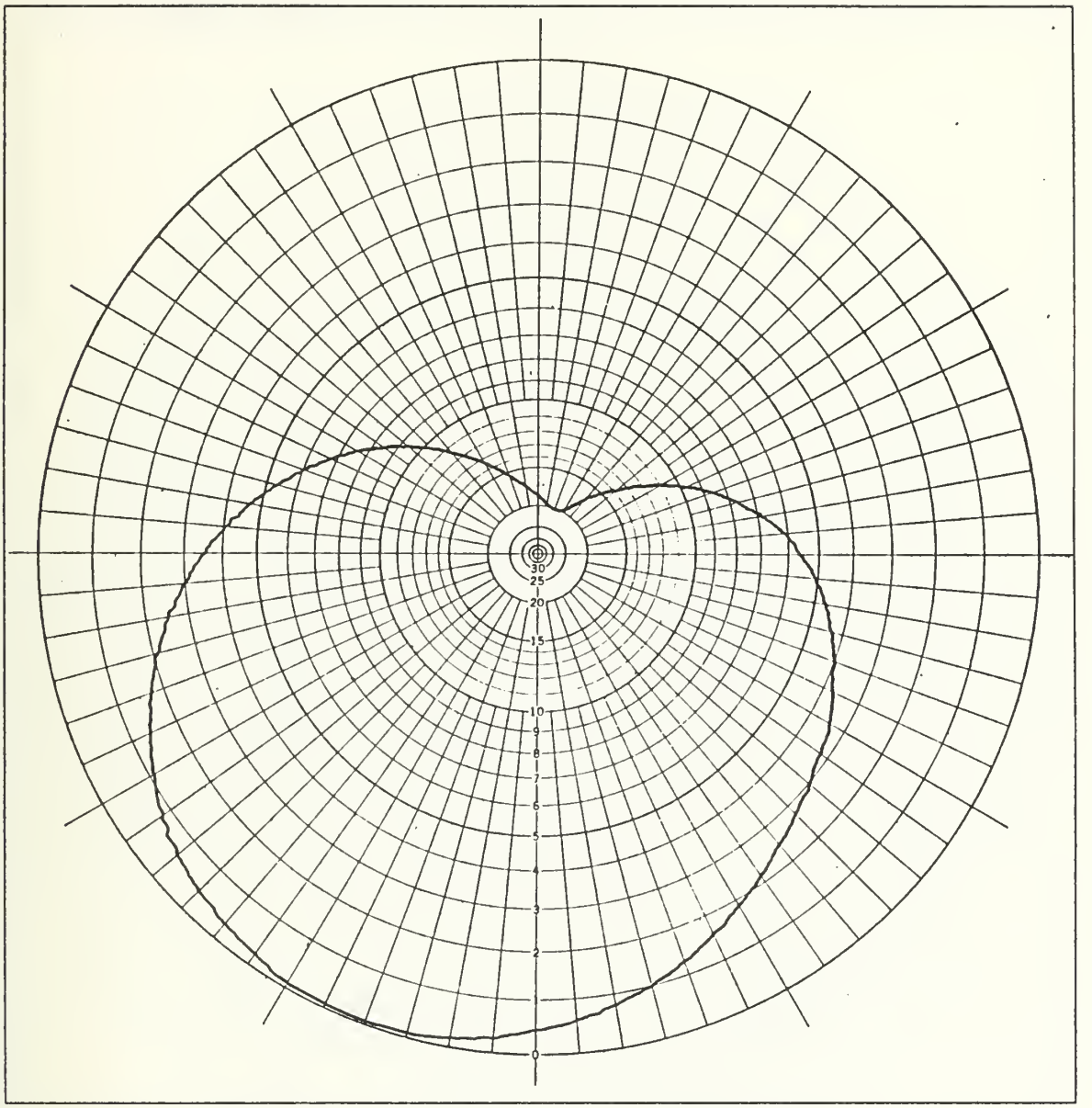

Figure 44. 55 MHz Harness, F = 54.00 MHz, Laboratory Plot

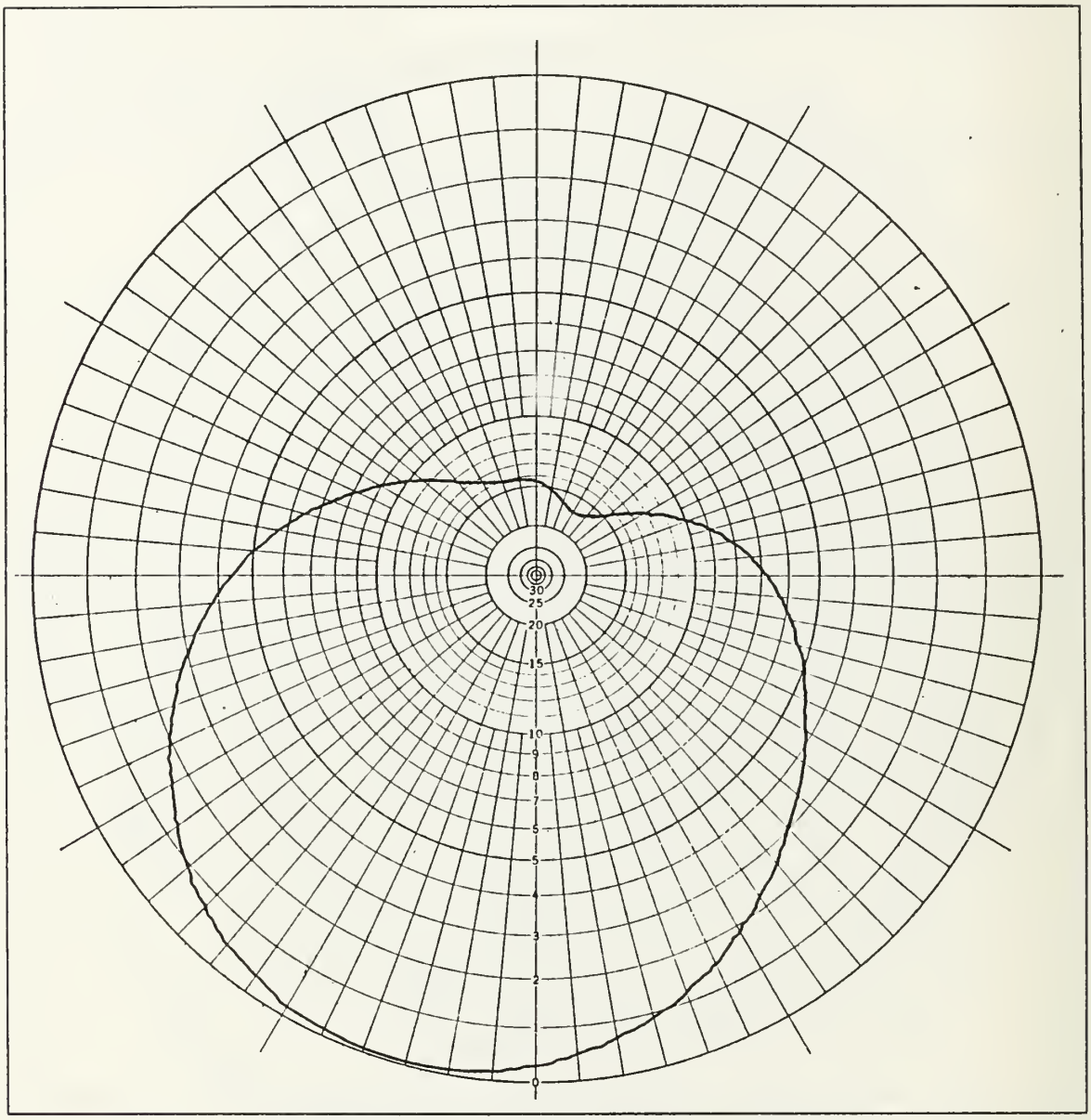

Figure 45. 55 MHz Harness, F = 54.50 MHz, Laboratory Plot

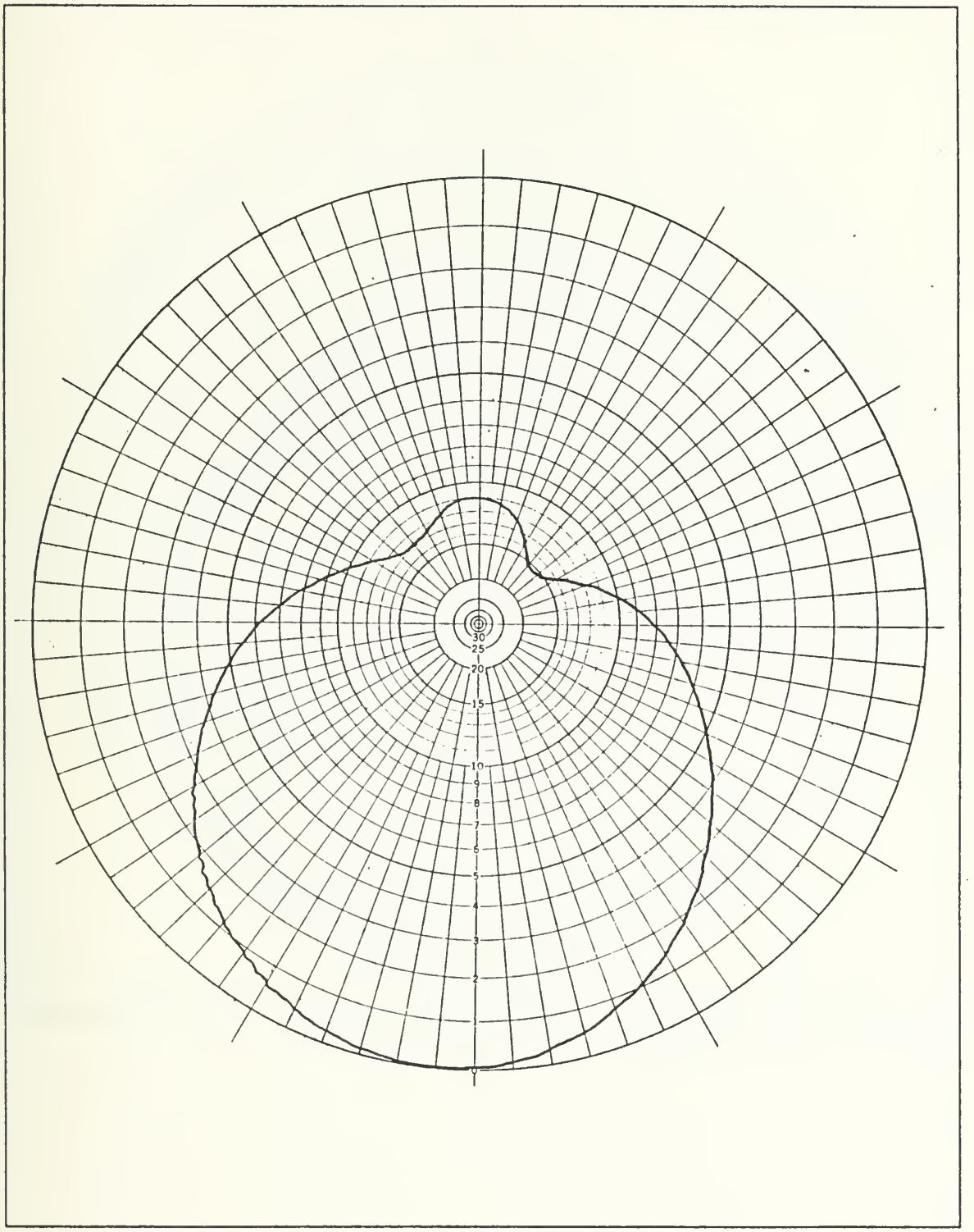

Figure 46. 55 MHz Harness, F = 55.00 MHz, Laboratory Plot

2. 60 MHz Feed Harness

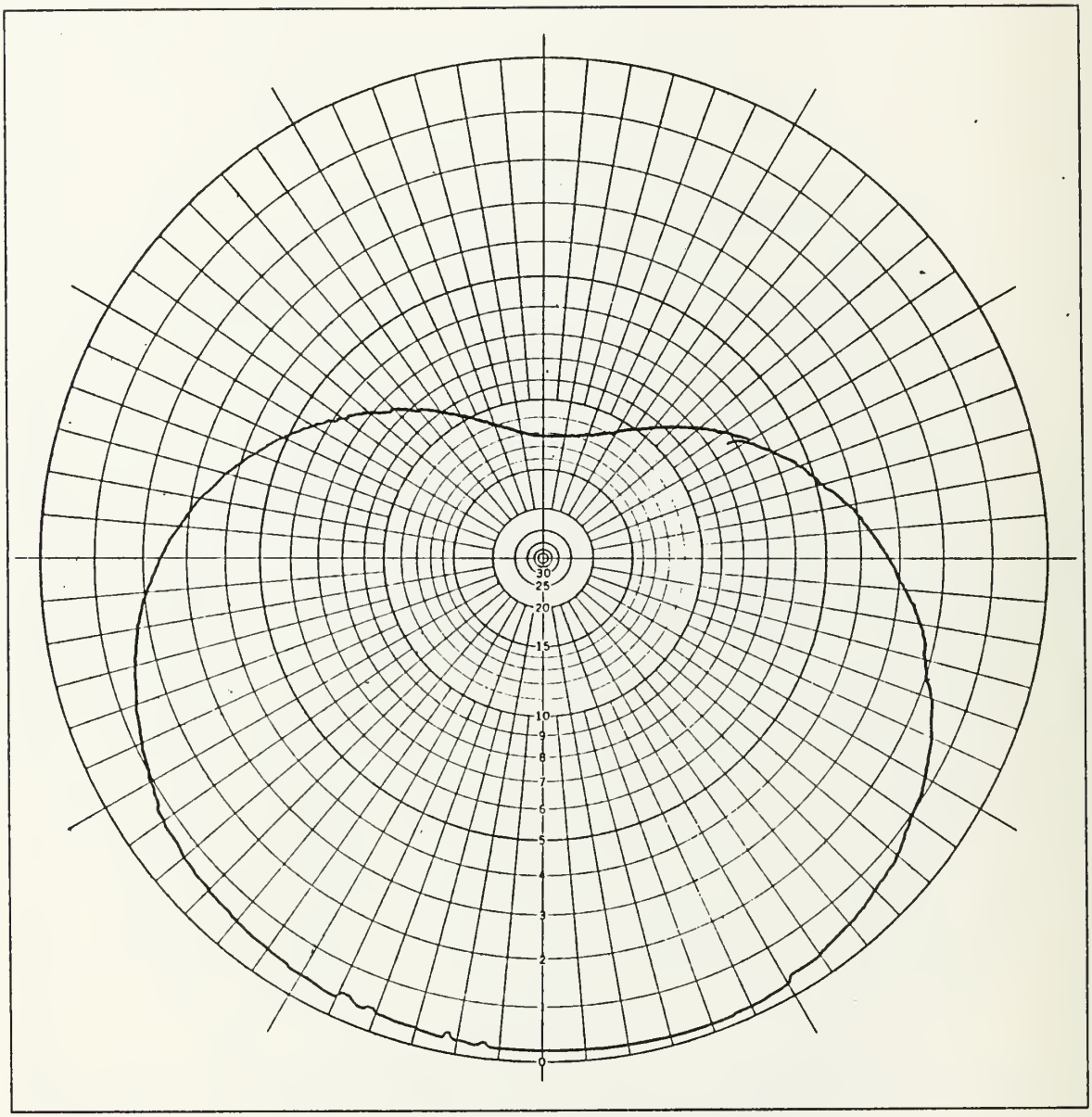

Figure 47. 60 MHz Harness, F = 58.50 MHz, Laboratory Plot

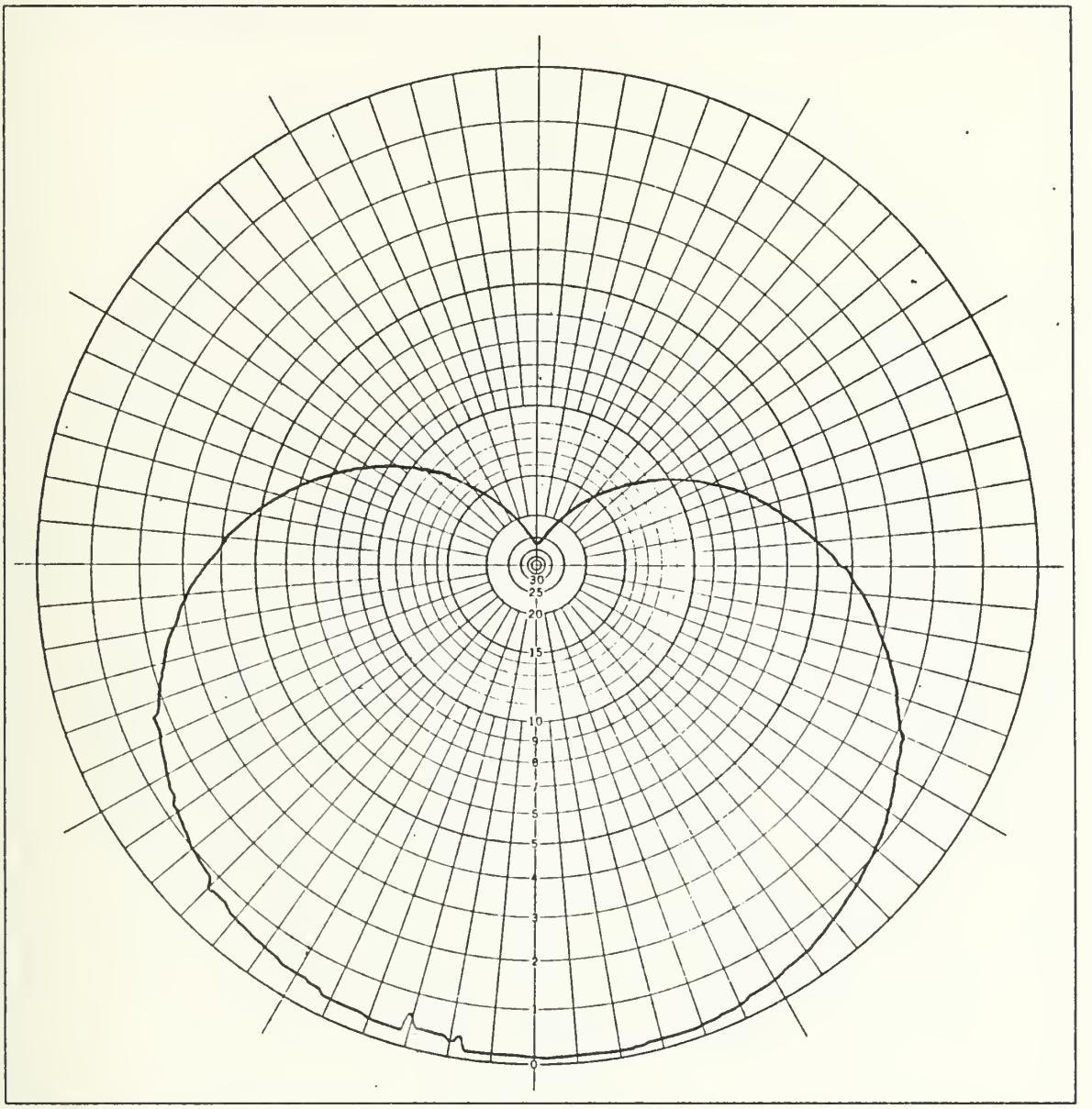

Figure 48. 60 MHz Harness, F = 59.00 MHz, Laboratory Plot

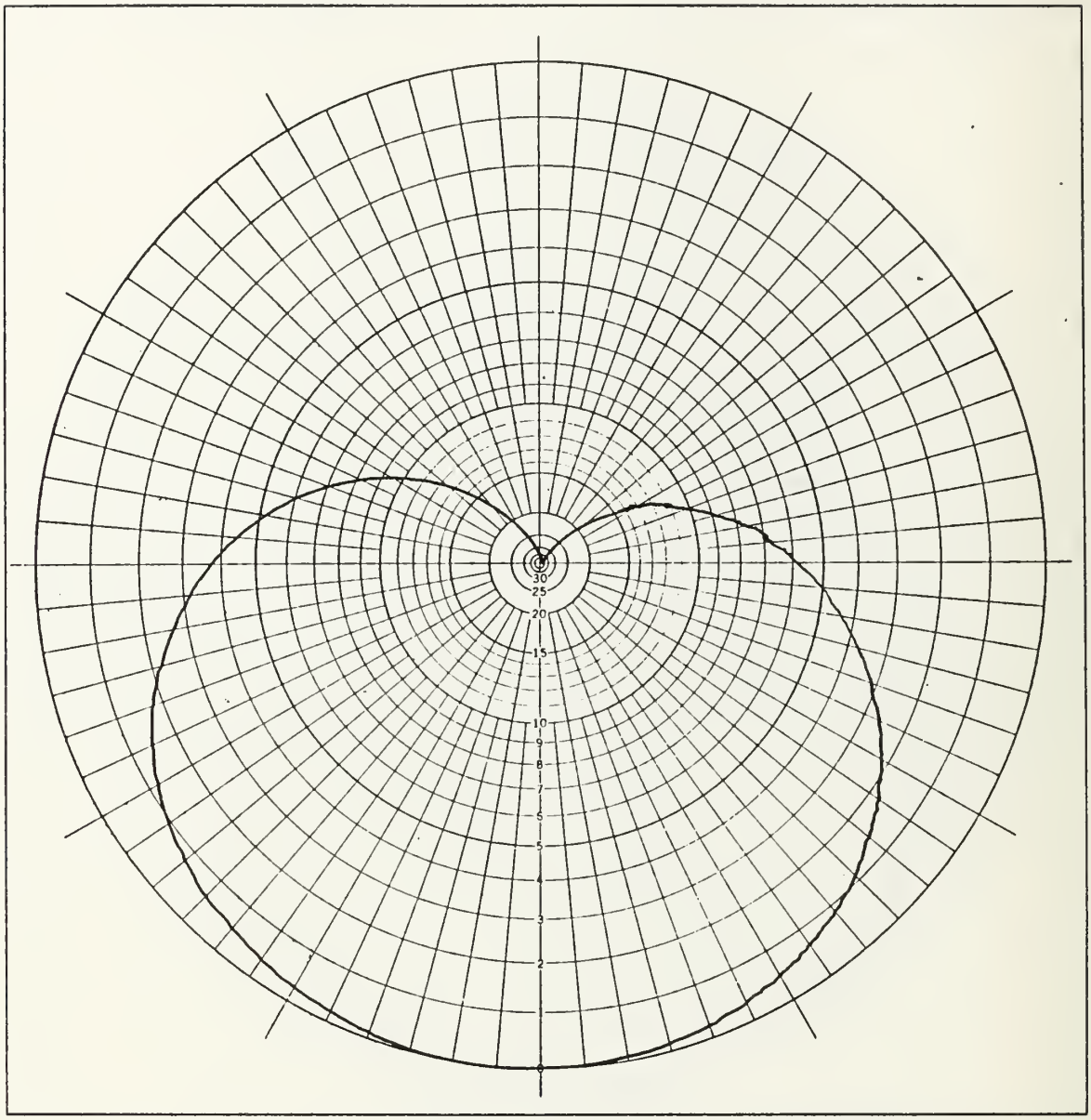

Figure 49. 60 MHz Harness, F = 59.35 MHz, Laboratory Plot

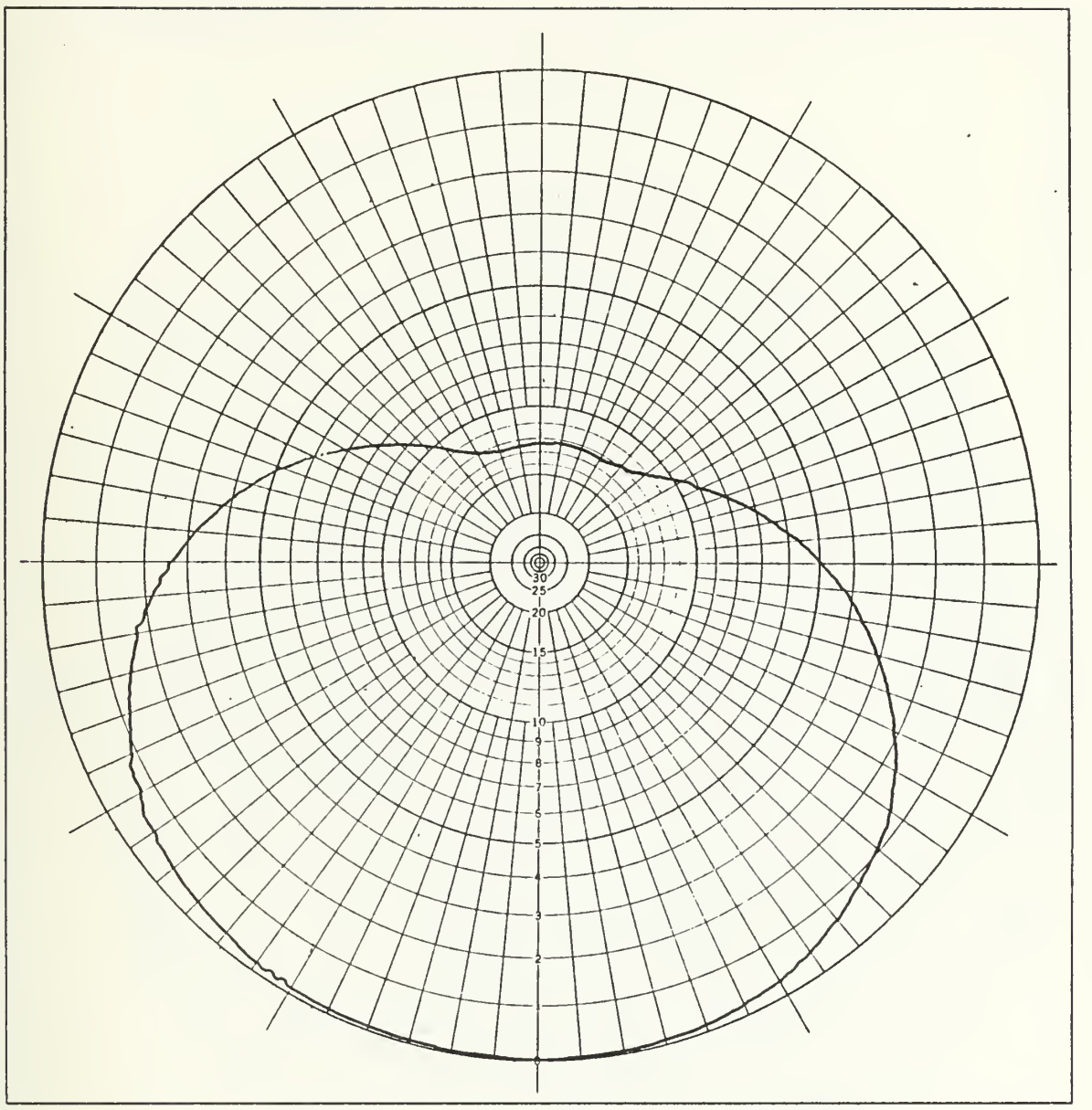

Figure 50. 60 MHz Harness, F = 60.00 MHz, Laboratory Plot

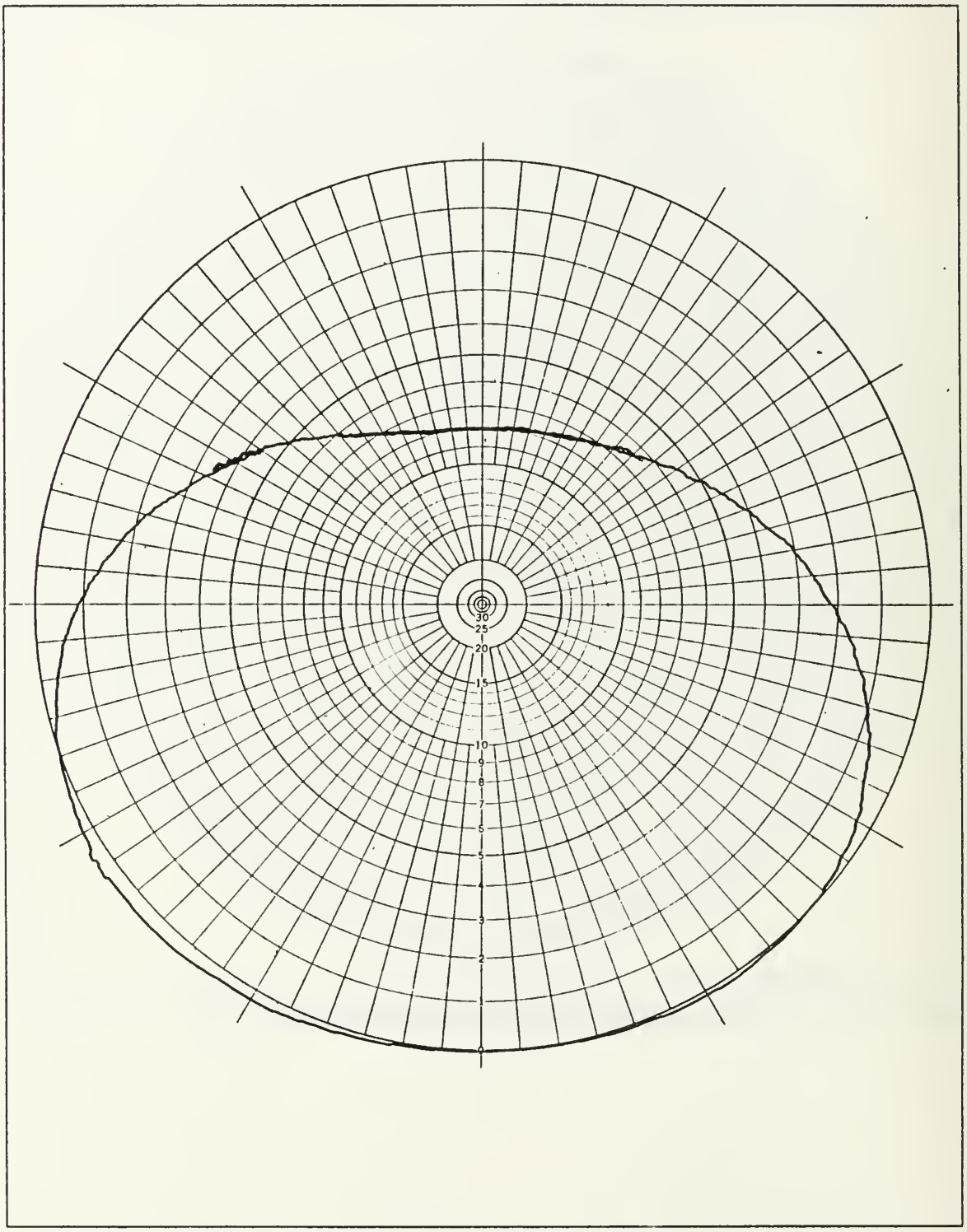

Figure 51. 60 MHz Harness, F = 60.50 MHz, Laboratory Plot

3. 66 MHz Feed Harness

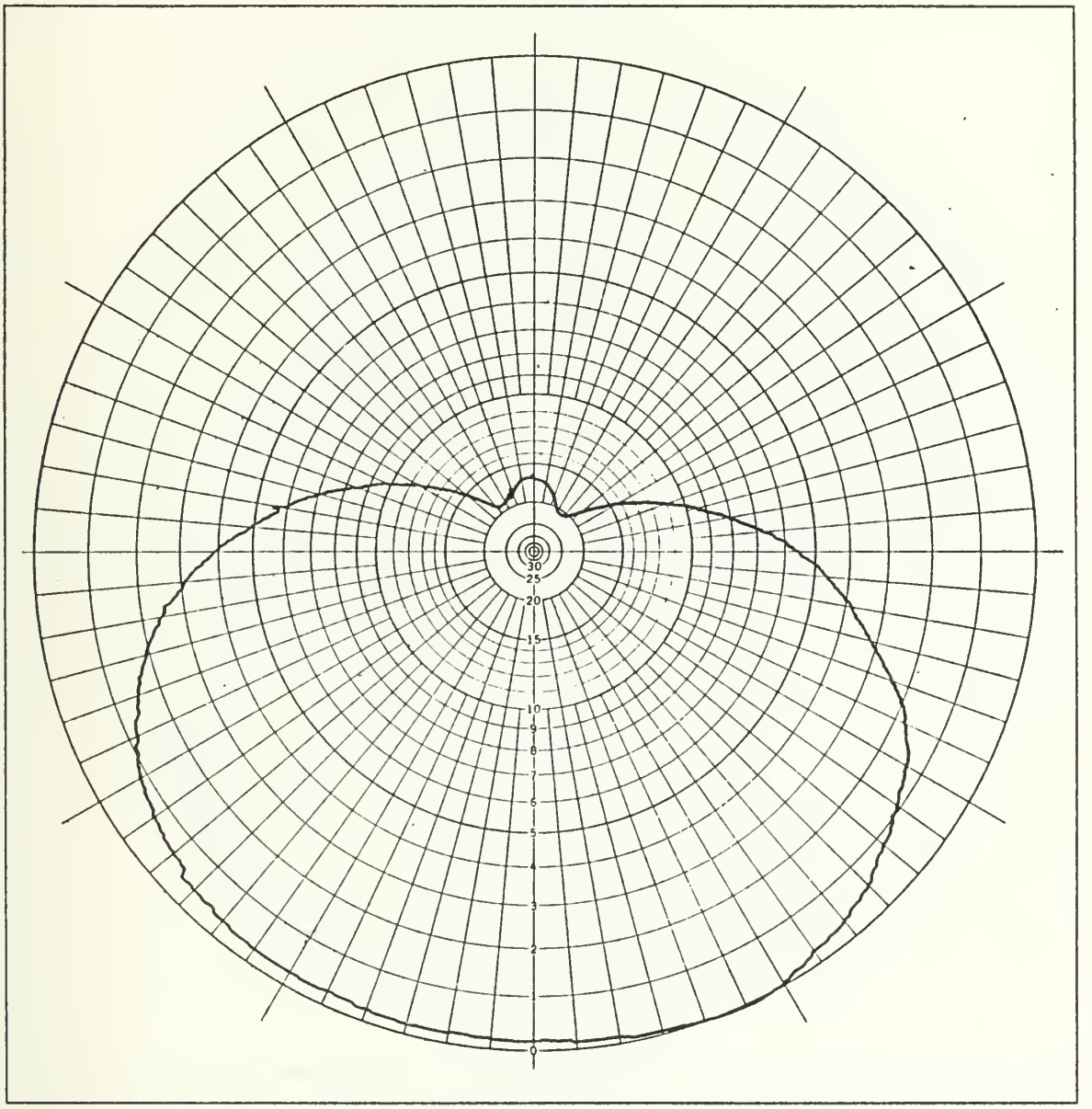

Figure 52. 66 MHz Harness, F = 64.00 MHz, Laboratory Plot

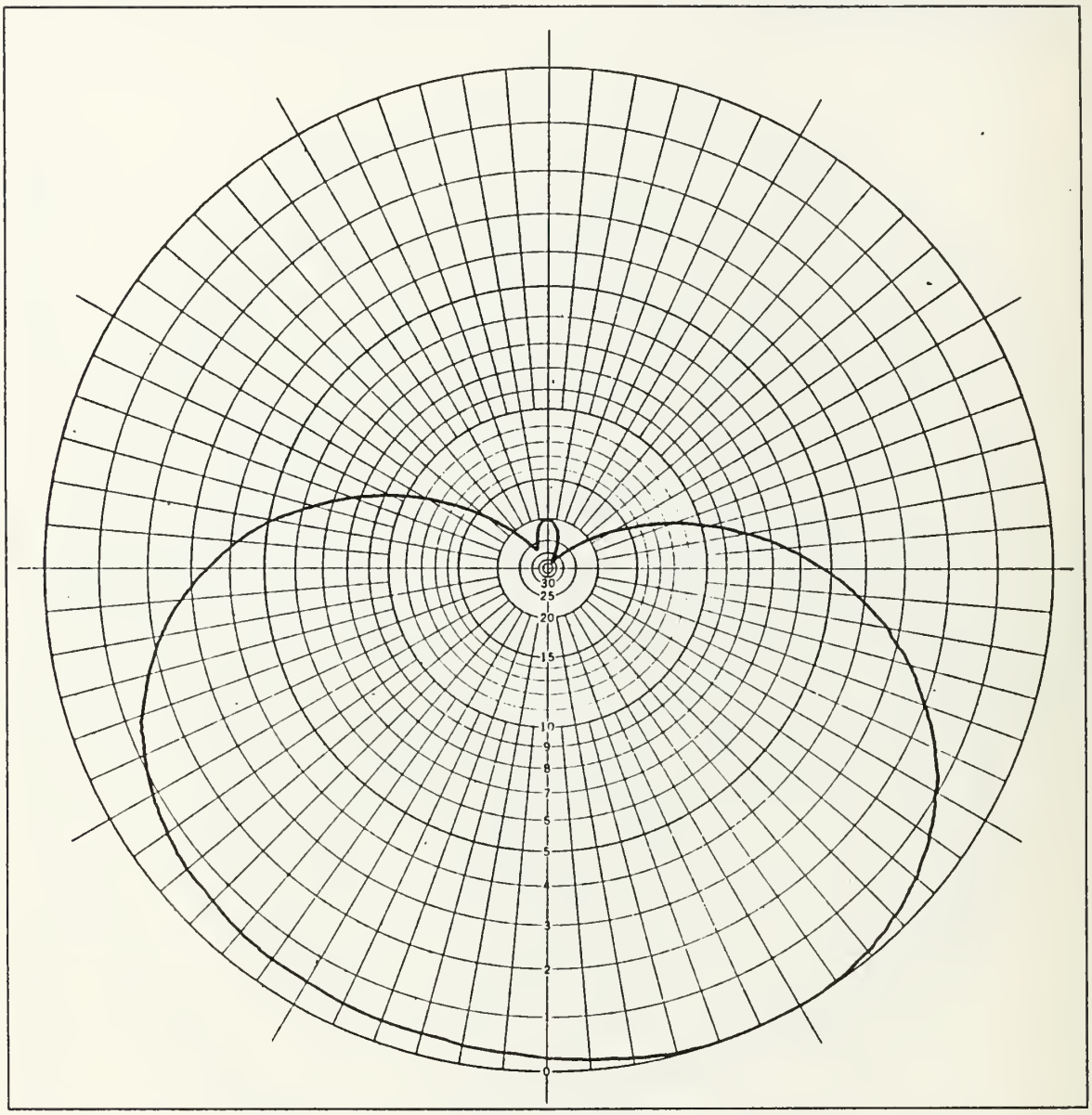

Figure 53. 66 MHz Harness, F = 64.50 MHz, Laboratory Plot

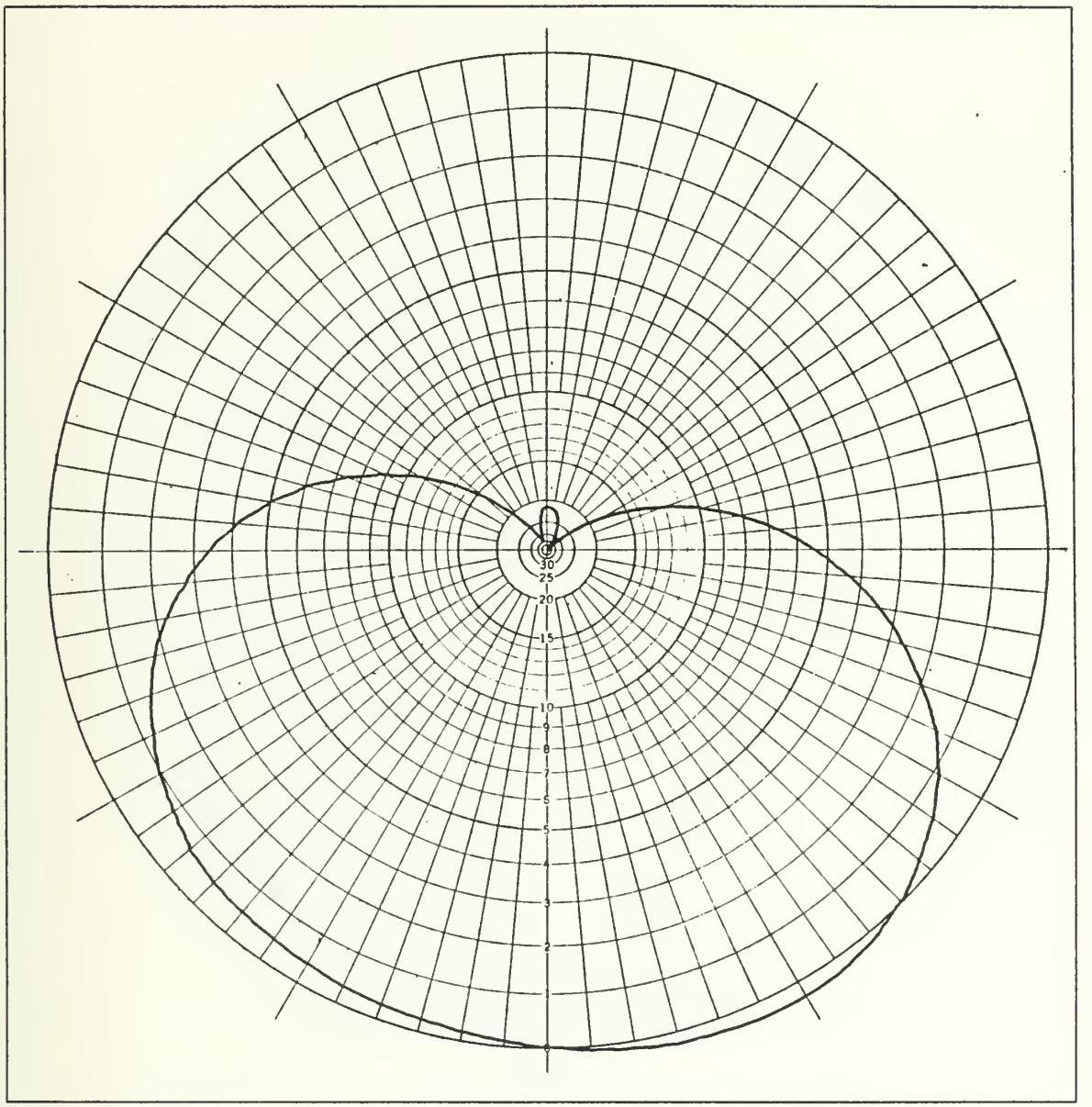

Figure 54. 66 MHz Harness, F = 65.00 MHz, Laboratory Plot

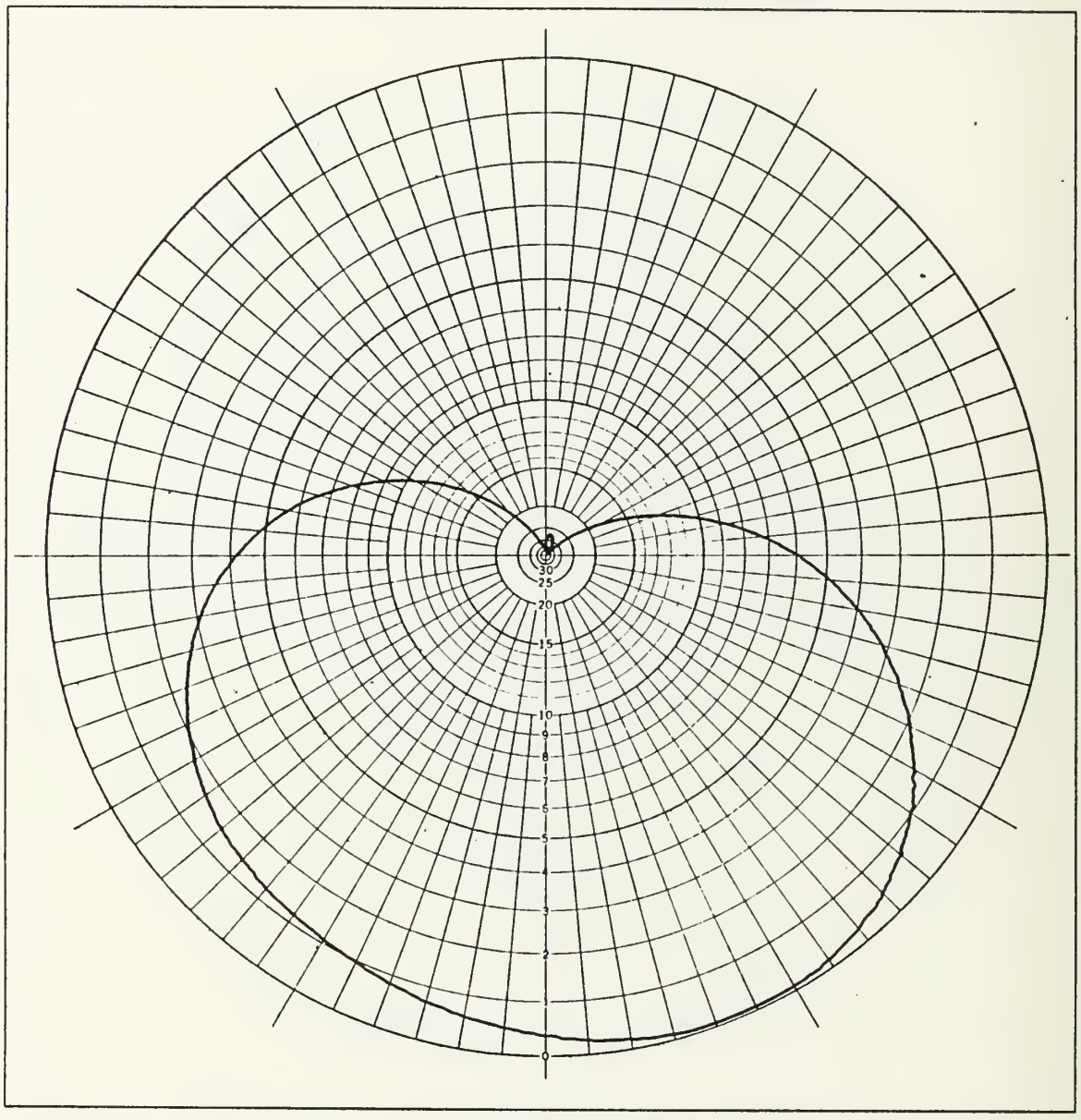

Figure 55. 66 MHz Harness, F = 65.50 MHz, Laboratory Plot

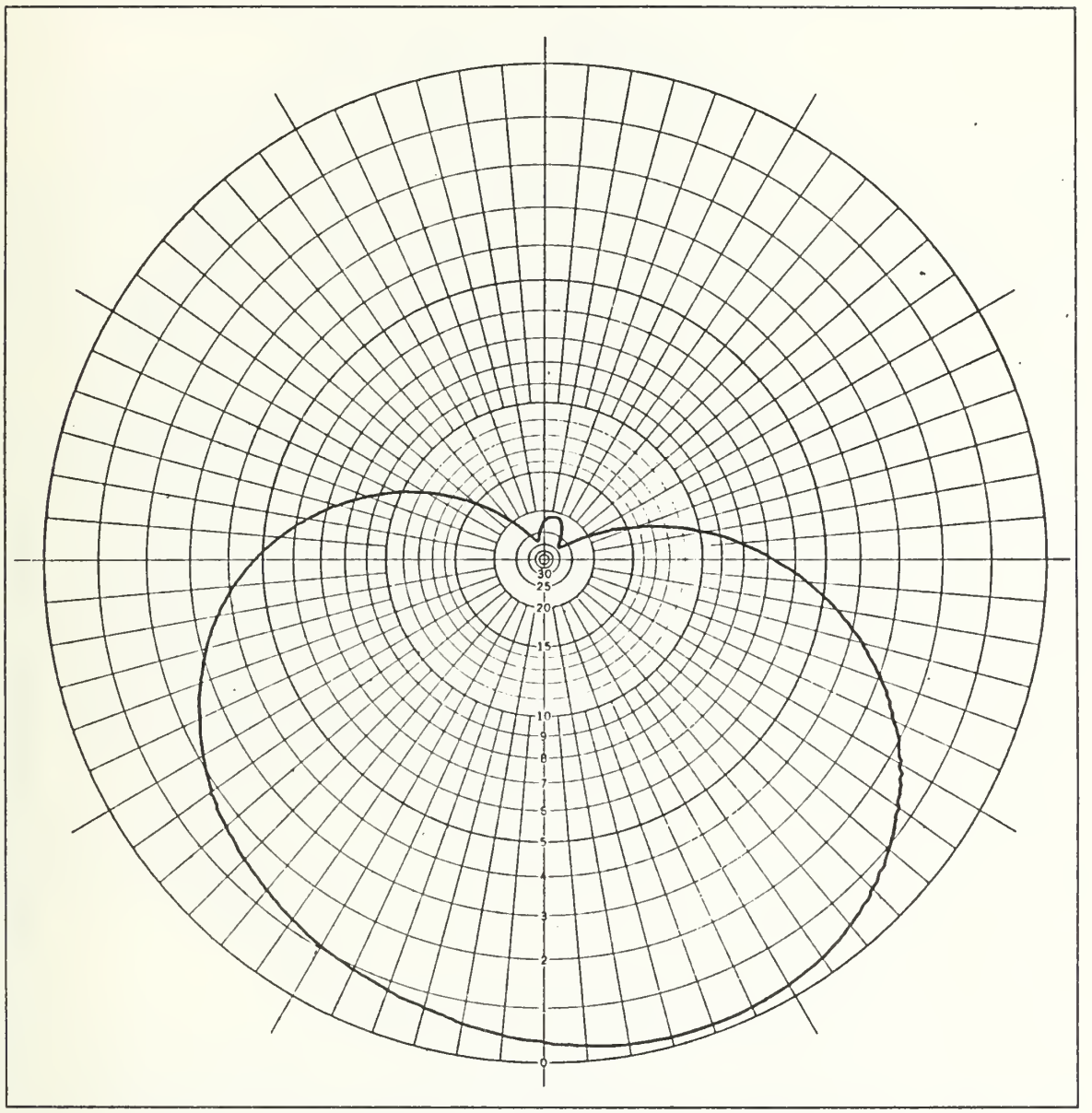

Figure 56. 66 MHz Harness, F = 66.00 MHz, Laboratory Plot

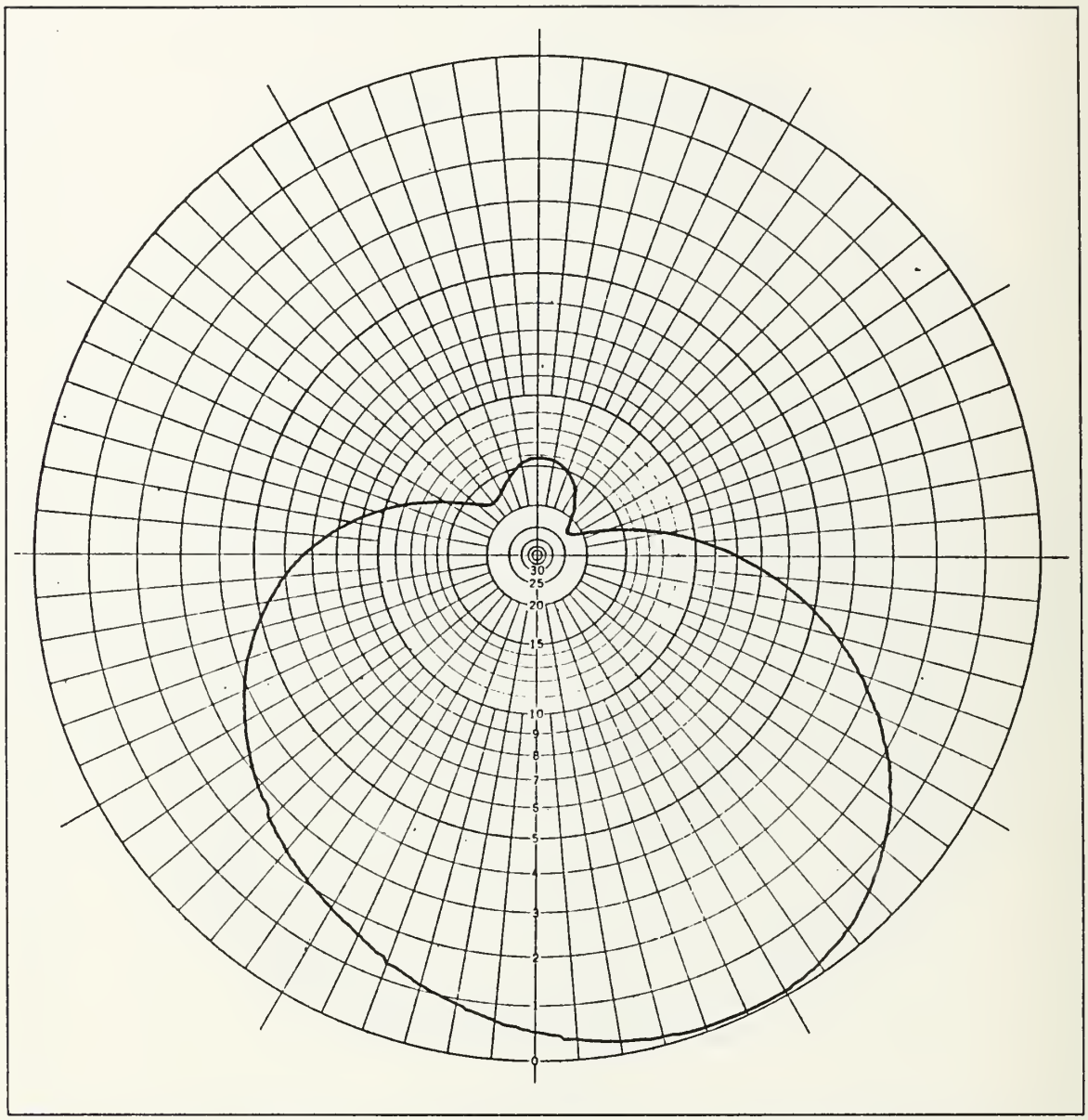

Figure 57. 66 MHz Harness, F = 66.50 MHz, Laboratory Plot

APPENDIX D. NEC DATASETS

A. ELEMENT ADMITTANCE AND MUTUAL ADMITTANCE

The dataset below was used to find the currents at the bases of the two monopoles of the test structures investigated. The current in segment one of tag one is the element admittance, and the current in segment one of tag two (the base of the other monopole) is the mutual admittance. These admittance values are used as shown in Appendix A to find the impedance matrix for the test structure.

```
CM TEST STRUCTURE #1.  TWO QTR WAVE MONOPOLES ABOVE AN ARTIFICIAL
CM GROUND PLANE WITH RADIALS AT 90 DEGREES TO DRIVEN MONOPOLES.
CM ONLY ONE MONOPOLE DRIVEN
CM ENTIRE STRUCTURE ELEVATED 10 METERS ABOVE GROUND.
CE
GW 1,5,0,0.625,10,0,0.625,11.25,0.006
GW 2,5,0,-0.625,10,0,-0.625,11.25,0.006
GW 3,5,0,0.625,10,-1.25,0.625,10,0.006
GW 4,5,0,0.625,10,0,1.875,10,0.006
GW 5,5,0,0.625,10,1.25,0.625,10,0.006
GW 6,5,0,.625,10,0,-.625,10,0.006
GW 7,5,0,-0.625,10,1.25,-0.625,10,0.006
GW 8,5,0,-0.625,10,0,-1.875,10,0.006
GW 9,5,0,-0.625,10,-1.25,-0.625,10,0.006
GE
FR 0,0,0,0,60
EX 0,1,1,0,1,0
PL 3,2,0,4
RP 0,1,361,1501,80,0,0,1
XQ
EN
```

B. GROUND RADIALS AT 120 DEGREE ANGLE TO MONOPOLES

This dataset was used to investigate the effects of putting the ground radials at an angle of 120 degrees to the monopoles. The corresponding radiation pattern plot is in Appendix C.

```
CM TEST STRUCTURE #2.  TWO QTR WAVE MONOPOLES IN FREE SPACE
CM WITH RADIALS AT 120 DEGREES TO DRIVEN MONOPOLES
CM MONOPOLES DRIVEN VIA TL SECTIONS TO GET PROPER CURRENTS
CE
GW 1,5,0,0.625,0,0,0.625,1.25,0.006
GW 2,5,0,-0.625,0,0,-0.625,1.25,0.006
GW 3,5,0,0.625,0,-1.083,0.625,-0.625,0.006
GW 4,5,0,0.625,0,0,1.708,-0.625,0.006
```

```
GW 5,5,0,0.625,0,1.083,0.625,-0.625,0.006
GW 6,5,0,.625,0,0,-.625,0,0.006
GW 7,5,0,-0.625,0,1.083,-0.625,-0.625,0.006
GW 8,5,0,-0.625,0,0,-1.708,-0.625,0.006
GW 9,5,0,-0.625,0,-1.083,-0.625,-0.625,0.006
GW 99,1,10000,10000,10000,10000,10000.05,10000,5E-4
GE
FR 0,0,0,0,60
TL 1,1,99,1,50,1.336,0,0,0,0
TL 2,1,99,1,50,1.865,0,0,0,0
EX 0,99,1,0,1,0
PL 3,2,0,4
RP 0,1,361,1501,90,0,0,1
XQ
EN
```

C. GROUND RADIALS AT 135 DEGREE ANGLE TO MONOPOLES

The dataset below was used to find the effects of drooping the ground radials at an angle of 135 degrees from the radiating monopoles. The radiation pattern plot for this dataset is in Appendix C.

```
CM TEST STRUCTURE #3.  TWO QTR WAVE MONOPOLES IN FREE SPACE
CM WITH RADIALS AT 135 DEGREES TO DRIVEN MONOPOLES.
CM MONOPOLES EXCITED VIA TL SECTIONS
CE
GW 1,5,0,0.625,0,0,0.625,1.25,0.006
GW 2,5,0,-0.625,0,0,-0.625,1.25,0.006
GW 3,5,0,0.625,0,-0.884,0.625,-0.884,0.006
GW 4,5,0,0.625,0,0,1.509,-0.884,0.006
GW 5,5,0,0.625,0,0.884,0.625,-0.884,0.006
GW 6,5,0,.625,0,0,-.625,0,0.006
GW 7,5,0,-0.625,0,0.884,-0.625,-0.884,0.006
GW 8,5,0,-0.625,0,0,-1.509,-0.884,0.006
GW 9,5,0,-0.625,0,-0.884,-0.625,-0.884,0.006
GW 99,1,10000,10000,10000,10000,10000.05,10000,5E-4
GE
FR 0,0,0,0,60
TL 1,1,99,1,50,1.256,0,0,0,0
TL 2,1,99,1,50,1.737,0,0,0,0
EX 0,99,1,0,1,0
PL 3,2,0,4
RP 0,1,361,1501,90,0,0,1
XQ
EN
```

D. GROUND RADIALS AT 150 DEGREE ANGLE TO MONOPOLES

The following dataset was used to investigate the effects of drooping the ground radials at an angle of 150 degrees from the radiating monopoles. The radiation pattern plot for this dataset is in Appendix C.

```
CM TEST STRUCTURE #4.  TWO QTR WAVE MONOPOLES IN FREE SPACE
CM WITH RADIALS AT 150 DEGREES TO DRIVEN MONOPOLES
CM BOTH MONOPOLES EXCITED VIA TL SECTIONS
CE
GW 1,5,0,0.625,0,0,0.625,1.25,0.006
GW 2,5,0,-0.625,0,0,-0.625,1.25,0.006
GW 3,5,0,0.625,0,-0.625,0.625,-1.083,0.006
GW 4,5,0,0.625,0,0,1.250,-1.083,0.006
GW 5,5,0,0.625,0,0.625,0.625,-1.083,0.006
GW 6,5,0,.625,0,0,-.625,0,0.006
GW 7,5,0,-0.625,0,0.625,-0.625,-1.083,0.006
GW 8,5,0,-0.625,0,0,-1.250,-1.083,0.006
GW 9,5,0,-0.625,0,-0.625,-0.625,-1.083,0.006
GW 99,1,10000,10000,10000,10000,10000.05,10000,5E-4
GE
TL 1,1,99,1,50,1.214,0,0,0,0
TL 2,1,99,1,50,1.662,0,0,0,0
FR 0,0,0,0,60
EX 0,1,1,0,1,0
PL 3,2,0,4
RP 0,1,361,1501,90,0,0,1
XQ
EN
```

E. TEST STRUCTURE SIMULATION OVER IMPERFECT GROUND

The NEC dataset below was used to add the effects of imperfect ground to the test structure model.

```
CM TEST STRUCTURE #1.  TWO QTR WAVE MONOPOLES ABOVE AN ARTIFICIAL
CM GROUND PLANE WITH RADIALS AT 90 DEGREES TO DRIVEN MONOPOLES.
CM CURRENT FEED ACCOMPLISHED USING TWO TL SECTIONS.
CM ENTIRE STRUCTURE ELEVATED 10 METERS ABOVE GROUND.
CM 9M MAST WITH 1M INSULATING SECTION SUPPORT USED.
CM GOOD GROUND:  EPSILON=34, SIGMA=.15
CE
GW 1,5,0,0.625,10,0,0.625,11.25,0.006
GW 2,5,0,-0.625,10,0,-0.625,11.25,0.006
GW 3,5,0,0.625,10,-1.25,0.625,10,0.006
GW 4,5,0,0.625,10,0,1.875,10,0.006
GW 5,5,0,0.625,10,1.25,0.625,10,0.006
GW 6,5,0,.625,10,0,-.625,10,0.006
GW 7,5,0,-0.625,10,1.25,-0.625,10,0.006
GW 8,5,0,-0.625,10,0,-1.875,10,0.006
GW 9,5,0,-0.625,10,-1.25,-0.625,10,0.006
GW 10,5,0,0,0,0,0,9,.02
```

```
GW 99,1,10000,10000,10000,10000,10000.05,10000,5E-4
GE
FR 0,0,0,0,60
GN 0,0,0,34,.15
TL 1,1,99,1,50,2.067,0,0,0,0
TL 2,1,99,1,50,2.428,0,0,0,0
EX 0,99,1,0,1,0
PL 3,2,0,4
RP 0,1,361,1501,80,0,0,1
XQ
EN
```

F. SURFACE WAVE MODEL OF PROTOTYPE ANTENNA

The NEC dataset below was used to model the prototype antenna over imperfect ground with the effects of the surface wave included. Note that prior to using this listing, it was necessary to create the required lookup table of ground characteristics using SOMNEC. The SOMNEC card required to get a lookup table for poor ground is shown below.

```
2.5,.00022,60.
```

Note that the epsilon, sigma and frequency values (2.5, 0.00022, 60), must match those in the NEC dataset being used.

```
CM SURFACE WAVE STUDY-- TWO QTR WAVE MONOPOLES ABOVE AN ARTIFICIAL
CM GROUND PLANE WITH RADIALS AT 90 DEGREES TO DRIVEN MONOPOLES.
CM CURRENT FEED ACCOMPLISHED USING TWO TL SECTIONS.
CM ENTIRE STRUCTURE ELEVATED 10 METERS ABOVE GROUND.
CM 9M METALLIC MAST WITH 1M INSULATING SECTION USED.
CM SURFACE WAVE INCLUDED VERSION OF GP10M3B STRUCTURE
CM GROUND CHARACTERISTICS:  EPSILON=2.5, SIGMA=.00022
CE
GW 1,5,0,0.625,10,0,0.625,11.25,0.006
GW 2,5,0,-0.625,10,0,-0.625,11.25,0.006
GW 3,5,0,0.625,10,-1.25,0.625,10,0.006
GW 5,5,0,0.625,10,1.25,0.625,10,0.006
GW 6,5,0,.625,10,0,-.625,10,0.006
GW 7,5,0,-0.625,10,1.25,-0.625,10,0.006
GW 9,5,0,-0.625,10,-1.25,-0.625,10,0.006
GW 10,5,0,0,0,0,0,9,.02
GW 99,1,10000,10000,10000,10000,10000.05,10000,5E-4
GE
FR 0,0,0,0,60
GN 2,0,0,0,2.5,.00022
TL 1,1,99,1,50,2.067,0,0,0,0
TL 2,1,99,1,50,2.428,0,0,0,0
EX 0,99,1,0,165.567,0
PL 3,2,1,0
```

```
RP 1,1,361,1000,10,0,0,1,1000
PL 3,2,2,0
RP 1,1,361,1000,10,0,0,1,1000
PL 3,2,3,0
RP 1,1,361,1000,10,0,0,1,1000
XQ
EN
```

This dataset produces all data needed to plot the vertical, horizontal and radial components of the total field at the specified observation points, 1000 meters from the test antenna in this case.

LIST OF REFERENCES

1. Kraus, John D., *Antennas,* McGraw-Hill Book Co., New York, 1950.

2. Jordan, Edward C. and Balmain, Keith G., *Electromagnetic Waves and Radiating Systems,* Prentice-Hall, Inc., Englewood Cliffs, NJ, 1968.

3. American Radio Relay League, *The ARRL Antenna Book,* 15th ed., American Radio Relay League, Newington, CT, 1988.

4. Christman, Al, "Elevated Vertical Antenna Systems," *QST,* v. 72, pp. 35-42, American Radio Relay League, Newington, CT, August 1988.

5. Logan, J. C. and Rockway, J. W., *The New MININEC (Version 3): A Mini-Numerical Electromagnetics Code,* Naval Ocean Systems Center, San Diego, CA, September 1986.

6. Breakall, J. K. and others, *Antenna Engineering Handbook,* v. 1, p. 19, Lawrence Livermore National Laboratory, Livermore, CA, 1987.

7. Christman, Al, "A Voltage-matching Method for Feeding Two-tower Arrays," *IEEE Transactions on Broadcasting,* v. BC-33, No. 2, pp. 33-42, June 1987.

8. Melody, James V., "An HF Phased Array Using Twisted-wire Hybrid Directional Couplers," *ARRL Antenna Compendium,* v. 1, pp. 67-71, American Radio Relay League, Newington, CT, 1985.

9. Mathsoft Inc., *MATHCAD Users Manual,* Mathsoft, Inc., Cambridge, MA. 1988.

INITIAL DISTRIBUTION LIST

		No. Copies
1.	Defense Technical Information Center Cameron Station Alexandria, VA 22304-6145	2
2.	Library, Code 0142 Naval Postgraduate School Monterey, CA 93943-5002	2
3.	U. S. Marine Corps Research, Development and Acquisition Command Marine Corps Combat Development Center Quantico, VA 22134	2
4.	Communication Officers School Marine Corps Combat Development Center Quantico, VA 22134	2
5.	Professor R. W. Adler Code 62Ab Naval Postgraduate School Monterey, CA 93943	10
6.	Professor J. K. Breakall Code 62Bk Naval Postgraduate School Monterey, CA 93943	5
7.	Commandant of the Marine Corps Code TE 06 Headquarters U. S. Marine Corps Washington, D.C. 20380-0001	1
8.	Major K. A. Vincent USMC ASST PM (Terminal Systems) COMM NAV Code C2C MCRDAC Quantico, VA 22134	5
9.	Professor Al Christman Electrical Engineering Department Grove City College Grove City, PA 16127	1
10.	Commander U.S. Army Information Systems Engineering Command ASB-SET-P (Janet McDonald) Fort Huachuca, AZ 85613-5300	1

11. Capt R. J. Gillespie Sr. USMC — 1
Development Center
C3 Division
MCDEC
Quantico, VA 22134-5080

12. Gerald A. Clapp — 1
Code 808
Naval Ocean Systems Center
271 Catalina Boulevard
San Diego, CA 92152

13. Jim Logan — 1
Code 822 (T)
Naval Ocean Systems Center
271 Catalina Boulevard
San Diego, CA 92152

14. Chairman, Code 62 — 1
Department of Electrical and Computer Engineering
Naval Postgraduate School
Monterey, CA 93943-5000

Th
V6
c.

Thesis
V6865 Vincent
c.1 Deep null antennas and
their applications to
tactical VHF radio
communications.

28 MAY 91 37870

Thesis
V6865 Vincent
c.1 Deep null antennas and
their applications to
tactical VHF radio
communications.

AMERICAN BINDERY
TOPEKA KANSAS

Deep null antennas and their application
3 2768 000 81965 0
DUDLEY KNOX LIBRARY